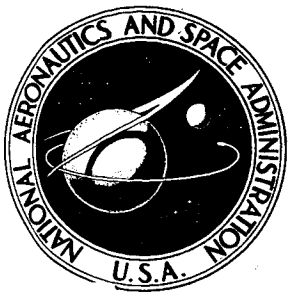


# NASA CONTRACTOR REPORT



## NASA CR-345

NASA CR-345

N66-14051

FORM 108M-202

(ACQUISITION NUMBER)	(FORM)
164	1
(OFFICE)	(CODE)
	32
(NASA CONTRACT NUMBER)	(CATEGORY)

# IMPROVED ANALYTIC LONGITUDINAL RESPONSE ANALYSIS FOR AXISYMMETRIC LAUNCH VEHICLES

## VOLUME I - LINEAR ANALYTIC MODEL

by *J. S. Archer and C. P. Rubin*

GPO PRICE \$ \_\_\_\_\_

CFSTI PRICE(S) \$ 5.00

Prepared under Contract No. NAS 1-4351 by  
TRW SPACE TECHNOLOGY LABORATORIES  
Redondo Beach, Calif.  
for Langley Research Center

Hard copy (HC) \_\_\_\_\_

Microfiche (MF) \_\_\_\_\_

# 653 July 65

IMPROVED ANALYTIC LONGITUDINAL RESPONSE ANALYSIS  
FOR AXISYMMETRIC LAUNCH VEHICLES

VOLUME I - LINEAR ANALYTIC MODEL

By J. S. Archer and C. P. Rubin

Distribution of this report is provided in the interest of information exchange. Responsibility for the contents resides in the author or organization that prepared it.

Prepared under Contract No. NAS 1-4351 by  
TRW SPACE TECHNOLOGY LABORATORIES  
Redondo Beach, Calif.

for Langley Research Center

NATIONAL AERONAUTICS AND SPACE ADMINISTRATION

---

For sale by the Clearinghouse for Federal Scientific and Technical Information  
Springfield, Virginia 22151 - Price \$5.00

## ACKNOWLEDGEMENT

The authors wish to acknowledge the technical guidance and assistance provided in a consulting capacity by Professor Y. C. Fung and Professor W. T. Thomson. Also, the performance of detailed calculations by Mrs. N. H. Piatt provided invaluable support for the theoretical developments.

## CONTENTS

Section		Page
1	INTRODUCTION . . . . .	1.1
2	ANALYTICAL MODEL . . . . .	2.1
3	SHELL COMPONENT STIFFNESS AND MASS MATRICES . . . . .	3.1
	3.1 Shell Stiffness Matrix . . . . .	3.2
	3.2 Shell Mass Matrix . . . . .	3.7
4	FLUID COMPONENT MASS MATRIX . . . . .	4.1
5	LAUNCH VEHICLE COORDINATE SYSTEMS . . . . .	5.1
	5.1 Local Coordinate Distortions . . . . .	5.1
	5.2 System Coordinate Point Displacements . . . . .	5.1
	5.3 Local to System Coordinate Transformation for Shell Component . . . . .	5.4
	5.4 Local to System Coordinate Transformation for Fluid Component . . . . .	5.8
6	LAUNCH VEHICLE STIFFNESS AND MASS MATRIX SYNTHESIS . . . . .	6.1
7	DYNAMIC RESPONSE EQUATIONS . . . . .	7.1
	7.1 Natural Frequency Equations . . . . .	7.1
	7.2 Steady-State Response Equations . . . . .	7.1
8	DIGITAL PROGRAM ARRANGEMENT . . . . .	8.1
9	DATA SETUP . . . . .	9.1
	9.1 Vehicle Subdivision . . . . .	9.1
	9.2 Input Description . . . . .	9.2
10	NOTATION . . . . .	10.1
11	REFERENCES . . . . .	11.1
 Appendices		
A	SHELL GEOMETRY AND ENERGY EXPRESSIONS . . . . .	A.1
B	INITIAL STRESSES IN SHELL ELEMENTS . . . . .	B.1

CONTENTS (Continued)

Appendices	Page
C	FLUID MASS MATRIX EXPRESSIONS . . . . . C. 1 C. 1 Case I. Upper Bulkhead Convex Upward, Lower Bulkhead Convex Downward . . . . . C. 1 C. 2 Case II. Upper Bulkhead Convex Downward, Lower Bulkhead Convex Downward . . . . . C. 4 C. 3 Case III. Upper Bulkhead Convex Upward, Lower Bulkhead Convex Upward . . . . . C. 8
D	CALCULATION OF THE SHELL STIFFNESS AND MASS MATRICES . . . . . D. 1 D. 1 Functional Flow Chart for Calculation of Shell Stiffness and Mass Matrices . . . . . D. 2 D. 2 Gaussian Weighting Matrix Tables . . . . . D. 4 D. 3 Assembly of $[rKMF]$ for $M = 1, 2, \dots, 13$ . . . . . D. 4 D. 4 Initial Stress for Conic . . . . . D. 7 D. 5 Initial Stress for Ellipsoidal Bulkhead . . . . . D. 8
E	CALCULATION OF FLUID MASS MATRIX . . . . . E. 1 E. 1 Functional Flow Chart for Calculation of Fluid Mass Matrix . . . . . E. 2 E. 2 General Matrix Equation for Mass Matrix $[\bar{M}]$ . . . . . E. 3 E. 3 Case I . . . . . E. 9 E. 3.1 Integral Equation Relationships . . . . . E. 9 E. 3.2 Integration Limit Data . . . . . E. 13 E. 3.3 Specific Matrix Data . . . . . E. 15 E. 4 Case II . . . . . E. 19 E. 4.1 Integral Equation Relationships . . . . . E. 19 E. 4.2 Integration Limit Data . . . . . E. 22 E. 4.3 Specific Matrix Data . . . . . E. 23 E. 5 Case III . . . . . E. 27 E. 5.1 Integral Equation Relationships . . . . . E. 27 E. 5.2 Integration Limit Data . . . . . E. 32 E. 5.3 Specific Matrix Data . . . . . E. 33 E. 6 Lagrangian Weighting Matrix Tables . . . . . E. 36
F	SAMPLE INPUT DATA . . . . . F. 1

## ILLUSTRATIONS

Figure		Page
1	Summary of Technical Approach . . . . .	1.4
2	Vehicle Components . . . . .	2.2
3	Tank Configuration . . . . .	2.3
4	Displacements of Shell of Revolution . . . . .	3.9
5	Conical Shell Component . . . . .	3.9
6	Ellipsoidal Bulkhead Component . . . . .	3.10
7	Definition of Fluid Motions . . . . .	4.4
8	Conical Shell Component System Coordinate Arrangement . . . . .	5.11
9	Convex Upward Ellipsoidal Shell Component System Coordinate Arrangement . . . . .	5.12
10	Convex Downward Ellipsoidal Shell Component System Coordinate Arrangement . . . . .	5.12
11	Vehicle System Coordinates . . . . .	6.4
12	Digital Program Arrangement . . . . .	8.4
A.1	Meridian of Shell of Revolution . . . . .	A.4
A.2	Conical Shell . . . . .	A.4
A.3	Ellipsoidal Shell . . . . .	A.5
C.1	Case I Tank Configuration . . . . .	C.14
C.2	Case II Tank Configuration . . . . .	C.15
C.3	Case III Tank Configuration . . . . .	C.15
F.1	Typical One-Stage Launch Vehicle . . . . .	F.2
F.2	System Components and Coordinates . . . . .	F.3

## 1. INTRODUCTION

This report describes an improved linear analytical model and digital program developed for the calculation of axisymmetric launch vehicle steady-stage response to applied axisymmetric sinusoidal loads. The detailed computer programming manual for the digital program is contained in Volume II of this report.

In the evaluation of launch vehicle behavior, it is necessary to study the response of the entire vehicle to a wide variety of dynamic loadings to insure the structural integrity and stability of the system. Much effort has already gone into the development of techniques to calculate the vehicle response to lateral and longitudinal loadings using distributed and lumped spring-mass models and techniques for theoretical and empirical modeling of the vehicle behavior.<sup>1,2</sup> However, experimental data indicate that these procedures are unsatisfactory in several respects. For example, accurate representation of important structural shell characteristics and realistic coupling of the fluids with the detailed structural behavior of tank walls and bulkheads are omitted.

The approach described herein overcomes the above noted deficiencies. A finite element technique is utilized to construct the total launch vehicle stiffness matrix  $[K]$  and mass matrix  $[M]$  by subdividing the prototype structure into a set of (1) axisymmetric shell components, (2) fluid components, and (3) spring-mass components. In this way, it is possible to represent as separate shell units the fairing, interstage structure, bulkheads, tank walls and engine thrust structure, and to conveniently provide for the inertial and stiffness characteristics of equipment, engines and vehicle supporting structure.

The stiffness and mass matrices for the complete launch vehicle are obtained by superposition of the stiffness and mass matrices of the individual shell, fluid and spring-mass components which are computed using a Rayleigh-Ritz approach. Fluid motions are assumed to be consistent with the shell component distortions. The superposition technique assures displacement compatibility and force equilibrium at the joints between components. After the complete system stiffness and mass

matrices have been formulated, displacement boundary conditions are introduced by removing appropriate rows and columns corresponding to points on the vehicle and its supports which are rigidly restrained from motion.

The coupled system natural frequencies and mode shapes are obtained from the eigenvalue equation constructed with the total stiffness and mass matrices

$$[K] \{a\} - p^2 [M] \{a\} = 0 \quad (1.1)$$

in which  $p$  is the circular frequency of the system and  $\{a\}$  is the modal vector whose components are the longitudinal, radial and rotational displacements at discrete points on the vehicle. The steady-state response due to simple harmonic loads is determined using a standard modal response procedure which expresses the total displacement, velocity, acceleration and force responses as the linear superposition of the individual modal responses based on an assumed modal damping.

The procedure will handle shell components with a wide range of geometries. It includes shell effects in the tank and bulkhead structure, but avoids the need for including detailed local deformation, such as at shell discontinuities, which are unimportant in determining the total dynamic behavior of the vehicle. The approach has the capability of representing the tank or stage of most interest in great detail and those of least interest with minimum detail, as desired, thereby minimizing the computation time required and remaining within the maximum limitations of standard eigenvalue routines. The formulation of the problem is subdivided into well-defined portions, leading to efficient coding and easy modification for later incorporation of asymmetric shell behavior and even more detailed treatment of the fluid behavior.

The analytical procedure discussed herein is summarized in Figure 1. The launch vehicle analytical model is discussed in Section 2. The equations for the shell and fluid component stiffness and mass matrices are developed in Sections 3 and 4, respectively. The coordinate representation which forms the framework for the vehicle model, and the construction of stiffness and mass matrices for the complete launch vehicle, are discussed



in Sections 5 and 6, respectively. The method for computing the dynamic response is discussed in Section 7. The computer program arrangement is described in Section 8 and detailed input data requirements for the computer program are itemized in Section 9. A complete list of symbols is provided in Section 10.

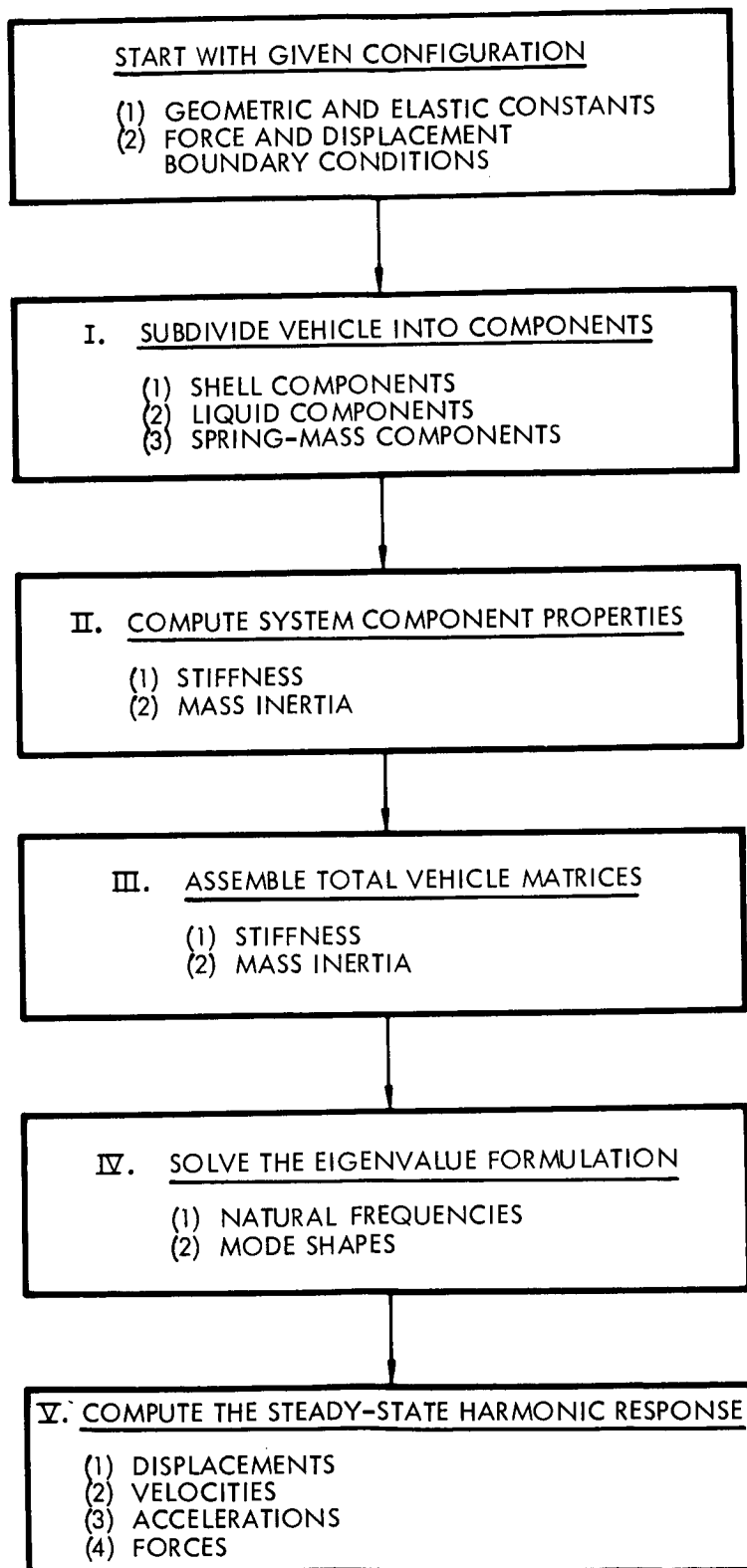


Figure 1. Summary of Technical Approach

## 2. ANALYTICAL MODEL

As illustrated in Figure 2, the vehicle structure is subdivided into a consistent set of shell components, a, fluid components, b, and multi-coordinate spring-mass components, c. The total vehicle which may be represented is limited to one with not more than six (6) fluid components. The total number of shell components which may be represented shall not exceed forty (40). The characteristics of the spring-mass components representing such equipment as engines and mass-elastic supports are provided directly by low order ( $\leq 10$ ) stiffness and mass matrices. The total number of spring-mass components may not exceed thirty (30). The vehicle behavior is described in terms of motions of discrete points on the vehicle located at intersections of shell components, at lumped masses, and at intermediate points on the shell elements. The number of nonfixed degrees-of-freedom by which the behavior of the system is described may not exceed eighty (80).

The specific shell components to be used are conical frustums (which include cylindrical shells as a special case) and ellipsoidal bulkheads (which include hemispherical shells as a special case). Within the domain of thin shell theory, the shell components may have orthotropic properties and a linear thickness variation in the meridional direction. Local thickening of a shell at a bulkhead or wall joint may be handled by using an equivalent local hoop stiffener which is provided as input in the form of an additional spring-mass component. Initial static stresses based on membrane theory are accounted for in determining the stiffness matrix for the shell components.

The most general fluid component may be in contact with an ellipsoidal upper bulkhead, a conical tank wall, and a conical or ellipsoidal lower bulkhead. The bulkhead shell elements may be convex down or up with fluid at any desired depth on either side, both sides or neither side. The tank configurations which are considered are illustrated in Figure 3.

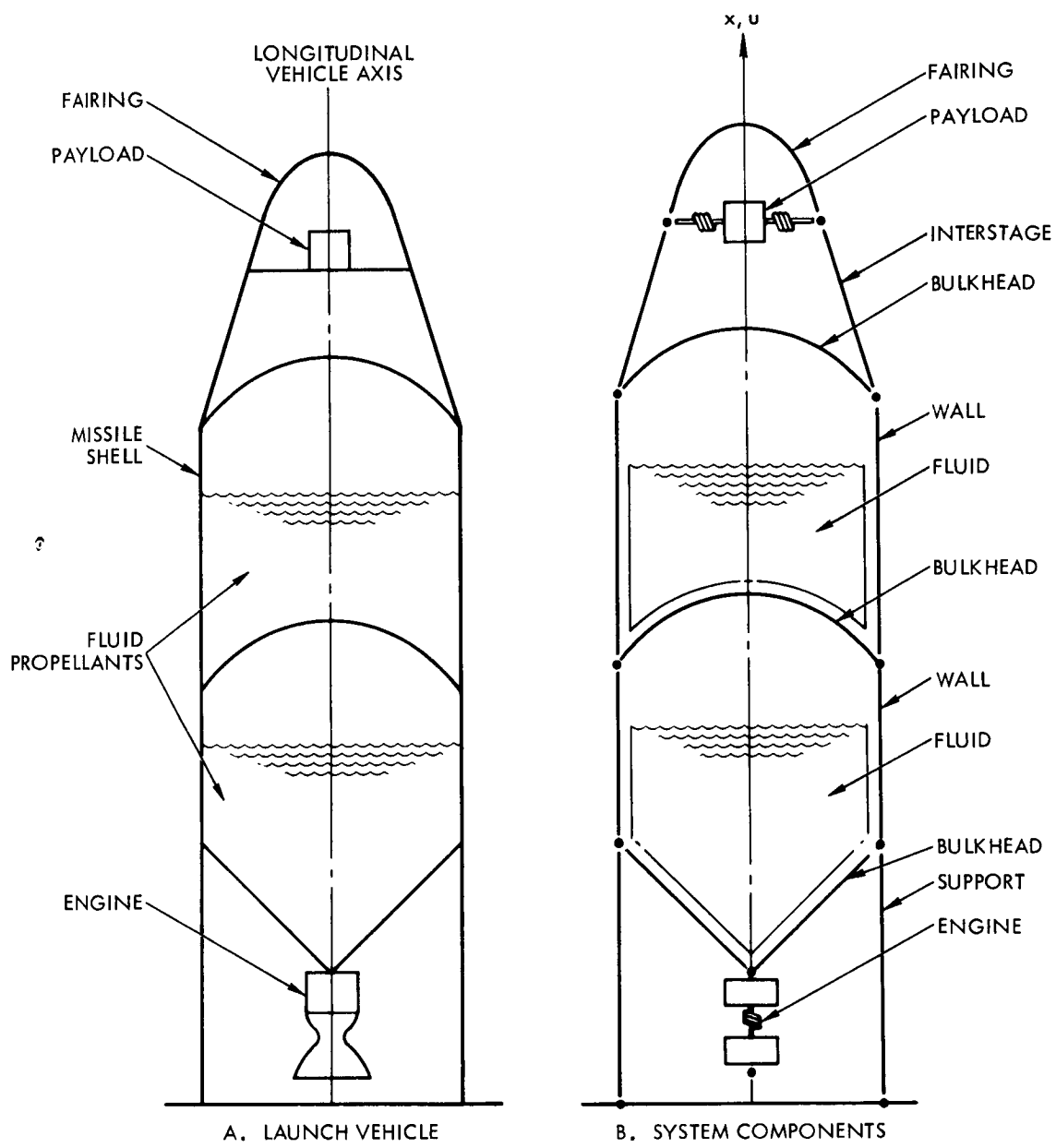
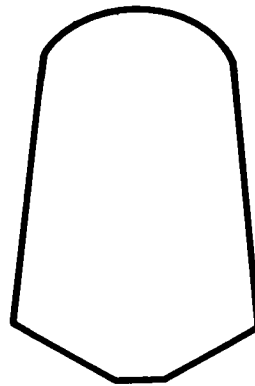
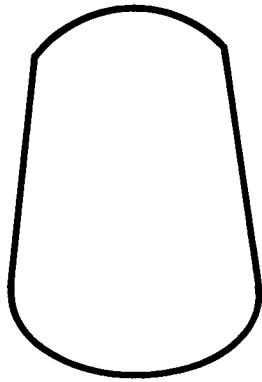
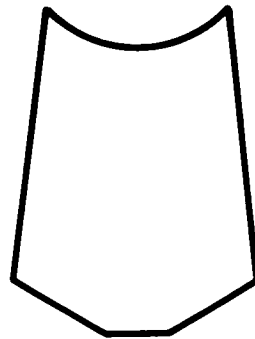
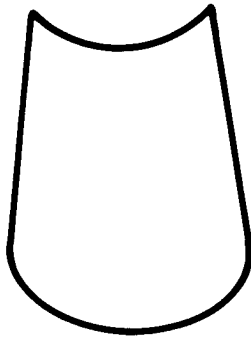


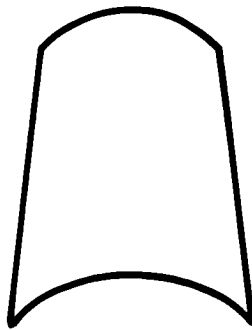
Figure 2. Vehicle Components



SIMPLE TANKS



INVERTED UPPER BULKHEAD TANKS



INVERTED LOWER BULKHEAD TANKS

Figure 3. Tank Configurations

### 3. SHELL COMPONENT STIFFNESS AND MASS MATRICES

The displacements of an individual shell component (Figure 4) are approximated in the Rayleigh-Ritz manner by a finite series of functions having the form

$$u(\xi) = \sum_{k=1}^{\bar{U}} \bar{a}_k u_k(\xi) \quad , \quad \bar{U} \leq 11 \quad (3.1)$$

$$v(\xi) = \sum_{\ell=1}^{\bar{V}} \bar{\beta}_\ell v_\ell(\xi) \quad , \quad \bar{V} \leq 11$$

in which  $\xi$  is a dimensionless variable and  $0 \leq \xi \leq 1$ . For conical frustums, Figure 5,  $\xi = s/l \sin \phi_0$ . For convex upward ellipsoidal shells, Figure 6,  $\xi = \phi/\phi_0$ , and for convex downward ellipsoidal shells,  $\xi = (\pi - \phi)/(\pi - \phi_0)$ .

The assumed mode shapes  $u_k(\xi)$  and  $v_\ell(\xi)$  consist of polynomial terms sufficient to represent all modes of shell distortion, including longitudinal stretching, radial dilatation and rigid body displacements. The specific shape of the assumed modes is determined within the limitations of a tenth order polynomial, as follows:

$$u_k(\xi) = \sum_{n=0}^{10} a_{kn} \xi^n \quad (3.2)$$

$$v_\ell(\xi) = \sum_{n=0}^{10} b_{\ell n} \xi^n$$

in which  $[a_{kn}] = [A]_{(\bar{U} \times 11)}$  and  $[b_{\ell n}] = [B]_{(\bar{V} \times 11)}$  define the polynomial functions associated with the local coordinates  $(\bar{a}_k)$  and  $(\bar{\beta}_\ell)$ , respectively.  $[A]$  and  $[B]$  are furnished as input to provide maximum flexibility in the selection of the assumed coordinate functions. It should be understood that the  $\bar{a}_k$  and the  $\bar{\beta}_\ell$  are the unknown generalized coordinates associated with the shell component, whereas the  $a_{kn}$  and  $b_{\ell n}$  are definite arbitrarily specified coefficients which determine the functions  $u_k(\xi)$  and  $v_\ell(\xi)$ .

### 3.1 SHELL STIFFNESS MATRIX

The shell stiffness matrix is constructed from the potential energy function  $V$  derived in Appendix A. For the generalized displacement (Equation 3.1), the stiffness matrix is defined by

$$\begin{aligned}
 [\bar{K}_a]_{((\bar{U}+\bar{V})_x(\bar{U}+\bar{V}))} = & \begin{bmatrix} \frac{\partial^2 V}{\partial \bar{a}_1 \partial \bar{a}_1} & \dots & \frac{\partial^2 V}{\partial \bar{a}_1 \partial \bar{a}_U} & | & \frac{\partial^2 V}{\partial \bar{a}_1 \partial \bar{\beta}_1} & \dots & \frac{\partial^2 V}{\partial \bar{a}_1 \partial \bar{\beta}_V} \\ \vdots & & \vdots & & \vdots & & \vdots \\ \frac{\partial^2 V}{\partial \bar{a}_U \partial \bar{a}_1} & \dots & \frac{\partial^2 V}{\partial \bar{a}_U \partial \bar{a}_U} & | & \frac{\partial^2 V}{\partial \bar{a}_U \partial \bar{\beta}_1} & \dots & \frac{\partial^2 V}{\partial \bar{a}_U \partial \bar{\beta}_V} \\ \dots & & \dots & & \dots & & \dots \\ \frac{\partial^2 V}{\partial \bar{\beta}_1 \partial \bar{a}_1} & \dots & \frac{\partial^2 V}{\partial \bar{\beta}_1 \partial \bar{a}_U} & | & \frac{\partial^2 V}{\partial \bar{\beta}_1 \partial \bar{\beta}_1} & \dots & \frac{\partial^2 V}{\partial \bar{\beta}_1 \partial \bar{\beta}_V} \\ \vdots & & \vdots & & \vdots & & \vdots \\ \frac{\partial^2 V}{\partial \bar{\beta}_V \partial \bar{a}_1} & \dots & \frac{\partial^2 V}{\partial \bar{\beta}_V \partial \bar{a}_U} & | & \frac{\partial^2 V}{\partial \bar{\beta}_V \partial \bar{\beta}_1} & \dots & \frac{\partial^2 V}{\partial \bar{\beta}_V \partial \bar{\beta}_V} \end{bmatrix} \quad (3.3)
 \end{aligned}$$

which is consistent with the Rayleigh-Ritz procedure and in which, for example

$$\begin{aligned}
 \frac{\partial^2 V}{\partial \bar{a}_k \partial \bar{\beta}_l} = & 2\pi \int_s \gamma a \left\{ \left[ C_{11} \frac{\partial \epsilon_\phi}{\partial \bar{a}_k} + C_{12} \frac{\partial \epsilon_\theta}{\partial \bar{a}_k} \right] \frac{\partial \epsilon_\phi}{\partial \bar{\beta}_l} + \left[ C_{12} \frac{\partial \epsilon_\phi}{\partial \bar{a}_k} + C_{22} \frac{\partial \epsilon_\theta}{\partial \bar{a}_k} \right] \frac{\partial \epsilon_\theta}{\partial \bar{\beta}_l} \right. \\
 & + \left[ C_{33} \frac{\partial K_\phi}{\partial \bar{a}_k} + C_{34} \frac{\partial K_\theta}{\partial \bar{a}_k} \right] \frac{\partial K_\phi}{\partial \bar{\beta}_l} + \left[ C_{34} \frac{\partial K_\phi}{\partial \bar{a}_k} + C_{44} \frac{\partial K_\theta}{\partial \bar{a}_k} \right] \frac{\partial K_\theta}{\partial \bar{\beta}_l} \\
 & \left. + N_\phi^o \frac{\partial \rho}{\partial \bar{a}_k} \frac{\partial \rho}{\partial \bar{\beta}_l} \right\} ds \quad (3.4)
 \end{aligned}$$

and

$$k = 1 \dots \bar{U}$$

$$l = 1 \dots \bar{V}$$

The strains ( $\epsilon_\phi$ ,  $\epsilon_\theta$ ), curvatures ( $K_\phi$ ,  $K_\theta$ ) and meridional rotation  $\rho$  are defined in terms of the displacements in Appendix A by Equations (A.13) through (A.17). The quantities  $C_{11}$ ,  $C_{12}$ ,  $C_{22}$ ,  $C_{33}$ ,  $C_{34}$  and  $C_{44}$  are the orthotropic stress-strain coefficients which are functions of the dimensionless parameter  $\xi$ . For the present analytical model, these coefficients are approximated by the following polynomial equations:

$$\{\bar{C}(\xi)\} = \begin{Bmatrix} C_{11}(\xi) \\ C_{12}(\xi) \\ C_{22}(\xi) \end{Bmatrix} = \{\bar{C}(0)\} + \xi \left( \{\bar{C}(1)\} - \{\bar{C}(0)\} \right) \quad (3.5)$$

$$\{\bar{\bar{C}}(\xi)\} = \begin{Bmatrix} C_{33}(\xi) \\ C_{34}(\xi) \\ C_{44}(\xi) \end{Bmatrix} = -\frac{9}{2} \left( \xi - \frac{1}{3} \right) \left( \xi - \frac{2}{3} \right) (\xi - 1) \{\bar{\bar{C}}(0)\}$$

$$+ \frac{27}{2} \xi \left( \xi - \frac{2}{3} \right) (\xi - 1) \left\{ \bar{\bar{C}}\left(\frac{1}{3}\right) \right\}$$

$$- \frac{27}{2} \xi \left( \xi - \frac{1}{3} \right) (\xi - 1) \left\{ \bar{\bar{C}}\left(\frac{2}{3}\right) \right\}$$

$$+ \frac{9}{2} \xi \left( \xi - \frac{1}{3} \right) \left( \xi - \frac{2}{3} \right) \left\{ \bar{\bar{C}}(1) \right\}$$

The quantities  $\{\bar{C}(0)\}$ ,  $\{\bar{C}(1)\}$ ,  $\{\bar{\bar{C}}(0)\}$ ,  $\left\{ \bar{\bar{C}}\left(\frac{1}{3}\right) \right\}$ ,  $\left\{ \bar{\bar{C}}\left(\frac{2}{3}\right) \right\}$  and  $\left\{ \bar{\bar{C}}(1) \right\}$  are provided as input.

$N_\phi^0$  is the initial meridional stress caused by tank pressures and longitudinal vehicle accelerations (prestress and static longitudinal acceleration stress). These initial stresses are derived in Appendix B using membrane theory, which is a reasonable first order approximation, except in very localized areas where the bending stresses predominate.



This simplifies the calculation of the initial stresses which are readily obtained from the membrane equations of equilibrium. Expressions for the initial stresses for conical shell components are given in Equations (B. 1) through (B. 6), for the upright ellipsoidal bulkheads in Equations (B. 7) through (B. 11), and for the inverted ellipsoidal bulkheads in Equations (B. 12) through (B. 15). The computation of these stresses is included as an integral part of the digital program.

After substitution of the displacements (3. 1) into (3. 3), the shell component stiffness matrix becomes

$$\begin{aligned}
 [\bar{K}_a] = 2\pi \int r & \left( K_1 \cdot \{\dot{u}\} \cdot \{\dot{u}\}^T + K_2 \{\ddot{u}\} \cdot \{\ddot{u}\}^T + K_3 [\{\dot{u}\} \cdot \{\ddot{u}\}^T + \{\ddot{u}\} \cdot \{\dot{u}\}^T] \right. \\
 & + K_4 [\{\dot{v}\} \cdot \{\dot{v}\}^T + \{\dot{v}\} \cdot \{\dot{v}\}^T] + K_5 \{\dot{v}\} \cdot \{\dot{v}\}^T + K_6 \{\dot{v}\} \cdot \{\dot{v}\}^T \\
 & + K_7 \{\ddot{v}\} \cdot \{\ddot{v}\}^T + K_8 [\{\dot{v}\} \cdot \{\ddot{v}\}^T + \{\ddot{v}\} \cdot \{\dot{v}\}^T] \\
 & + K_9 [\{\dot{v}\} \cdot \{\dot{u}\}^T + \{\dot{u}\} \cdot \{\dot{v}\}^T] + K_{10} [\{\dot{v}\} \cdot \{\dot{u}\}^T + \{\dot{u}\} \cdot \{\dot{v}\}^T] \\
 & + K_{11} [\{\ddot{v}\} \cdot \{\dot{u}\}^T + \{\dot{u}\} \cdot \{\ddot{v}\}^T] + K_{12} [\{\dot{v}\} \cdot \{\ddot{u}\}^T + \{\ddot{u}\} \cdot \{\dot{v}\}^T] \\
 & \left. + K_{13} [\{\ddot{v}\} \cdot \{\ddot{u}\}^T + \{\ddot{u}\} \cdot \{\ddot{v}\}^T] \right) r_1 d\phi
 \end{aligned} \tag{3. 6}$$

in which

$$\{\mathbf{u}\} = \begin{Bmatrix} u_1(\xi) \\ \vdots \\ u_{\bar{U}}(\xi) \\ \text{---} \\ 0_1 \\ \vdots \\ 0_{\bar{V}} \end{Bmatrix} \qquad \{\mathbf{v}\} = \begin{Bmatrix} 0_1 \\ \vdots \\ 0_{\bar{U}} \\ \text{---} \\ v_1(\xi) \\ \vdots \\ v_{\bar{V}}(\xi) \end{Bmatrix}$$

$$\frac{1}{r_1} \frac{d}{d\phi} \langle u \rangle = \langle \dot{u} \rangle = \begin{bmatrix} A \\ - \\ 0 \end{bmatrix} [\dot{D}] \langle \xi^n \rangle$$

$$\frac{1}{r_1} \frac{d}{d\phi} \langle \dot{u}_k \rangle = \langle \ddot{u}_k \rangle = \begin{bmatrix} A \\ - \\ 0 \end{bmatrix} [\dot{D}] [\dot{D}] \langle \xi^n \rangle$$

$$\frac{1}{r_1} \frac{d}{d\phi} \langle v_l \rangle = \langle \dot{v}_l \rangle = \begin{bmatrix} 0 \\ - \\ B \end{bmatrix} [\dot{D}] \langle \xi^n \rangle$$

$$\frac{1}{r_1} \frac{d}{d\phi} \langle \dot{v}_l \rangle = \langle \ddot{v}_l \rangle = \begin{bmatrix} 0 \\ - \\ B \end{bmatrix} [\dot{D}] [\dot{D}] \langle \xi^n \rangle$$

$$[\dot{D}] = D \left\{ \begin{array}{cccccccc} 0 & 0 & 0 & \cdot & \cdot & \cdot & 0 \\ 1 & 0 & 0 & \cdot & \cdot & \cdot & 0 \\ 0 & 2 & 0 & \cdot & \cdot & \cdot & 0 \\ \cdot & & & & & & \\ \cdot & & & & & & \\ \cdot & & & & & & \\ 0 & 0 & 0 & \cdot & \cdot & 10 & 0 \end{array} \right\} \quad (11 \times 11)$$

and

$$\begin{aligned} D &= \frac{1}{r_1 \phi_0} && \text{for convex upward ellipsoid,} \\ &= \frac{1}{r_1 (\phi_0 - \pi)} && \text{for convex downward ellipsoid,} \\ &= \frac{\sin \phi_0}{L} && \text{for a cone.} \end{aligned} \quad (3.7)$$

The constants K1 - K13 are defined as follows:

$$K1 = \left[ C_{11} \sin^2 \phi + C_{33} \frac{1}{r_1^2} \left( \sin \phi + \frac{\dot{r}_1}{r_1} \cos \phi \right)^2 \right. \\ \left. - C_{34} \frac{2 \cos^2 \phi}{r r_1} \left( \sin \phi + \frac{\dot{r}_1}{r_1} \cos \phi \right) + C_{44} \frac{\cos^4 \phi}{r^2} \right] + N_\phi^o \cos^2 \phi$$

$$K2 = C_{33} \cos^2 \phi$$

$$K3 = -C_{33} \frac{\cos \phi}{r_1} \left( \sin \phi + \frac{\dot{r}_1}{r_1} \cos \phi \right) + C_{34} \frac{\cos^3 \phi}{r}$$

$$K4 = C_{12} \frac{\cos \phi}{r}$$

$$K5 = C_{22} \frac{1}{r^2}$$

$$K6 = C_{11} \cos^2 \phi + C_{33} \frac{1}{r_1^2} \left( \cos \phi - \frac{\dot{r}_1}{r_1} \sin \phi \right)^2 \\ + C_{34} \frac{2 \sin \phi \cos \phi}{r r_1} \left( \cos \phi - \frac{\dot{r}_1}{r_1} \sin \phi \right) + C_{44} \frac{\sin^2 \phi \cos^2 \phi}{r^2} + N_\phi^o \sin^2 \phi$$

$$K7 = C_{33} \sin^2 \phi$$

$$K8 = C_{33} \frac{\sin \phi}{r_1} \left( \cos \phi - \frac{\dot{r}_1}{r_1} \sin \phi \right) + C_{34} \frac{\sin^2 \phi \cos \phi}{r}$$

$$K9 = -C_{12} \frac{\sin \phi}{r}$$

$$\begin{aligned}
K_{10} = & -C_{11} \sin \phi \cos \phi - C_{33} \frac{1}{r_1^2} \left( \cos \phi - \frac{\dot{r}_1}{r_1} \sin \phi \right) \left( \sin \phi + \frac{\dot{r}_1}{r_1} \cos \phi \right) \\
& - C_{34} \frac{\sin \phi \cos \phi}{r r_1} \left( \sin \phi + \frac{\dot{r}_1}{r_1} \cos \phi \right) + C_{34} \frac{\cos^2 \phi}{r r_1} \left( \cos \phi - \frac{\dot{r}_1}{r_1} \sin \phi \right) \\
& + C_{44} \frac{\sin \phi \cos^3 \phi}{r^2} + N_\phi^o \sin \phi \cos \phi
\end{aligned}$$

$$K_{11} = -C_{33} \frac{1}{r_1} \left( \sin \phi + \frac{\dot{r}_1}{r_1} \cos \phi \right) \sin \phi + C_{34} \frac{\sin \phi \cos^2 \phi}{r}$$

$$K_{12} = C_{33} \left( \cos \phi - \frac{\dot{r}_1}{r} \sin \phi \right) \frac{\cos \phi}{r_1} + C_{34} \frac{\sin \phi \cos^2 \phi}{r}$$

$$K_{13} = C_{33} \sin \phi \cos \phi \tag{3.8}$$

### 3.2 SHELL MASS MATRIX

The shell mass matrix associated with the generalized coordinates  $\bar{\alpha}_k, \bar{\beta}_l$  is derived by operating on the expression for the kinetic energy T. For each shell component, the mass matrix is defined by

$$p^2 \left[ \overline{M}_a \right] (\overline{U} + \overline{V})_x (\overline{U} + \overline{V}) = \begin{bmatrix} \frac{\partial^2 T}{\partial \overline{a}_1 \partial \overline{a}_1} \dots \frac{\partial^2 T}{\partial \overline{a}_1 \partial \overline{a}_U} & & \\ \vdots & \vdots & \\ \frac{\partial^2 T}{\partial \overline{a}_U \partial \overline{a}_1} \dots \frac{\partial^2 T}{\partial \overline{a}_U \partial \overline{a}_U} & & \\ \hline & & \frac{\partial^2 T}{\partial \overline{\beta}_1 \partial \overline{\beta}_1} \dots \frac{\partial^2 T}{\partial \overline{\beta}_1 \partial \overline{\beta}_V} \\ & & \vdots \\ & & \frac{\partial^2 T}{\partial \overline{\beta}_V \partial \overline{\beta}_1} \dots \frac{\partial^2 T}{\partial \overline{\beta}_V \partial \overline{\beta}_V} \end{bmatrix} \quad \begin{matrix} \text{(Zero)} \\ \\ \\ \text{(Zero)} \end{matrix} \quad (3.9)$$

After substitution of Equations (3.1) into the kinetic energy expression in Equation (3.9), the mass matrix assumes the form<sup>3</sup>

$$\left[ \overline{M}_a \right] = 2\pi\gamma_a \int \text{tr} \left( \{u\} \cdot \{u\}^T + \{v\} \cdot \{v\}^T \right) ds \quad (3.10)$$

where  $\gamma_a$  is the shell mass density.

The detailed equations for the calculation of the stiffness and mass matrices of the shell components are presented in Appendix D. The equations are written in matrix notation to accommodate the Gaussian weighted matrix<sup>5</sup> integration scheme.

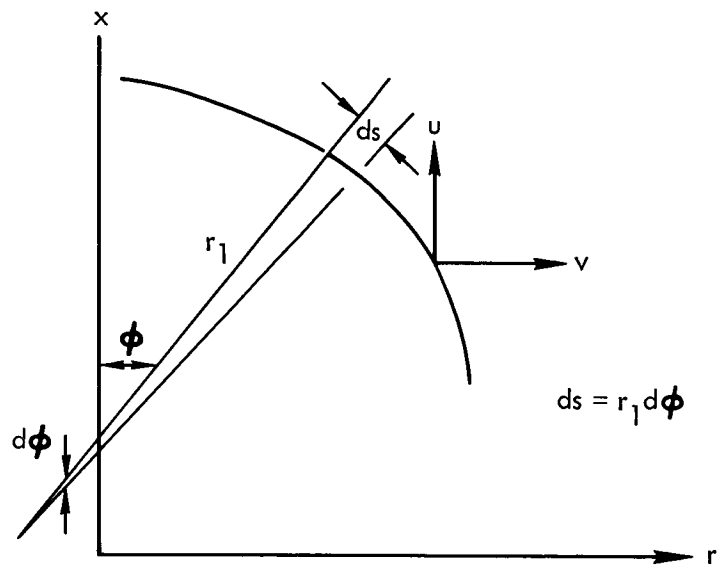
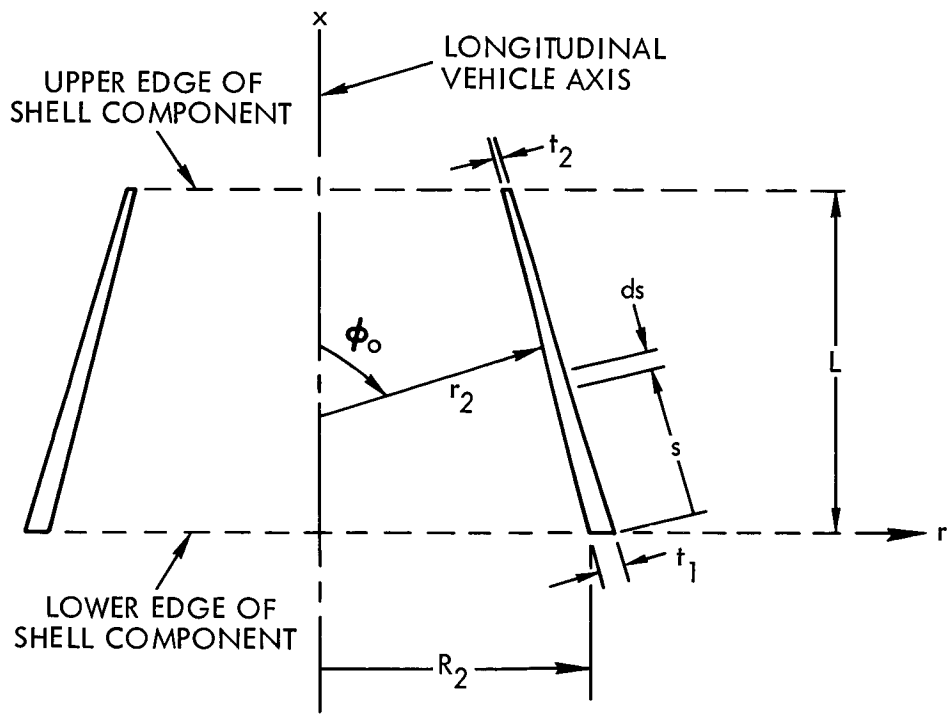
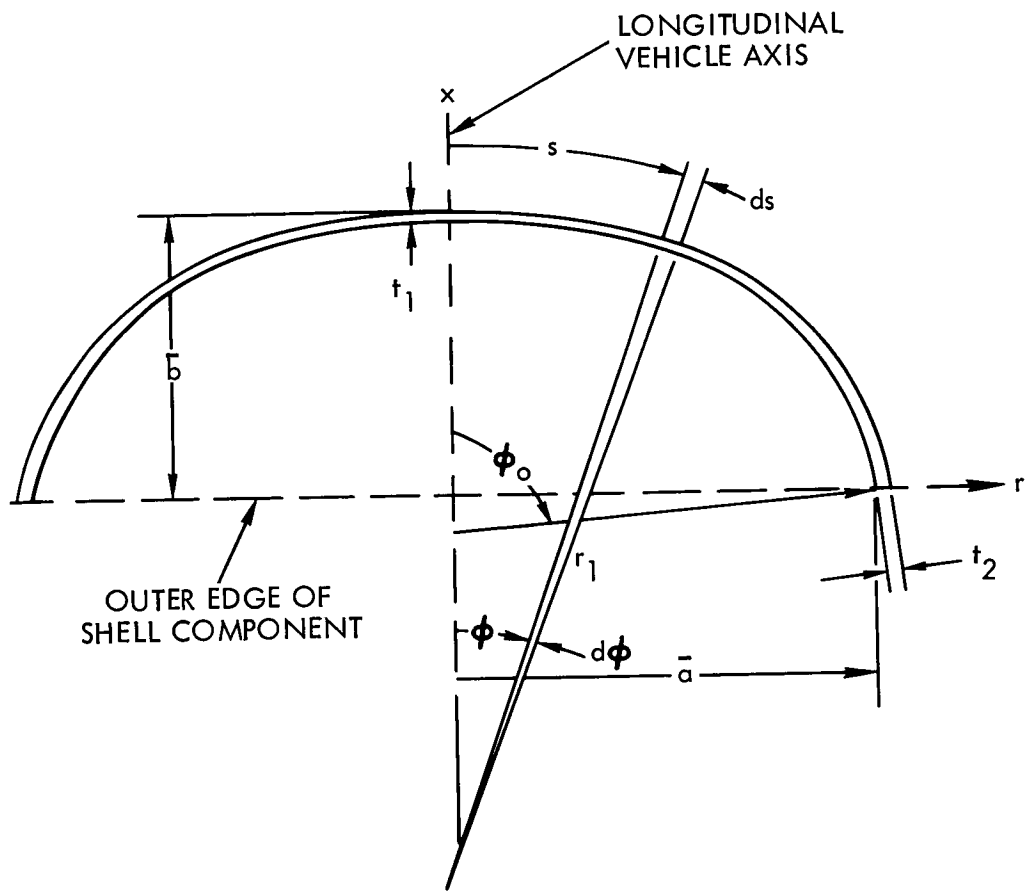


Figure 4. Displacements of Shell of Revolution



(TRANSVERSE CROSS-SECTION THROUGH LONGITUDINAL AXIS)

Figure 5. Conical Shell Component



(TRANSVERSE CROSS-SECTION THROUGH LONGITUDINAL AXIS)

Figure 6. Ellipsoidal Bulkhead Component

#### 4. FLUID COMPONENT MASS MATRIX

In addition to the mass and stiffness matrices for the shell components, the inertial effects due to the presence of liquid propellants in the vehicle fuel tanks must be considered. The linear analytical model does not include, however, the effective fluid stiffness caused by changes in the fluid head during shell distortions as this is a higher order nonlinear effect.

The general fluid component  $b$  is enclosed by three shell components, consisting of conical and ellipsoidal shells of revolution. The specific tank configurations which are included in the present model have been illustrated in Figure 3. For a typical fluid component, as shown in Figure 7, the tank is divided into three shells in which the upper bulkhead is referred to as shell  $a_1$ , the tank wall as shell  $a_2$ , and the lower bulkhead as shell  $a_3$ .

The fluid motions are a function of the generalized displacements for shell components,  $a_1$ ,  $a_2$  and  $a_3$ . For the  $u_k(\xi)$  or  $v_l(\xi)$  of each shell element defined by Equation (3.2), there is an associated fluid motion  $\hat{u}_m(x)$  and  $\hat{v}_m(x, \hat{r})$ , where  $1 \leq m \leq \bar{W}$  and  $\bar{W} = (\bar{U} + \bar{V})_{a_1} + (\bar{U} + \bar{V})_{a_2} + (\bar{U} + \bar{V})_{a_3}$ .  $\hat{u}_m(x)$  is the fluid displacement parallel to the  $x$ -axis (longitudinal axis of the vehicle) associated with the tank shell generalized displacement  $m$ .  $\hat{v}_m(x, \hat{r})$  is the fluid displacement parallel to the  $r$ -axis (radial axis of the vehicle) associated with the tank shell generalized displacement  $m$ .

The general form of the fluid mass matrix consistent with the fluid displacement may be expressed as<sup>3</sup>

$$[\bar{M}_b]_{(\bar{W} \times \bar{W})} = 2\pi\gamma_b \int_{-\bar{H}_3}^H \int_0^{\hat{r}} \left( \{\hat{u}(x)\} \{\hat{u}(x)\}^T + \{\hat{v}(x, \hat{r})\} \{\hat{v}(x, \hat{r})\}^T \right) d\hat{r} dx \quad (4.1)$$

where

$$\{\hat{u}(x)\} \equiv \begin{Bmatrix} \hat{u}_1(x) \\ \vdots \\ \hat{u}_{\bar{W}}(x) \end{Bmatrix}, \quad \{\hat{v}(x, \hat{r})\} \equiv \begin{Bmatrix} \hat{v}_1(x, \hat{r}) \\ \vdots \\ \hat{v}_{\bar{W}}(x, \hat{r}) \end{Bmatrix} \quad (4.2)$$

$\gamma_b$  is the fluid mass density and matrix  $[\bar{M}_b]$  is of order  $\bar{W}$ .



The fluid motion  $\hat{u}_m(x)$  is assumed independent of location  $\hat{r}$  and is obtained by treating the fluid as incompressible and inviscid. From these assumptions,  $\hat{u}_m(x)$  is equal to the change in volume below a given location  $x$  divided by the corresponding tank cross sectional area. Thus (see Figure 7),

$$\{\hat{u}(x)\} = -\frac{2}{r^2} \int_{-\bar{H}_3}^x r \left( \cot \phi \{ \overline{u(\xi)} \}_b + \{ \overline{v(\xi)} \}_b \right) dx \quad (4.3)$$

where

$$\{ \overline{u(\xi)} \}_b = \begin{Bmatrix} u_1(\xi) \\ \vdots \\ u_{\bar{U}_1}(\xi) \\ \text{---} \\ 0_1 \\ \vdots \\ 0_{\bar{V}_1} \\ \text{---} \\ u_1(\xi) \\ \vdots \\ u_{\bar{U}_2}(\xi) \\ \text{---} \\ 0_1 \\ \vdots \\ 0_{\bar{V}_2} \\ \text{---} \\ u_1(\xi) \\ \vdots \\ u_{\bar{U}_3}(\xi) \\ \text{---} \\ 0_1 \\ \vdots \\ 0_{\bar{V}_3} \end{Bmatrix} \quad \text{and} \quad \{ \overline{v(\xi)} \}_b = \begin{Bmatrix} 0_1 \\ \vdots \\ 0_{\bar{U}_1} \\ \text{---} \\ v_1(\xi) \\ \vdots \\ v_{\bar{V}_1}(\xi) \\ \text{---} \\ 0_1 \\ \vdots \\ 0_{\bar{U}_2} \\ \text{---} \\ v_1(\xi) \\ \vdots \\ v_{\bar{V}_2}(\xi) \\ \text{---} \\ 0_1 \\ \vdots \\ 0_{\bar{U}_3} \\ \text{---} \\ v_1(\xi) \\ \vdots \\ v_{\bar{V}_3}(\xi) \end{Bmatrix} \quad (4.4)$$

$(\bar{W} \times 1)$    $(\bar{W} \times 1)$

Fluid sloshing motions which disturb the planar character of the assumed longitudinal motion are beyond the scope of this treatment, but may be superimposed as generalized sloshing modes independent of the shell distortions. Consistent with the assumed longitudinal fluid motion  $\hat{u}_k(x)$  and the axisymmetric nature of the linear model, the radial fluid motion  $\hat{v}_k(x, \hat{r})$  varies linearly with space coordinate  $\hat{r}$ . At a particular longitudinal location  $x$ , the radial fluid motion is a function of the radial motion of the adjacent tank shell boundary and of the longitudinal fluid motion. Thus

$$\{\hat{v}(x, \hat{r})\} = \frac{\hat{r}}{r} \left( \cot \phi \{u(\xi)\}_b + \{v(\xi)\}_b - \cot \phi \{\hat{u}(x)\} \right) \quad (4.5)$$

Upon substituting Equations (4.3) and (4.5) into (4.1) and integrating with respect to  $r$ , one obtains

$$[\bar{M}_b] = \pi \gamma_b \int_{-\bar{H}_3}^H \left( \frac{4}{r^2} \left\{ \frac{r^2}{2} \hat{u}(x) \right\} \left\{ \frac{r^2}{2} \hat{u}(x) \right\}^T + \frac{1}{2} \{r\hat{v}(x, r)\} \{r\hat{v}(x, r)\}^T \right) dx \quad (4.6)$$

where

$$\left\{ \frac{r^2}{2} \hat{u}(x) \right\} = - \int_{-\bar{H}_3}^x r \left( \cot \phi \{u(\xi)\}_b + \{v(\xi)\}_b \right) dx$$

and

$$\{r\hat{v}(x, r)\} = r \cot \phi \{u(\xi)\}_b + r\{v(\xi)\}_b - r \cot \phi \{\hat{u}(x)\} \quad (4.7)$$

The detailed expressions developed for evaluating Equation (4.6) for various cases are summarized in Appendix C.

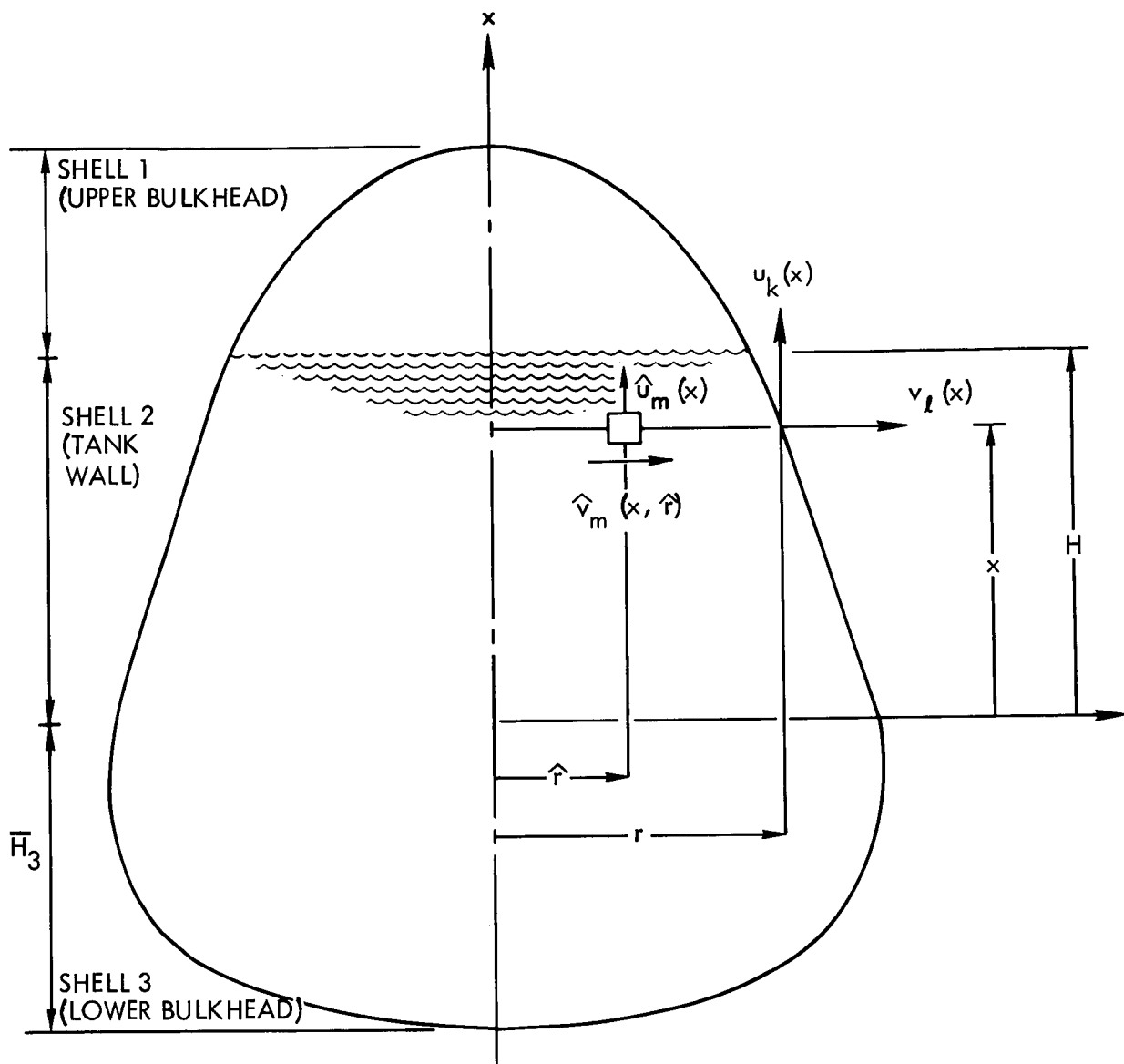


Figure 7. Definition of Fluid Motions

## 5. LAUNCH VEHICLE COORDINATE SYSTEMS

### 5.1 LOCAL COORDINATE DISTORTIONS

The matrices for the shell and fluid components are derived in Sections 3 and 4, respectively, using a system of generalized coordinate displacements (local coordinates), as given by Equations (3.1) and (3.2) to describe the shell distortion. These equations may be written in matrix notation in the following form:

$$u(\xi) = [\bar{a}_k] [A] \{\xi\} = [\xi] [A]^T \{\bar{a}_k\} \quad (5.1)$$

and

$$v(\xi) = [\bar{\beta}_l] [B] \{\xi\} = [\xi] [B]^T \{\bar{\beta}_l\} \quad (5.2)$$

where

$$\begin{aligned} [\bar{a}_k] &= [\bar{a}_1 \cdot \cdot \cdot \bar{a}_{\bar{U}}] \\ [\bar{\beta}_l] &= [\bar{\beta}_1 \cdot \cdot \cdot \bar{\beta}_{\bar{V}}] \\ [\xi] &= [1(\xi)(\xi)^2 \cdot \cdot \cdot (\xi)^{10}] \end{aligned} \quad (5.3)$$

$\bar{U}$  and  $\bar{V}$  are constants provided as input which define the number of local coordinates selected for representing shell distortions in the longitudinal and radial directions, respectively, for a particular component.

### 5.2 SYSTEM COORDINATE POINT DISPLACEMENTS

In order to work with reference to a space frame, however, it is necessary to transform the generalized coordinates to space coordinates designated as system coordinates. The system coordinates represent displacement and rotations at specific points on each shell component, connections of spring-mass components, and applications of force inputs at arbitrary stations along the vehicle.

For each shell component, system coordinates are provided to represent displacements in the longitudinal and radial directions at equally spaced intervals along the shell meridian, and tangential rotations at the edges of the shell (see Figures 8, 9 and 10). Longitudinal displacements  $\{u(\xi_i)\}$

at locations  $\xi_i = (U - i)/(U - 1)$ , where  $i = 1, 2, \dots, U$  are expressed [using Equation (5.1)] as

$$\left\{ u(\xi_i) \right\}_{(U \times 1)} = [U][A]^T \left\{ \bar{a}_k \right\} \quad (5.4)$$

where

$$[U] = \begin{bmatrix} 1_1 & \xi_1 & \dots & (\xi_1)^{10} \\ \vdots & \vdots & & \vdots \\ \vdots & \vdots & & \vdots \\ 1_U & \xi_U & \dots & (\xi_U)^{10} \end{bmatrix} \quad (5.5)$$

Longitudinal displacements  $\left\{ v(\xi_j) \right\}$  at locations  $\xi_j = (V - j)/(V - 1)$ , where  $j = 1, 2, \dots, V$ , are similarly expressed (using Equation (5.2)) as

$$\left\{ v(\xi_j) \right\}_{(V \times 1)} = [V][B]^T \left\{ \bar{\beta}_l \right\} \quad (5.6)$$

where

$$[V] = \begin{bmatrix} 1_1 & \xi_1 & \dots & (\xi_1)^{10} \\ \vdots & \vdots & & \vdots \\ \vdots & \vdots & & \vdots \\ 1_V & \xi_V & \dots & (\xi_V)^{10} \end{bmatrix} \quad (5.7)$$

The scalar quantities  $U$  and  $V$  are constants provided as input which define the number of system coordinate point displacements to be provided in the longitudinal and radial directions, respectively, for a given shell component. These are related to  $\bar{U}$  and  $\bar{V}$ , as discussed in Section 5.3. The shell rotations,  $\rho_1$  and  $\rho_2$ , are evaluated at  $\xi = 1$  and  $0$ , respectively, and by Equation (A.17) can be shown to have the following form:

$$\begin{Bmatrix} \rho_1 \\ \rho_2 \end{Bmatrix} = [D_1][A]^T \left\{ \bar{a} \right\} + [D_2][B]^T \left\{ \bar{\beta} \right\} \quad (5.8)$$

where

$$[D_1] = D_1 \begin{bmatrix} 0 & 1 & 2 & \dots & 9 & 10 \\ 0 & 1 & 0 & \dots & 0 & 0 \end{bmatrix}_{(2 \times 11)}$$

and

$$[D_2] = D_2 \begin{bmatrix} 0 & 1 & 2 & \dots & 9 & 10 \\ 0 & 1 & 0 & \dots & 0 & 0 \end{bmatrix}_{(2 \times 11)} \quad (5.9)$$

$$D_1 = \frac{\cos \phi_o \sin \phi_o}{L} \text{ for conical frustums}$$

$$\frac{\cos \phi_o}{(r_1)_o \phi_o} \text{ for convex upward ellipsoidal bulkheads, and}$$

$$\frac{\cos \phi_o}{(r_1)_o (\phi_o - \pi)} \text{ for convex downward ellipsoidal bulkheads}$$

$$D_2 = \frac{\sin^2 \phi_o}{L} \text{ for conical frustums,}$$

$$\frac{\sin \phi_o}{(r_1)_o \phi_o} \text{ for convex upward ellipsoidal bulkheads, and}$$

$$\frac{\sin \phi_o}{(r_1)_o (\phi_o - \pi)} \text{ for convex downward ellipsoidal bulkheads.}$$

where  $(r_1)_o$  is  $r_1$  evaluated at  $\phi = \phi_o$

The total vector of system coordinates displacements for shell component "a" is defined from Equations (5.4), 5.6) and 5.8) as

$$\{a_a\}_{(\bar{U}+\bar{V}) \times 1} = \begin{Bmatrix} u(\xi_i) \\ v(\xi_j) \\ \rho_1 \\ \rho_2 \end{Bmatrix} \quad (5.10)$$

As indicated in Figures 8, 9 and 10, each displacement and rotation coordinate is identified by a number  $C$  where  $1 \leq C \leq N_C$  and  $N_C$  is defined as the total number of system coordinates used in the vehicle model. The identification numbers  $C$  may be arbitrarily specified on the vehicle independent of location and, hence, must be identified with the vector  $\{a_a\}$  components in the input data. For this purpose, a vector  $\{C_a\}$  is provided for each shell component  $a$  with the identification numbers illustrated in Figures 8, 9 and 10 arranged consistent with Equations (5.4), (5.6) and (5.10). Thus, in general,

$$\{C_a\} = \begin{Bmatrix} C_1 \\ \vdots \\ C_U \\ C_{U+1} \\ \vdots \\ C_{U+V} \\ C_{\rho_1} \\ C_{\rho_2} \end{Bmatrix} \quad (5.11)$$

For ellipsoidal bulkhead components, vector elements  $C_{U+V}$  and  $C_{\rho_2}$  are omitted.

### 5.3 LOCAL TO SYSTEM COORDINATE TRANSFORMATION FOR SHELL COMPONENT

The local coordinate displacements for shell component "a" are related to the system coordinate displacements by the transformation  $[T_a]$  as follows:

Consolidating the arrangement of local coordinate displacements, as defined in Equations (5.1), (5.2) and (5.3), let

$$\{\bar{a}_a\}_{(\bar{U}+\bar{V}) \times 1} = \begin{Bmatrix} \bar{a}_k \\ \bar{\beta}_l \end{Bmatrix} \quad (5.12)$$

Consistent with the system coordinate displacement vector  $\{a_a\}$  given by Equations (5.4), (5.6) and (5.8), the transformation matrix  $[T_a]$  which relates local to system coordinates, is defined by the equation

$$\{a_a\} = [T_a]^{-1} \{\bar{a}_a\} \quad (5.13)$$

where, in general,

$$[T_a]^{-1} = \begin{bmatrix} [U] & 0 \\ 0 & [V] \\ [D_1] & [D_2] \end{bmatrix} \begin{bmatrix} [A]^T & 0 \\ 0 & [B]^T \end{bmatrix} \quad (5.14)$$

Thus

$$\{\bar{a}_a\} = [T_a] \{a_a\} \quad (5.15)$$

It is apparent that computation of the matrix  $[T_a]$  requires inversion of the matrix  $[T_a]^{-1}$ , which must therefore be nonsingular, square, and of order  $(\bar{U} + \bar{V})$ . This may require modification of the general Equation (5.14), as discussed below. Special attention must be given the scalar quantities  $U$ ,  $V$ ,  $\bar{U}$ ,  $\bar{V}$  and the matrices  $[A]$ ,  $[B]$ ,  $[D_1]$ ,  $[D_2]$  to satisfy the above conditions consistent with the shell component boundary conditions.

For ellipsoidal bulkheads, the  $[A]$  and  $[B]$  matrices are selected so that the displacement  $v(0)$  and the rotation  $\rho_2$  are equal to zero to satisfy the conditions imposed by axial symmetry. This implies that for ellipsoidal bulkheads  $U = \bar{U}$ ,  $V = \bar{V}$ , which requires that the last row of  $[V]$ ,  $[D_1]$  and  $[D_2]$  in Equation (5.14) be removed. For a conical bulkhead,  $[B]$  is selected so that  $v(0)$  is zero. This case requires that the last row of  $[V]$  be removed, and  $U + 1 = \bar{U}$ ,  $V = \bar{V}$ . For cylindrical shells,  $U = \bar{U}$ ,  $V = \bar{V} - 2$ . For other cases,  $U + V + 2 = \bar{U} + \bar{V}$  is a necessary condition. The following example matrices fulfill the above requirements.



For nonbulkhead components:

$$\begin{aligned}
 [A]_{(\bar{U}_{x11})} = & \begin{bmatrix} 1 & 0 & 0 & 0 & 0 & 0 & 0 & 0 & 0 & 0 & 0 \\ 0 & 1 & 0 & 0 & . & . & . & . & . & . & . \\ 0 & 0 & 1 & 0 & . & . & . & . & . & . & . \\ 0 & 0 & 0 & 1 & . & . & . & . & . & . & 0 \end{bmatrix} & (5.16) \\
 & \text{(Illustrated for } \bar{U} = 4)
 \end{aligned}$$

$$\begin{aligned}
 [B]_{(\bar{V}_{x11})} = & \begin{bmatrix} 1 & 0 & 0 & . & . & . & . & . & . & . & 0 \\ 0 & 1 & 0 & 0 & . & . & . & . & . & . & . \\ 0 & 0 & 1 & 0 & 0 & . & . & . & . & . & . \\ 0 & 0 & 0 & 1 & 0 & 0 & . & . & . & . & . \\ 0 & 0 & 0 & 0 & 1 & 0 & . & . & . & . & . \\ 0 & 0 & 0 & 0 & 0 & 1 & 0 & . & . & . & . \end{bmatrix} & (5.17) \\
 & \text{(Illustrated for } \bar{V} = 6)
 \end{aligned}$$

For ellipsoidal bulkhead components:

$$\begin{aligned}
 [A]_{(\bar{U}_{x11})} = & \begin{bmatrix} 1 & 0 & 0 & . & . & . & . & . & . & . & 0 \\ 0 & 0 & 1 & 0 & . & . & . & . & . & . & 0 \\ 0 & 0 & 0 & 1 & . & . & . & . & . & . & . \\ 0 & 0 & 0 & 0 & 1 & . & . & . & . & . & 0 \end{bmatrix} & (5.18) \\
 & \text{(Illustrated for } \bar{U} = 4)
 \end{aligned}$$

$$\begin{aligned}
 [B]_{(\bar{V}_{x11})} = & \begin{bmatrix} 0 & 1 & 0 & 0 & . & . & . & . & . & . & 0 \\ 0 & 0 & 1 & 0 & . & . & . & . & . & . & . \\ 0 & 0 & 0 & 1 & 0 & . & . & . & . & . & . \\ 0 & 0 & 0 & 0 & 1 & . & . & . & . & . & 0 \end{bmatrix} & (5.19) \\
 & \text{(Illustrated for } \bar{V} = 4)
 \end{aligned}$$

For the simple unit diagonal  $[A]$  and  $[B]$  matrices illustrated, the matrix  $[T_a]^{-1}$  may be poorly conditioned and difficult to invert accurately if  $\bar{U}$  and/or  $\bar{V}$  are equal to or greater than six (6). For these cases it is recommended that Shifted Chebyshev Polynomial Coefficients<sup>10</sup> (see Table 1) be used for the  $[A]$  and  $[B]$  matrices to improve the accuracy of the matrix  $[T_a]$  calculation. Using Table 1, Equations (5.16), (5.17), (5.18) and (5.19) become, respectively,

For nonbulkhead components:

$$[A]_{(\bar{U} \times 11)} = \begin{bmatrix} 1 & 0 & 0 & 0 & 0 & 0 & 0 & 0 & 0 & 0 & 0 \\ -1 & 2 & 0 & 0 & . & . & . & . & . & . & . \\ 1 & -8 & 8 & 0 & . & . & . & . & . & . & . \\ -1 & 18 & -48 & 32 & . & . & . & . & . & . & 0 \end{bmatrix} \quad (5.20)$$

(Illustrated for  $\bar{U} = 4$ )

$$[B]_{(\bar{V} \times 11)} = \begin{bmatrix} 1 & 0 & 0 & . & . & . & . & . & . & . & 0 \\ -1 & 2 & 0 & 0 & . & . & . & . & . & . & . \\ 1 & -8 & 8 & 0 & 0 & . & . & . & . & . & . \\ -1 & 18 & -48 & 32 & 0 & 0 & . & . & . & . & . \\ 1 & -32 & 160 & -256 & 128 & 0 & . & . & . & . & . \\ -1 & 50 & -400 & 1120 & -1280 & 512 & 0 & . & . & . & . \end{bmatrix} \quad (5.21)$$

(Illustrated for  $\bar{V} = 6$ )

For ellipsoidal bulkhead components:

$$[A]_{(\bar{U} \times 11)} = \begin{bmatrix} 1 & 0 & 0 & . & . & . & . & . & . & . & 0 \\ 1 & 0 & 8 & 0 & . & . & . & . & . & . & 0 \\ -1 & 0 & -48 & 32 & 0 & . & . & . & . & . & . \\ 1 & 0 & 160 & -256 & 128 & . & . & . & . & . & 0 \end{bmatrix} \quad (5.22)$$

(Illustrated for  $\bar{U} = 4$ )

$$\left[ B \right]_{(\bar{V} \times 11)} = \begin{bmatrix} 0 & 2 & 0 & 0 & . & . & . & . & . & . & 0 \\ 0 & -8 & 8 & 0 & . & . & . & . & . & . & . \\ 0 & 18 & -48 & 32 & 0 & . & . & . & . & . & . \\ 0 & -32 & 160 & -256 & 128 & . & . & . & . & . & 0 \end{bmatrix} \quad (5.23)$$

(Illustrated for  $\bar{V} = 4$ )

#### 5.4 LOCAL TO SYSTEM COORDINATE TRANSFORMATION FOR FLUID COMPONENT

As illustrated in Figure 7, and discussed in Section 4, the distortion of each fluid component "b" is a function of the distortion of the three enclosing shell components a1, a2 and a3. The local to system coordinate transformation matrix  $\left[ T_b \right]$  for the fluid component is thus obtained as a combination of the shell component transformations  $\left[ T_a \right]$  for a = a1, a2 and a3, as follows:

Consolidating the arrangement of local coordinate displacements, as defined by Equations (4.4) and (5.12), let

$$\left\{ \bar{a}_b \right\} = \left\{ \begin{array}{l} \left\{ \bar{a}_{a1} \right\} \\ \left\{ \bar{a}_{a2} \right\} \\ \left\{ \bar{a}_{a3} \right\} \end{array} \right\} \quad (5.24)$$

Consistent with Equation (5.10), let the consolidated vector of system coordinate displacements be

$$\left\{ a_b \right\} = \left\{ \begin{array}{l} \left\{ a_{a1} \right\} \\ \left\{ a_{a2} \right\} \\ \left\{ a_{a3} \right\} \end{array} \right\} \quad (5.25)$$

Corresponding to Equations (5.15), (5.24) and (5.25), the transformation matrix  $[T_b]$  is defined by

$$\{\bar{a}_b\} = [T_b] \{a_b\} \quad (5.26)$$

where

$$[T_b] = \left( \begin{array}{c|c|c} [T_{a1}] & 0 & 0 \\ \hline 0 & [T_{a2}] & 0 \\ \hline 0 & 0 & [T_{a3}] \end{array} \right)_{(\bar{W} \times \bar{W})} \quad (5.27)$$

From Equations (5.10) and (5.25), it is noted that the coordinate identification vector for fluid component b is obtained as a combination of the shell coordinate identification vectors  $\{C_a\}$ , defined in Equation (5.11), for  $a = a1, a2$  and  $a3$ , as follows:

$$\{C_b\} = \left\{ \begin{array}{c} \{C_{a1}\} \\ \{C_{a2}\} \\ \{C_{a3}\} \end{array} \right\} \quad (5.28)$$

Table 1. Shifted Chebyshev Polynomial Coefficients for Use in Constructing Matrices [A] and [B]

1	0	0	0	0	0	0	0	0	0	0	0	0	0	0	0	0	0	0	0	0	0	0	0	0	0		
-1	2	0	0	0	0	0	0	0	0	0	0	0	0	0	0	0	0	0	0	0	0	0	0	0	0	0	
1	-8	8	0	0	0	0	0	0	0	0	0	0	0	0	0	0	0	0	0	0	0	0	0	0	0	0	0
-1	18	-48	32	0	0	0	0	0	0	0	0	0	0	0	0	0	0	0	0	0	0	0	0	0	0	0	0
1	-32	160	-256	128	0	0	0	0	0	0	0	0	0	0	0	0	0	0	0	0	0	0	0	0	0	0	0
-1	50	-400	1120	-1280	512	0	0	0	0	0	0	0	0	0	0	0	0	0	0	0	0	0	0	0	0	0	0
1	-72	840	-3584	6192	-6144	2048	0	0	0	0	0	0	0	0	0	0	0	0	0	0	0	0	0	0	0	0	0
-1	98	-1568	9408	-26880	39424	-28672	8192	0	0	0	0	0	0	0	0	0	0	0	0	0	0	0	0	0	0	0	0
1	-128	2688	-21504	84480	-180224	212992	-131072	32768	0	0	0	0	0	0	0	0	0	0	0	0	0	0	0	0	0	0	0
-1	162	-4320	44352	-228096	658944	-1118208	1105920	-589824	131072	0	0	0	0	0	0	0	0	0	0	0	0	0	0	0	0	0	0
1	-200	6600	-84880	549120	-2050048	4659200	-6553600	5570560	-2621440	524288	0	0	0	0	0	0	0	0	0	0	0	0	0	0	0	0	0

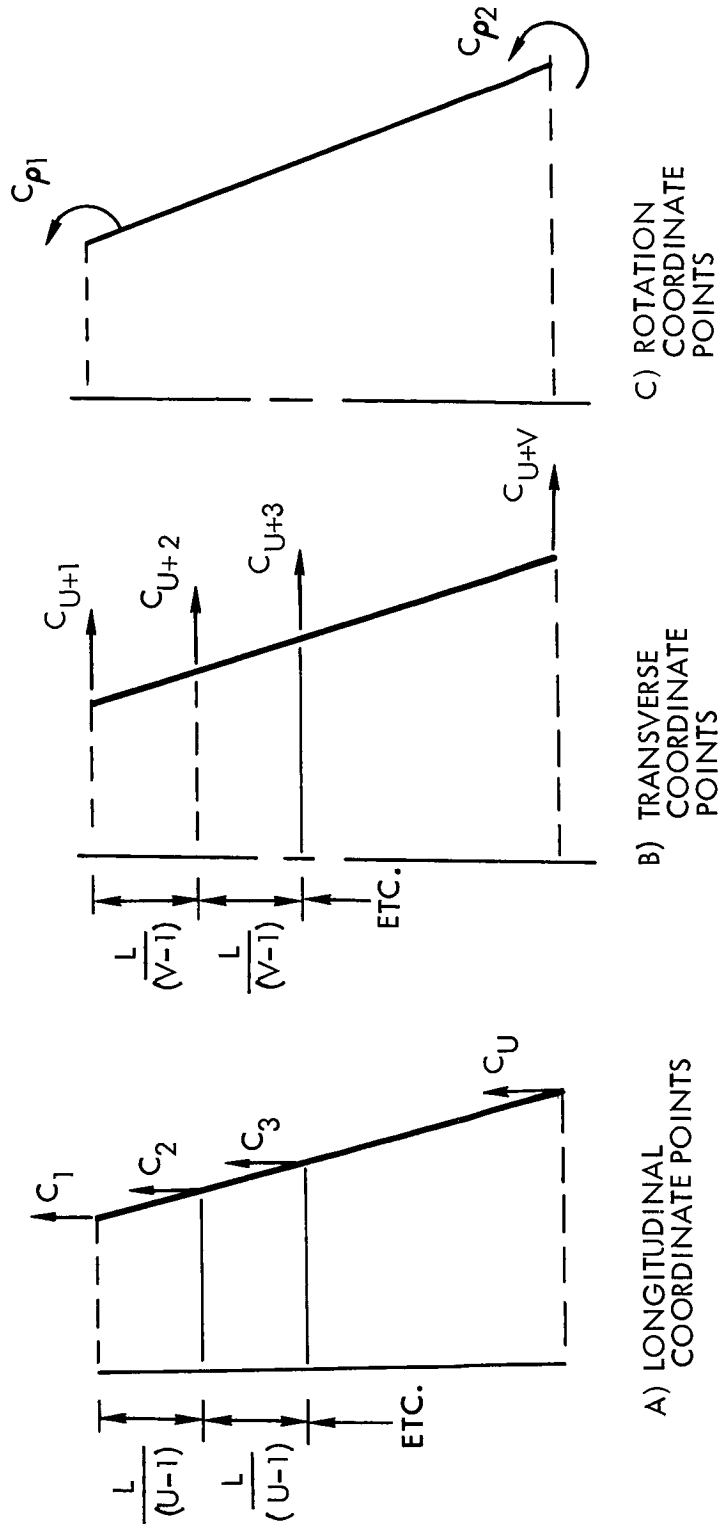


Figure 8. Conical Shell Component System Coordinate Arrangement

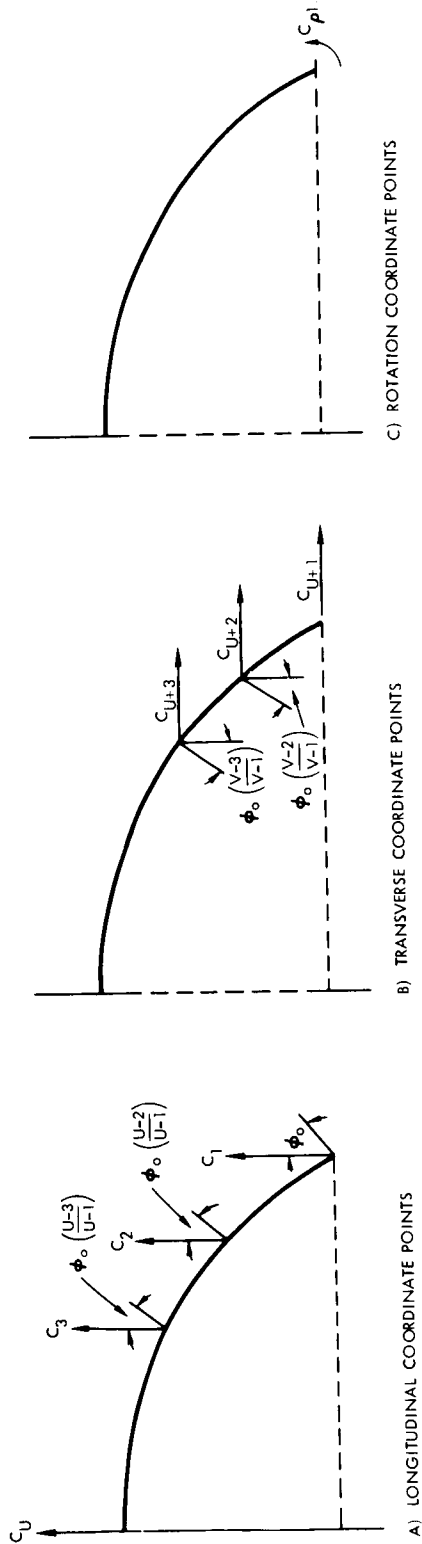


Figure 9. Convex Upward Ellipsoidal Shell, Component System Coordinate Arrangement

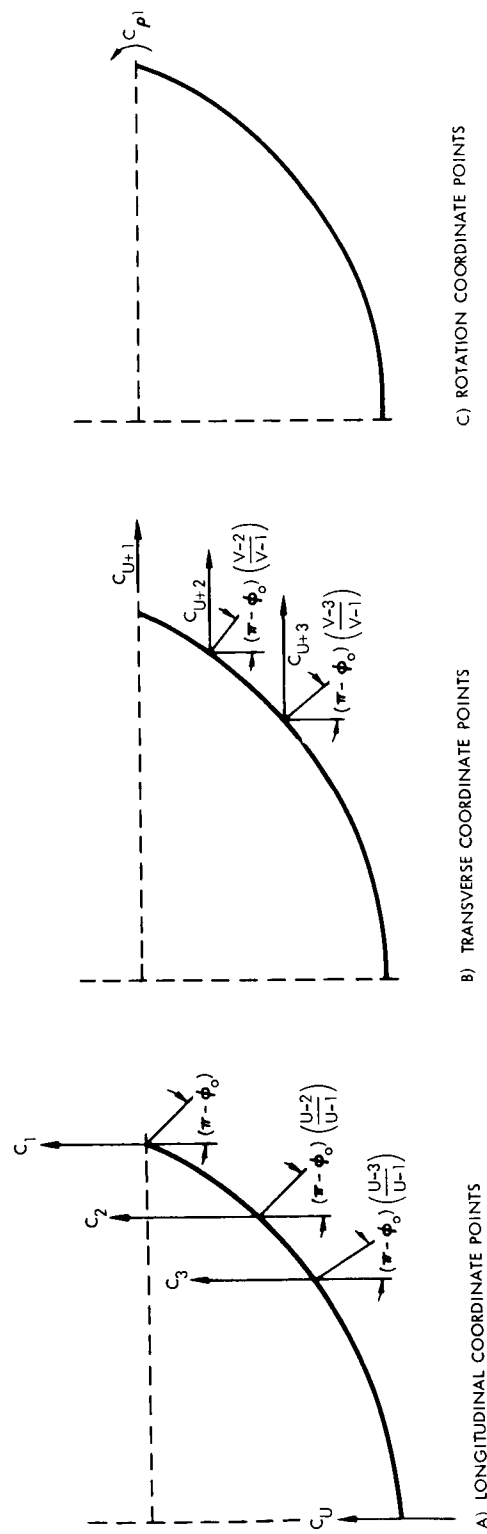


Figure 10. Convex Downward Ellipsoidal Shell, Component System Coordinate Arrangement

## 6. LAUNCH VEHICLE STIFFNESS AND MASS MATRIX SYNTHESIS

In order to construct the total vehicle stiffness and mass matrices referenced to a common coordinate system, the individual component stiffness and mass matrices are expressed in terms of the system coordinates developed in Section 5.2. For each shell and fluid component  $e$ , the matrices, transformed<sup>4</sup> to system coordinates, become

$$\left[ K_e \right] = \left[ T_e \right]^T \left[ \bar{K}_e \right] \left[ T_e \right]$$

and

$$\left[ M_e \right] = \left[ T_e \right]^T \left[ \bar{M}_e \right] \left[ T_e \right]$$

(6.1)

where  $\left[ T_e \right]$  is the transformation matrix defined in Equation (5.13) for shell components and in Equation (5.26) for fluid components.  $\left[ \bar{K}_e \right]$  and  $\left[ \bar{M}_e \right]$  are the stiffness and mass matrices related to the local coordinate system. The stiffness and mass matrices for the spring mass components do not undergo the transformation Equation (6.1), since they already exist as input data in terms of the system coordinate displacements.

The total system stiffness and mass matrices are synthesized by expanding each of the component matrices Equation (6.1) into an enlarged matrix which is of the same order as the total system matrix and which is related to the set of system coordinates for the total vehicle, as shown in Figure 11. This is accomplished by superimposing each of the component matrices after an additional transformation, as described below.

As indicated in Figures 8, 9, 10 and 11 and discussed in Section 5.2, each system displacement and rotation coordinate is defined by an identification number  $C$  ( $C = 1, 2, \dots, N_c$ ) arbitrarily specified to suit the convenience of the analyst. It is desirable, however, to reserve the identification numbers  $(N_c)$ ,  $(N_c - 1)$ ,  $\dots$ ,  $(N_c - N_o + 1)$  for the  $N_o$  system coordinates to be used for rigid supports to preserve a one-to-one correspondence in the digital program output between the identification numbers and the coordinate row-column location in the total system matrices.



The arrangement of the coordinates in the total system displacement vector  $\{a\}$  of order  $N_C$  is made to coincide with the coordinate identification numbers  $C$ . Thus, the transformation matrix  $[\Delta_e]$  relating the total system displacements  $\{a\}$  to the component  $e$  system displacements  $\{a_e\}$  is defined as

$$\{a_e\} = [\Delta_e] \{a\} . \quad (6.2)$$

The elements  $\delta_{rs}$  of  $[\Delta_e]$  are determined to be zero or unity from the relations

$$\begin{aligned} \delta_{rs} &= 1 \text{ when } s = C_r \\ &= 0 \text{ when } s \neq C_r \end{aligned} \quad (6.3)$$

where  $C_r$  is the  $r$ -th element of the coordinate identification vector  $\{C_e\}$  for component  $e$  [see Equations (5.11) and 5.28)].

The total stiffness and mass matrices are obtained using transformation matrices  $[\Delta_e]$  in the following summation equations

$$[K]_{(N_C \times N_C)} = \sum_{a=1}^{N_S} [\Delta_a]^T [K_a] [\Delta_a] + \sum_{c=1}^{N_M} [\Delta_c]^T [K_c] [\Delta_c] \quad (6.4)$$

and

$$\begin{aligned} [M]_{(N_C \times N_C)} &= \sum_{a=1}^{N_S} [\Delta_a]^T [M_a] [\Delta_a] + \sum_{b=1}^{N_F} [\Delta_b]^T [M_b] [\Delta_b] \\ &+ \sum_{c=1}^{N_M} [\Delta_c]^T [M_c] [\Delta_c] \end{aligned} \quad (6.5)$$

in which  $N_C$ ,  $N_S$ ,  $N_F$  and  $N_M$  are the total number of system coordinates, shell components, fluid components and spring-mass components, respectively. The matrices  $[K_a]$ ,  $[M_a]$  and  $[M_b]$  are, respectively, the stiffness and mass matrices for the shell components and the mass matrix for the fluid components, as defined by Equation (6.1).

The superposition technique assures displacement compatibility and force equilibrium at the joints between components. Displacement boundary conditions are imposed on the total stiffness and mass matrix by removing appropriate rows and columns of coefficients corresponding to points on the vehicle and its support which are rigidly restrained from motion. Due to storage limitations in the digital program, the order of the resulting total stiffness and mass matrix must not exceed 80.

Additional limitations are placed on the size of the component matrices utilized in Equations (6.4) and (6.5). The shell component stiffness and mass matrices,  $[K_a]$  and  $[M_a]$ , must have an order no larger than 22. For the fluid mass matrix,  $[M_b]$ , the order must not exceed 35, and for the spring-mass component stiffness and mass matrices,  $[K_c]$  and  $[M_c]$ , the order must not exceed 10.

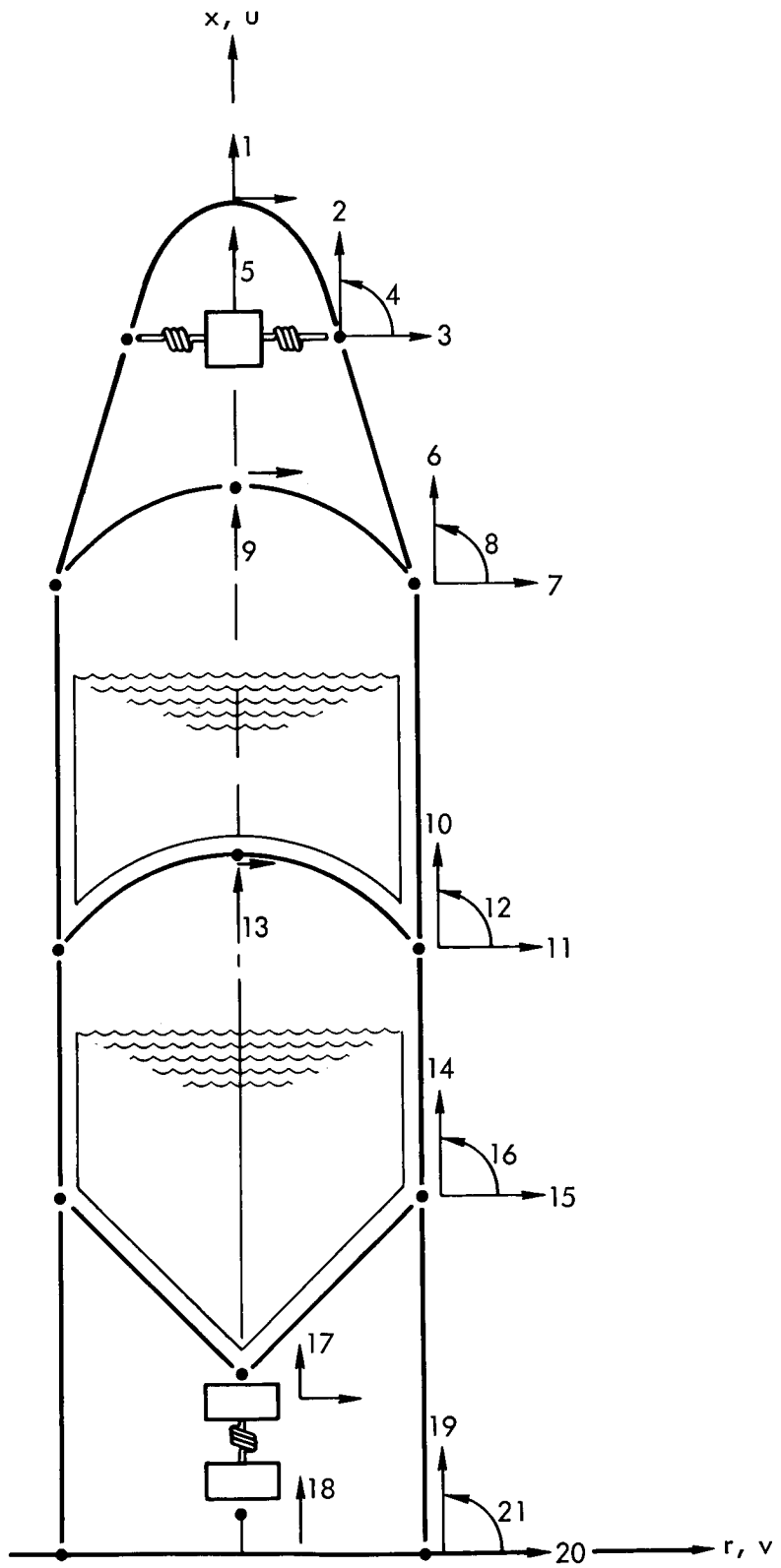


Figure 11. Vehicle System Coordinates

## 7. DYNAMIC RESPONSE EQUATIONS

### 7.1 NATURAL FREQUENCY EQUATIONS

The total stiffness and mass matrices which are derived in Section 6 are used for computation of the natural frequencies and mode shapes from the eigenvalue equation

$$[K] \{a\} - p^2 [M] \{a\} = 0 \quad (7.1)$$

in which  $p$  is the circular frequency of the launch vehicle and  $\{a\}$  is the modal vector whose elements are the longitudinal, radial and rotational system coordinate displacements defined in Section 5 and illustration in Figure 11. This equation is solved to obtain the natural frequencies  $p_t$  and the mode shapes for all modes,  $t$ , which are arranged in a square modal matrix  $\{a\}$  of order  $N_c - N_o$ . Each column,  $\{a_t\}$ , of  $\{a\}$ , is the mode  $t$  displacement vector with system coordinate elements, whereas each row,  $[a_s]$ , of  $\{a\}$ , is the system coordinate  $s$  displacement vector with natural mode elements.

### 7.2 STEADY-STATE RESPONSE EQUATIONS

The steady-state response due to simple harmonic loads of frequency  $\omega$  is determined using a standard modal technique. The elements of the load vector  $\{P\}$  of order  $(N_c - N_o)$  represent axisymmetric forces (longitudinal and radial) or moments, depending on whether the associated coordinate is a displacement or a rotation. The displacement response  $\{R\}$  at coordinates  $s$  ( $s = 1, 2, \dots, (N_c - N_o)$ ) on the launch vehicle is expressed as the linear superposition of the individual modal responses based on an assumed modal damping factor  $\eta_k$  which is the ratio of the actual damping to the critical damping for each mode and has the form<sup>4</sup>

$$\{R\} = \left\{ \bar{R} \sin \{\omega t - \bar{\delta}\} \right\}$$

where

$$\left\{ \bar{R}^2 \right\} = \left( [a] \left\{ \frac{Q_t \sin \delta_t}{m_t (p_t^2 z_t)} \right\} \right)^2 + \left( [a] \left\{ \frac{Q_t \cos \delta_t}{m_t (p_t^2 z_t)} \right\} \right)^2 \quad (7.2)$$

$$\{\bar{\delta}\} = \left\{ \tan^{-1} \frac{\left[ \begin{array}{c} \{a_s\} \\ \left\{ \frac{Q_t \sin \delta_t}{m_t (p_t^2 z_t)} \right\} \end{array} \right]}{\left[ \begin{array}{c} \{a_s\} \\ \left\{ \frac{Q_t \cos \delta_t}{m_t (p_t^2 z_t)} \right\} \end{array} \right]} \right\} \quad (7.3)$$

$$Q_t = \{a_t\}^T \{P\}$$

$$m_t = \{a_t\}^T [M] \{a_t\}$$

$$p_t^2 z_t = \left[ \left( p_t^2 - \omega^2 \right)^2 + 4 p_t^2 \eta_t^2 \omega^2 \right]^{1/2} \quad (7.4)$$

and

$$\delta_t = \tan^{-1} \frac{2 \eta_t \left( \frac{p_t}{\omega} \right)}{\left( \frac{p_t}{\omega} \right)^2 - 1}$$

In these equations,  $\delta_t = \pi$  when  $p_t = 0$ , and  $\delta_t = 0$  when  $p_t \neq 0$ ,  $\omega = 0$ .  $\{\bar{R}\}$  and  $\{\bar{\delta}\}$  represent, respectively, the vectors of steady-state displacement amplitude and the phase angle by which the forcing function leads (+) or lags (-) the response. The velocity  $\{\dot{R}\}$  and acceleration  $\{\ddot{R}\}$  responses are obtained from the relations

$$\{\dot{R}\} = \omega \left\{ \bar{R} \sin \left( \omega t - \left( \frac{\pi}{2} + \bar{\delta} \right) \right) \right\} \quad (7.5)$$

$$\{\ddot{R}\} = -\omega^2 \left\{ \bar{R} \sin (\omega t - \bar{\delta}) \right\}$$

The internal forces (or moments)  $\{S_a\}$  acting at each point along the vehicle on each shell component  $a$  are obtained from the equation

$$\{S_a\}_{((\bar{U}+\bar{V}) \times 1)} = \{\bar{S} \sin (\omega t - \bar{\delta})\} \quad (7.6)$$

where

$$\begin{aligned} \{\bar{S}^2\}_{(\bar{U}+\bar{V}) \times 1} &= \left( [K_a] [\Delta_a] \langle \bar{R} \sin \bar{\delta} \rangle \right)^2 + \left( [K_a] [\Delta_a] \langle \bar{R} \cos \bar{\delta} \rangle \right)^2 \\ \{\bar{\delta}\}_{(\bar{U}+\bar{V}) \times 1} &= \left\{ \tan^{-1} \left( \frac{[K_s] [\Delta_a] \langle \bar{R} \sin \bar{\delta} \rangle}{[K_s] [\Delta_a] \langle \bar{R} \cos \bar{\delta} \rangle} \right) \right\} \end{aligned} \quad (7.7)$$

$\{\bar{S}\}$  and  $\{\bar{\delta}\}$  represent, respectively, the amplitude and phase angle of the internal forces.  $[K_s]$  is row  $s$  ( $s = 1, 2, \dots, (\bar{U} + \bar{V})_a$ ) of the shell element stiffness matrix  $[K_a]$ .  $\langle \bar{R} \rangle$  and  $\langle \bar{\delta} \rangle$  are obtained from Equation (7.3).

## 8. DIGITAL PROGRAM ARRANGEMENT

The analytic model developed in the previous sections is used as the basis for a digital computer program to determine the vibration characteristics and steady-state response of a launch vehicle subjected to axisymmetric sinusoidal loads. The program is written in Fortran IV language for use on an IBM 7094 computer having 32K magnetic core storage locations. The functional operations and the overall program arrangement are illustrated in Figure 12. Each of the operations enclosed by a block represents an independent link in the computer program. This feature facilitates the task of making future modifications or expansions of the program.

The input data necessary to initiate the program sequence is discussed in detail in Section 9. After the data has been processed, the program proceeds to develop the stiffness and mass matrices for each of the shell components. The functional operations required to perform these computations and the form of the equations used in the digital program are provided in Appendix D. Consistent with the matrix formulation of the basic equations, the numerical integration is performed using a sixteen point Gaussian<sup>5</sup> weighted matrix integration scheme.

In a similar fashion, the fluid mass matrix for each fluid component is constructed. The functional flow diagram and the basic equations required to describe the three fluid tank configurations considered in the present analytical model are presented in detail in Appendix E. Unlike the formulation for the shell stiffness and mass matrices, the equations for the fluid mass matrix involve a double integration. For this computation, a double Lagrangian<sup>6</sup> weighted matrix integration scheme was found most suitable. This technique employs two 11-point Lagrangian weighting matrices in sequence to provide a 22 point approximation.

The component matrix construction is concluded with the setting up of the stiffness and mass matrices, provided as input data, of the spring-mass components.

The shell, fluid and spring-mass component stiffness and mass matrices are then synthesized into a total vehicle system stiffness and mass matrix, according to the steps presented in Section 6. Utilizing these matrices, the natural frequency equation, Equation (7.1), is formulated and subsequently solved using a standard digital eigenvalue routine which solves matrices up to order 80.

The program user now has the option of 1) continue the analysis and move directly to the computation of the steady-state response, or 2) to temporarily stop the solution after the free vibrations stage for the purpose of examining the output before proceeding with the computation of the steady-state response. This option enables the user to examine the results of the computation for the natural frequencies and mode shapes before determining the input for the modal damping and for the frequencies at which the launch vehicle is forced.

Checks on the accuracy and consistency of the various computations are performed throughout the program. The shell component stiffness matrices are subjected to longitudinal rigid body displacements to establish automatically that equilibrium is satisfied. For each shell component, the "equilibrium check" appears as output in the following form

$$\text{Equilibrium Check} = \frac{\sum \text{Longitudinal Rigid Body Displacement Forces}}{\sum_{i=1}^U k_{ii}} \quad (8.1)$$

where  $k_{ii}$  are the diagonal components of the shell component stiffness matrix  $[K_a]$  associated with the system coordinates and  $U$  is defined in Section 5.2 as the total number of longitudinal system coordinates associated with component  $a$ . If equilibrium is satisfied, Equation (8.1) will be equal to zero.

In a similar manner, the mass matrices for the shell and fluid components are subjected to unit accelerations to verify that the rigid body mass characteristics have been accurately represented. The "mass check" also appears as output and has the form

$$\text{Mass Check} = \frac{M_{\text{input}}}{M_{\text{computed}}} \quad (8.2)$$



where  $M_{\text{input}}$  is the total mass of the element, provided as input, and  $M_{\text{computed}}$  is the rigid body mass computed in the program. The elements of the mass matrix  $[M_e]$  are corrected by the "mass check" factor to provide the correct total mass representation for the structural component  $e$ , since  $M_{\text{computed}}$ , in general, will not agree with  $M_{\text{input}}$  due to the physical nature of the problem.

An additional check on the accuracy of the program is provided in the form of a  $[T_a]$  "inverse check." In developing the  $[T_a]$  transformation, Equation (5.15), it is necessary to take the inverse of  $[T_a]^{-1}$ . An indication of the conditioning of this matrix is furnished by the product

$$\text{Inverse Check} = [T_a] [T_a]^{-1} \quad (8.3)$$

which appears as output. The deviation of this product from a unit diagonal matrix provides an estimate of the accuracy of the computation for  $[T_a]$ . The incorporation of the three checks discussed above is a useful aid in assuring the reliability of the digital solution.

An additional feature which is incorporated in the program is the capability to stack cases, i. e., to solve numerous related problems in sequence by simply stacking the data input for each of the cases. The stacking capability can be utilized for

- 1) the solution of the complete problem, which may include the steady-state response or
- 2) the solution of the steady-state response using natural mode data previously stored on tape.

This feature provides for an efficient use of machine time by eliminating the need for reloading the program deck for successive cases.

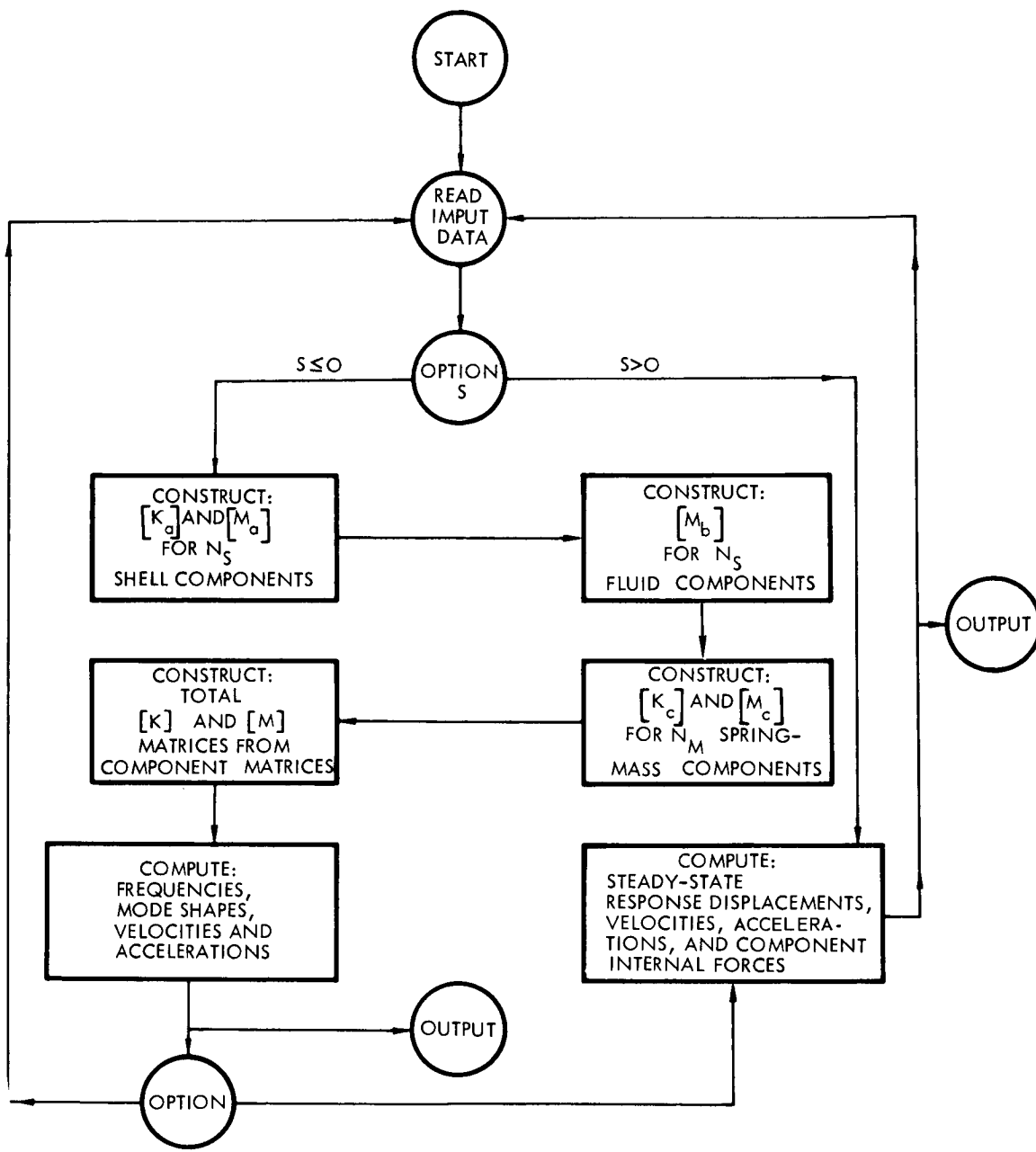


Figure 12. Digital Program Arrangement

## 9. DATA SETUP

### 9.1 VEHICLE SUBDIVISION

In order to prepare the input data, it is first necessary to subdivide the launch vehicle into a consistent set of axisymmetric shell components a, fluid components b, and spring-mass components c. Size limitations of the program require that

- 1) The total number of shell components shall not exceed forty (40),
- 2) The total number of fluid components shall not exceed six (6),
- 3) The total number of spring-mass components shall not exceed thirty (30), and
- 4) The order of the spring-mass stiffness and mass matrices must not exceed ten (10).

Subsequent to the vehicle subdivision, the location of the system coordinate displacements must be determined. The internal operations of the digital program require that

- 1) Longitudinal, radial and rotational coordinate displacements must be placed at each junction of two or more shell elements
- 2) Longitudinal and radial coordinate displacements are placed at each point lying on the vehicle longitudinal axes.

These locations are defined as the terminal points of each shell element. Additional longitudinal and radial coordinate displacements may be placed, as desired, at intermediate points uniformly spaced between the terminal points. Longitudinal, radial and rotational coordinates may also be used to describe the motions of the spring-mass elements.

The coordinate displacements are then identified by a consecutively numbered sequence. The arrangement of these numbers on the vehicle is arbitrary and is left up to the discretion of the analyst. However, the radial coordinate points lying on the vehicle axis are not to be identified with a number. This is necessary because the program must assume these displacements equal to zero, as is required by the axisymmetry of the vehicle, and thus they do not contribute to the degrees-of-freedom of the

system. These are defined as "unnumbered" coordinates and are utilized only in the preparation of the data input sheets for determining the value of U and V (see Figure 11).

In general, for a supported structure, some of the "numbered" coordinates may be assumed fixed or restrained from motion. The total number of "numbered" coordinates which are not fixed must not exceed eighty (80). In addition, the numbering sequence should be arranged so that the fixed coordinates are numbered last to insure consistency in the program output identification with the coordinate identification numbers.

The total number of coordinates for a shell component may not exceed 22, of which in general the number of longitudinal displacement coordinates may not exceed 11, and the number of lateral displacement coordinates may not exceed 10 (see Section 5.3). For the case of three shell components surrounding a fluid component, the total number of coordinates for the composite tank structure may not exceed 29.

## 9.2 INPUT DESCRIPTION

### System Input Data

#### 1) Heading

HHEAD is one line of BCD characters which will be printed as the title of the printed output. The number of BCD words (6 characters per word) must not exceed 11.

#### 2) Input Parameters

$N_C$  is the total number of system coordinates which include the fixed coordinates  $N_O$ .  $N_C - N_O$  must not exceed 80.

$N_S$  is the total number of shell components.  $N_S$  cannot be zero and must not exceed 40.

$N_F$  is the total number of fluid components.  $N_F$  must not exceed 6.

$N_M$  is the total number of spring-mass components.  $N_M$  must not exceed 30.

$N_O$  is the total number of fixed coordinates.  
 $N_C - N_O$  must not exceed 80.

3) Applied Loads and Forcing Frequencies (Section 7.2)

$N_L$  is the total number of discrete applied loads.  $N_L$  must not exceed 80.

$C_i$  is the applied load coordinates  $C_1, C_2, C_3, \dots, C_{N_L}$ .

$P_i$  is the discrete applied loads  $P_1, P_2, P_3, \dots, P_{N_L}$ .

$N_W$  is the number of sets of forcing function frequencies.

$f_i, \Delta f_i, m_i$   $f$  is the frequency of the forcing function in cycles per second ( $\omega = 2\pi f$ ). This program will compute the steady-state response for the frequencies  $f_i, f_i + \Delta f_i, f_i + 2\Delta f_i, \dots, f_i + (m_i - 1)\Delta f_i, i = 1, 2, \dots, N_W$ .

4) Modal Damping Factor

$N_{ET}$  is the number of input  $\eta$ . Program will generate a complete table of  $\eta$  by setting  $\eta_{(N_{ET}+1)}, \eta_{(N_{ET}+2)}, \dots, \eta_{(N_C - N_O)}$  equal to  $\eta_{N_{ET}}$

$\eta_k$  is the ratio of the assumed damping to the critical damping in mode  $k$

$$\eta_1, \eta_2, \eta_3, \dots, \eta_{N_{ET}}$$

5) Ratio of Acceleration

$g$  is the ratio of the vehicle acceleration to the acceleration of gravity.

## 6) Steady-State Response Option

- S is a fixed point word which controls the option of computing steady-state response.
- $S < 0$  indicates that the computation of the steady-state response is not included. The necessary data for the steady-state computation is saved on Tape 1 and 2.
- $S = 0$  indicates that the computation of the steady-state response is included.
- $S > 0$  is the option to compute the steady-state response only. The necessary data should be available on Tape 1 and 2. In addition the following System Input Data must be provided:
- S = 1, Heading [Item 1)], Input Parameters [Item 2)], and Modal Damping Factors [Item 4)].
- S = 2, Heading [Item 1)], Input Parameters [Item 2)], Applied Loads and Forcing Frequencies [Item 3)], Modal Damping Factors [Item 4)], and the option word  $opt_4$ .

## 7) Print Options

- $opt_1$  is an option word which controls the output of stiffness matrix and mass matrix of the shell and the fluid components.
- $opt_1 = 1$ , print the component matrices
- $opt_1 = 0$ , suppress the printing of component matrices.
- $opt_2$  is an option word which controls the printing of total stiffness matrix and total mass matrix.
- $opt_2 = 1$ , print the total stiffness and mass matrices.

$\text{opt}_2 = 0$ , suppress the printing of total stiffness and mass matrices.

$\text{opt}_3$  is an option word which sets the rigid body frequency to zero for computing the response.

$\text{opt}_3 = 1$ , set the first frequency to zero.

$\text{opt}_3 = 0$ , do not set the first frequency to zero.

$\text{opt}_4$  is an option word which controls the computation and printing of forces for the steady-state response.

$\text{opt}_4 = 1$ , compute and print the forces.

$\text{opt}_4 = 0$ , do not compute and print the forces.

$N_{EI}$  is the number of frequencies, mode shapes, velocities and accelerations that will be printed as the final output.

## 8) Polynomial Matrices (Section 5.3)

$N_P$  is the total number of polynomial matrices.

$\bar{U}_k$  is the number of rows of polynomial matrix  $[A]_{\bar{U}_k \times 11}$ . ( $\bar{U}_k \leq 11$ )

$\bar{V}_k$  is the number of rows of polynomial matrix  $[B]_{\bar{V}_k \times 11}$ . ( $\bar{V}_k \leq 11$ )

$[A]_k$  is  $\bar{U}_k \times 11$  polynomial matrix.

$[B]_k$  is  $\bar{V}_k \times 11$  polynomial matrix.

$k = 1, 2, 3, \dots, N_P$

The input sequence of the polynomial matrices establishes the identification number  $k$  which is referred by the shell components.

The subscript k is used as the polynomial matrix identification number by the shell components.

### Shell Component Input Data

1) I.D. Number

a is the identification number for shell component a where  $0 < a \leq N_S$

+ a indicates a conical shell component  
- a indicates an ellipsoidal shell component

2) Coordinates

U, V are the total number of system coordinates.  
 $\bar{U}$ ,  $\bar{V}$  are the total number of local coordinates  
 $\bar{U}$ ,  $\bar{V}$  must not exceed 11.

3) Coordinate I.D. Vector (Figures 8, 9, and 10)

$(ID)_i$  is the identification vector which is used to position the elements for building total stiffness and mass matrices. The length of the vector must be equal to  $\bar{U} + \bar{V}$  and the number must not be greater than  $N_C$ .

4) Polynomial Matrix Identification Number

k is the polynomial matrix identification number which refers to polynomial matrices  $[A]_k$  and  $[B]_k$  in the system input data.

5) Shell Geometric Data (Figures 4 and 5)

$\phi_o$  is the meridional angle for conical shell and is the edge meridional angle for ellipsoidal shell.  $\phi_o$  is input in degrees.

L is the height of conical shell  
+ L indicates converging upward  
- L indicates converging downward  
L = 0 for ellipsoidal shell input



$R_2$  is the lower radius of conical shell  
 $R_2 = 0$  for ellipsoidal shell input

$\bar{b}$  is the height of ellipsoidal shell  
+  $\bar{b}$  indicates convex upward  
-  $\bar{b}$  indicates convex downward  
 $\bar{b} = 0$  for conical shell input

$\bar{a}$  is the radius of the base of ellipsoidal shell,  $\bar{a} = 0$  for conical shell input

6) Orthotropic Shell Constants and Thickness (Equation 3.5)

$(C_{11})_p$  are orthotropic shell constants at two points  $\xi = 0, 1$  which are represented by  $p = 1, 2$ , respectively.

$(C_{12})_p$

$(C_{22})_p$

$(C_{33})_p$

$(C_{34})_p$

$(C_{44})_p$

are orthotropic shell constants at four points  $\xi = 0, 1/3, 2/3, 1$  which are represented by  $p = 1, 2, 3, 4$ , respectively.

$(t)_p$

are shell thickness at two points  $\xi = 0, 1$  which are represented by  $p = 1, 2$ , respectively.

7) Mass Density and Total Mass

$\gamma_a$

is the mass density of the shell component.

$M_a$

is the total mass of the shell component.

$M_a \neq 0$ , the ratio of the total mass  $M_a$  to the computed mass  $\bar{M}_a$  will be used as the scaling factor for the mass matrix. When  $\text{opt}_1 = 1$ , the scaling factor will be printed as the mass check of the mass matrix.

$M_a = 0$ , no scaling factor will be used for the mass matrix. When  $\text{opt}_1 = 1$ , the computed mass will be printed.

8) Initial Stress Data (Figures (B.1), (B.2) and )B.3))

- $H_i$  is the depth of interior fluid.  
 $w_i$  is the weight density of interior fluid.  
 $p_i$  is the uniform interior pressure.  
 $H_e$  is the depth of exterior fluid.  
 $w_e$  is the weight density of exterior fluid.  
 $p_e$  is the uniform exterior pressure  
 $W$  is the reactive force at upper edge of conical shell.  
+  $W$  produces tensile stresses.  
-  $W$  produces compressive stresses.  
 $W = 0$  for ellipsoidal shells.

Fluid Component Input Data

1) I.D. Number

- $b$  is the identification number for fluid component  $b$  where  $0 < b \leq N_F$ .

2) Associated Shell Components (Figure 7)

- $a_1$ ,  $a_2$ , and  $a_3$  are the identification numbers of the associated shell components

3) Fluid Data (Figure C.1)

- $H$  is the depth of fluid component.  
 $\gamma$  is the mass density of fluid component.  
 $M$  is the mass of fluid component.  $M \neq 0$ , the ratio of the total mass  $M$  to the computed mass  $\bar{M}$  will be used as the scaling factor for the mass matrix. When  $opt_1 = 1$ , the scaling factor will be printed as the mass check of the mass matrix.

$M = 0$ , no scaling factor will be used for the mass matrix. When  $opt_1 = 1$ , the computed mass will be printed.

### Spring-Mass Component Input Data

1) I.D. Number

$c$  is the identification number of spring-mass component  $c$  where  $0 < c \leq N_M$ .

2) Stiffness and Mass Matrices

$n$  is the order of the spring-mass component  $n$  must not exceed 10.

$[K]_c$  is  $n \times n$  stiffness matrix of spring-mass component.

$[M]_c$  is  $n \times n$  mass matrix of spring-mass component.

3) Coordinate I.D. Vector

$IDC_i$  is the identification vector which is used to position the elements for building the total stiffness and mass matrices. The length of the vector must be equal to  $n$  and the number must not be greater than  $N_C$ .

### 9.3 SAMPLE INPUT DATA SHEETS

Sample input data sheets are included to illustrate the input format. The data must be arranged in the order shown, that is,

- 1) System input data
- 2) Shell component input data
- 3) Fluid component input data
- 4) Spring-mass component input data

THE SYSTEM INPUT DATA

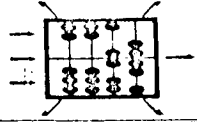
SPACE TECHNOLOGY LABORATORIES, INC.  
 COMPUTATION AND DATA REDUCTION CENTER

DATE \_\_\_\_\_ PAGE \_\_\_\_\_ OF \_\_\_\_\_

NAME \_\_\_\_\_ PRIORITY \_\_\_\_\_

PROBLEM NO. \_\_\_\_\_ KEYPUNCHED BY \_\_\_\_\_

NO. OF CARDS \_\_\_\_\_ VERIFIED BY \_\_\_\_\_



1 7 73

HHEAD

**X3**

SYMBOL	P R E	LOC.	VALUE	EXP.	73
NC	I	NC			
NS	I	NS			
NF	I	NF			
NM	I	NM			
NØ	I	NØ			
NL	I	NL			
C <sub>1</sub>	I	LDCRD			
C <sub>2</sub>	I				
.	.				
.	.				
.	.				
CNL	I				
P <sub>1</sub>		ALØAD			
P <sub>2</sub>					
.	.				
.	.				
PNL					
N <sub>W</sub>	I	NW			
ω <sub>1</sub>		ØMEGA			
Λ <sub>1</sub>					
m <sub>1</sub>	I				
.	.				
ω <sub>N<sub>W</sub></sub>					
Λ <sub>N<sub>W</sub></sub>					
m <sub>N<sub>W</sub></sub>	I				
NET	I	IETAK			
η <sub>1</sub>		ETAK			
η <sub>2</sub>					
.	.				

**X3**

SPACE TECHNOLOGY LABORATORIES, INC.  
COMPUTATION AND DATA REDUCTION CENTER

DATE \_\_\_\_\_

PAGE \_\_\_\_\_ OF \_\_\_\_\_

NAME \_\_\_\_\_

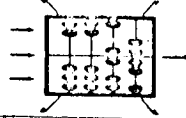
PRIORITY \_\_\_\_\_

PROBLEM NO. \_\_\_\_\_

KEYPUNCHED BY \_\_\_\_\_

NO. OF CARDS \_\_\_\_\_

VERIFIED BY \_\_\_\_\_



X3

SYMBOL	P R E	LOC.	VALUE	EXP.	73
.					
NET					
G		G			
S		I INS			
opt <sub>1</sub>		I IØPT1			
opt <sub>2</sub>		I IØPT2			
opt <sub>3</sub>		I IØPT3			
opt <sub>4</sub>		I IØPT4			
<sup>N</sup> EI		I NEI			
N <sub>P</sub>		I NP			
		END			
U <sub>k</sub>		I UBAR			
V <sub>k</sub>		I VBAR			
[A] <sub>k</sub>		M APØLY 11,11 OI,OJ			
[B] <sub>k</sub>		M BPØLY 11,11 OI,OJ			

X3



THE SHELL COMPONENT INPUT DATA

SPACE TECHNOLOGY LABORATORIES, INC.  
COMPUTATION AND DATA REDUCTION CENTER

DATE \_\_\_\_\_

PAGE \_\_\_\_\_ OF \_\_\_\_\_

NAME \_\_\_\_\_

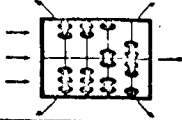
PRIORITY \_\_\_\_\_

PROBLEM NO. \_\_\_\_\_

KEYPUNCHED BY \_\_\_\_\_

NO. OF CARDS \_\_\_\_\_

VERIFIED BY \_\_\_\_\_



1	7		73
			<b>X3</b>

SYMBOL	P R E	LOC.	VALUE	17
				EXP.
a	I	INA		
U	I	IU		
V	I	IV		
$\bar{0}$	I	IUB		
$\bar{v}$	I	IVB		
(ID) <sub>1</sub>	I	IDVT		
(ID) <sub>2</sub>	I			
.	.			
.	.			
.	.			
(ID) $\bar{u}+\bar{v}$	I			
k	I	INK		
$\bar{0}$		PHIN		
L		XL		
R <sub>2</sub>		R2IN		
$\bar{b}$		BBAR		
$\bar{a}$		ABAR		
(C <sub>11</sub> ) <sub>1</sub>		C11I		
(C <sub>11</sub> ) <sub>2</sub>				
(C <sub>12</sub> ) <sub>1</sub>		C12I		
(C <sub>12</sub> ) <sub>2</sub>				
(C <sub>22</sub> ) <sub>1</sub>		C22I		
(C <sub>22</sub> ) <sub>2</sub>				
(C <sub>33</sub> ) <sub>1</sub>		C33I		
(C <sub>33</sub> ) <sub>2</sub>				
(C <sub>33</sub> ) <sub>3</sub>				
(C <sub>33</sub> ) <sub>4</sub>				
(C <sub>34</sub> ) <sub>1</sub>		C34I		
(C <sub>34</sub> ) <sub>2</sub>				
(C <sub>34</sub> ) <sub>3</sub>				
(C <sub>34</sub> ) <sub>4</sub>				
(C <sub>44</sub> ) <sub>1</sub>		C44I		
(C <sub>44</sub> ) <sub>2</sub>				

**X3**

SPACE TECHNOLOGY LABORATORIES, INC.  
COMPUTATION AND DATA REDUCTION CENTER

DATE \_\_\_\_\_

PAGE \_\_\_\_\_ OF \_\_\_\_\_

NAME \_\_\_\_\_

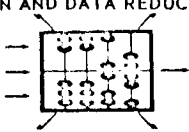
PRIORITY \_\_\_\_\_

PROBLEM NO. \_\_\_\_\_

KEYPUNCHED BY \_\_\_\_\_

NO. OF CARDS \_\_\_\_\_

VERIFIED BY \_\_\_\_\_



1		73
7		

X3

SYMBOL	P R E	LOC.	VALUE	EXP.
(C <sub>11</sub> ) <sub>3</sub>	19 37 55			
(C <sub>11</sub> ) <sub>4</sub>	20 38 56			
(t) <sub>1</sub>		THI		
(t) <sub>2</sub>				
Y <sub>a</sub>		DESTA		
K <sub>a</sub>		AM		
H <sub>i</sub>		HI		
w <sub>1</sub>		DESTI		
P <sub>i</sub>		PRI		
H <sub>c</sub>		WE		
w <sub>c</sub>		DESTE		
P <sub>c</sub>		FRE		
w		WFORC		
		ND		

X3



# THE FLUID COMPONENT INPUT DATA

IV-11

DATE \_\_\_\_\_

SPACE TECHNOLOGY LABORATORIES, INC.  
COMPUTATION AND DATA REDUCTION CENTER

PAGE \_\_\_\_ OF \_\_\_\_

NAME \_\_\_\_\_

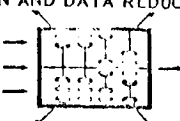
PRIORITY \_\_\_\_\_

PROBLEM NO. \_\_\_\_\_

KEYPUNCHED BY \_\_\_\_\_

NO. OF CARDS \_\_\_\_\_

VERIFIED BY \_\_\_\_\_



**X3**

SYMBOL	P R E	LOC.	VALUE	73	
				EXP.	
b	I	INB			
a <sub>1</sub>	I	IDA1			
a <sub>2</sub>	I	IDA2			
a <sub>3</sub>	I	IDA3			
H		HF			
Y		DESTF			
M		FM			
	E	ND			

**X3**

THE SPRING-MASS COMPONENT INPUT DATA

THE SPRING-MASS COMPONENT INPUT DATA

IV-12

SPACE TECHNOLOGY LABORATORIES, INC.  
COMPUTATION AND DATA REDUCTION CENTER

DATE \_\_\_\_\_

PAGE \_\_\_\_\_ OF \_\_\_\_\_

NAME \_\_\_\_\_

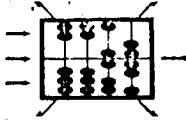
PRIORITY \_\_\_\_\_

PROBLEM NO. \_\_\_\_\_

KEYPUNCHED BY \_\_\_\_\_

NO. OF CARDS \_\_\_\_\_

VERIFIED BY \_\_\_\_\_



1	7	73
		X3

SYMBOL	P R E	LOC.	VALUE	EXP.	73
					17 35 53 71
c	I	INC			
n	I	IN			
[K] <sub>c</sub>	M	CK	10, 10		
		OI, OJ			
[M] <sub>c</sub>	M	CM	10, 10		
		OI, OJ			
(IDC) <sub>1</sub>	I	IDVTC			
(IDC) <sub>2</sub>	I				
.	.				
.	.				
(IDC) <sub>n</sub>	I				
	E	ND			

X3

## 10. NOTATION

$[ ]_{(1 \times j)}$	Row matrix of order $j$
$\{ \}_{(i \times 1)}$	Column matrix of order $i$
$[ ]_{(i \times j)}$	Rectangular matrix with $i$ rows and $j$ columns
$a, b, c$	Identification number for the shell, fluid and spring-mass components respectively
$a, b$	Semimajor and semiminor axes, respectively, of an ellipsoidal bulkhead
$\bar{a}, \bar{b}$	Edge radius and height, respectively, of an ellipsoidal bulkhead
$a_1, a_2, a_3$	Identification numbers for the shell components which enclose a fluid component
$[A]_{(\bar{U}_{x11})} \equiv [a_{kn}]$	Polynomial matrix associated with $u_k(\xi)$
$[B]_{(\bar{V}_{x11})} [b_{ln}]$	Polynomial matrix associated with $v_l(\xi)$
$\{C_e\}$	Coordinate identification vector for component $e$
$C_r$	$r^{\text{th}}$ component of $\{C_e\}$
$C_{11}(\xi), C_{12}(\xi), C_{22}(\xi)$	Orthotropic stress-strain coefficients
$C_{33}(\xi), C_{34}(\xi), C_{44}(\xi)$	Orthotropic moment-curvature coefficients
$ds$	Differential meridional distance along shell
$(\cdot) \equiv \frac{d(\cdot)}{ds}$	Derivative with respect to meridional distance $s$
$D_1, D_2$	Constants used to determine the rotation vector $\{\rho\}$
$[D_1]_{(2 \times 11)}, [D_2]_{(2 \times 11)}$	Matrices used in the definition of the rotation vector $\{\rho\}$

e	General identification number for vehicle components which may stand for a or b
g	Ratio of vehicle acceleration to acceleration of gravity
H	Total fluid level measured positive upward from the base of a2
$\bar{H}_1, \bar{H}_2, \bar{H}_3$	Fluid levels associated with tank shell sections a1, a2, a3
$[K]_{(N_c \times N_c)}$	Total launch vehicle stiffness matrix
$[K_a]_{((\bar{U} + \bar{V})_x (\bar{U} + \bar{V}))}$	Stiffness matrix for shell component a associated with the system coordinates
$[\bar{K}_a]_{((\bar{U} + \bar{V})_x (\bar{U} + \bar{V}))}$	Stiffness matrix for shell component a associated with the local coordinates
$[K_c]$	Stiffness matrix of spring-mass component c associated with the system coordinates
$[K_s]$	Row s ( $s = 1, 2, \dots (\bar{U} + \bar{V})_a$ ) of $[K_a]$
$K_\phi$	Shell meridional curvature
$K_\theta$	Shell hoop curvature
L	Length of conical shell
$m_t$	Generalized mass for mode t
$[M]$	Total mass matrix for the launch vehicle
$[M_a]$	Mass matrix for shell component a associated with the system coordinates
$[\bar{M}_a]$	Mass matrix for shell component a associated with the local coordinates
$[\tilde{M}_b]$	Mass matrix for fluid component b associated with the system coordinates

$[\bar{M}_b]$	Mass matrix for fluid component b associated with the local coordinates
$[M_c]$	Mass matrix for spring-mass component c associated with the system coordinates
$N_C$	Total number of system coordinates used in the vehicle model
$N_F$	Total number of fluid components used in the vehicle model
$N_M$	Total number of spring-mass components used in the vehicle model
$N_O$	Total number of fixed coordinates
$N_S$	Total number of shell components used in the vehicle model
$N_\phi^o$	Initial meridional stress
$p$	Circular frequency of the vehicle
$p_t$	Circular frequency of the vehicle for mode t
$\{P\} (N_C - N_O \times 1)$	Applied load vector
$Q_t$	Generalized force acting on mode t
$r$	Radial distance from the vehicle longitudinal axis to each point on the shell
$\overset{\wedge}{r}$	Radial distance from the vehicle longitudinal axis to each point in the fluid
$r_1$	Meridional radius of curvature of the shell
$r_2$	Hoop radius of curvature of the shell
$\{R\} (N_C \times 1)$	Displacement response vector
$\{\bar{R}\}$	Displacement response amplitude vector

$\{S_a\}_{(\bar{U}+\bar{V})_{x1}}$	Vector of internal forces or moments acting at each point of shell component a
$\{\bar{S}\}$	Amplitude vector of internal forces $\{S_a\}$
t	Identification number for a particular mode of vibration
t	Time
$[T_a]_{(\bar{U}+\bar{V})_{x1}(\bar{U}+\bar{V})}$	Transformation matrix which relates local to system coordinates in shell component a
$[T_b]_{(\bar{W}_{x1}\bar{W})}$	Transformation matrix which relates local to system coordinates in fluid component b
$\{U\}_{(\bar{U}+\bar{V})_{x1}}, \{V\}_{(\bar{U}+\bar{V})_{x1}}$	Longitudinal and radial displacement vectors, respectively, for shell components
$u_k(\xi), v(\xi)$	Generalized longitudinal and radial displacements, respectively, for shell components
$\{\hat{u}(x)\}_{(\bar{W}_{x1})} = \{\hat{u}_m(x)\}$	Longitudinal and radial fluid displacements, respectively
and	
$\{\hat{v}(x, r)\}_{(\bar{W}_{x1})} = \{\hat{v}_m(x, r)\}$	
U, V	Total number of longitudinal and radial system coordinates, respectively, associated with each shell component
$\bar{U}, \bar{V}$	Total number of longitudinal and radial local coordinates, respectively, associated with each shell component
$[U]_{(U_{x11})}, [V]_{(V_{x11})}$	Constant matrices used in the definition of the system coordinates
$w_i, w_e$	Fluid weight densities interior and exterior, respectively, to each shell component
$\bar{w}_i, \bar{w}_e$	Effective fluid weight densities equal to, respectively, $gw_i$ and $gw_e$
$\bar{W}$	The sum of $\bar{U} + \bar{V}$ for the three shells surrounding a fluid component

$x$	Longitudinal axis of the launch vehicle
$z_t$	Structural impedance for mode $t$
$\{a_a\}_{((\bar{U}+\bar{V}) \times 1)}$	Modal vector whose components are the longitudinal, radial and rotational system coordinate displacements for shell component $a$
$\{\bar{a}_a\}_{((\bar{U}+\bar{V}) \times 1)}$	Consolidated vector of local coordinates
$\{\bar{a}_k\}_{(\bar{U} \times 1)}, \{\bar{\beta}_l\}_{(\bar{V} \times 1)}$	Generalized coordinates in the longitudinal and radial directions, respectively
$[a]_{(N_C - N_O) \times (N_C - N_O)}$	Modal matrix with each column representing a vehicle mode shape
$[a_s]_{(1 \times (N_C - N_O))}$	Each row of $[a]$ which is a system coordinate "s" displacement vector with natural mode elements
$\{a_t\}_{(N_C - N_O) \times 1}$	Each column of $[a]$ which is a mode "t" displacement vector with system coordinate elements
$\gamma_a, \gamma_b$	Mass densities for shell and fluid components respectively
$\{\bar{\delta}\}_{((N_C - N_O) \times 1)}$	Vector of steady-state displacement phase angles
$\{\bar{\delta}\}_{((\bar{U}+\bar{V}) \times 1)}$	Vector of phase angles for the internal forces of each shell component
$[\Delta e]_{((\bar{U}+\bar{V}) \times N_C)} = [\delta_{rs}]$	Transformation matrix relating total system displacements to component 3 system displacements
$\epsilon_\phi, \epsilon_\theta$	Meridional and hoop strains, respectively, for the shell components
$\eta_t$	Ratio of actual damping to the critical damping for each mode $t$
$\{\xi\}$	Nondimensional variable describing location on each shell component

- $\rho$  Meridional rotation of the shell components
- $\phi$  Meridional angle
- $\omega$  Frequency of the forcing function in radians per second



## 11. REFERENCES

1. J.D. Wood, "Survey on Missile Structural Dynamics," EM 11-11, TRW Space Technology Laboratories, 1 June 1961.
2. R.A. Winje, J.H. Walker, and K.J. McKenna, "An Investigation of Low Frequency Longitudinal Vibration of the Titan II Missile During Stage I Flight," 6438-6001-RU000, TRW Space Technology Laboratories, 26 March 1964.
3. J.S. Archer, "Consistent Matrix Formulations for Structural Analysis Using Influence-Coefficient Techniques," Preprint No. 64-488, Am. Inst. Aeron. and Astronaut., June-July 1964.
4. Walter C. Hurty and Moshe F. Rubinstein, Dynamics of Structures, Prentice-Hall, Inc., 1964.
5. Handbook of Mathematical Functions with Formulas, Graphs and Mathematical Tables, U.S. Department of Commerce, National Bureau of Standards, Applied Mathematic Series, 1964.
6. Tables of Lagrangian Interpolation Coefficients, National Bureau of Standards, Computation Laboratories, New York, Columbia University Press.
7. S.P. Timoshenko and J.M. Gere, Theory of Elastic Stability, Second Ed., McGraw-Hill Book Co., Inc., 1961.
8. W. Flügge, Stresses in Shells, Springer-Verlag, pp. 18-24, 97, 355-359, 1960.
9. W.F. Thielemann, "New Developments in the Nonlinear Theories of the Buckling of Thin Cylindrical Shells." Proceedings of the Durant Centennial Conference, Pergamon Press, New York, 1960.
10. Cornelius Lanczos, Applied Analysis, Prentice-Hall, Inc., p. 516, 1956.

APPENDIX A  
SHELL GEOMETRY AND ENERGY EXPRESSIONS

The additional potential energy of a shell of revolution due to axisymmetric deformations is given in the form

$$V = \frac{1}{2} \int_s 2\pi r \left( N_\phi \epsilon_\phi + N_\theta \epsilon_\theta + M_\phi K_\phi + M_\theta K_\theta + N_\phi^0 \rho^2 \right) ds \quad (\text{A. 1})$$

in which the last term represents the work done by the initial meridional stress,  $N_\phi^0$ .<sup>7</sup> The initial hoop stress does not make a similar contribution to the potential energy since there is zero rotation in the hoop direction. In the notation of Flugge,<sup>8</sup> the strains ( $\epsilon_\phi$ ,  $\epsilon_\theta$ ), curvatures ( $K_\phi$ ,  $K_\theta$ ) and the meridional rotation  $\rho$  are expressed in terms of the displacements  $\bar{v}$  and  $\bar{w}$  (see Figure A. 1) as follows:

$$\epsilon_\phi = \frac{1}{r_1} \left( \frac{d\bar{v}}{d\phi} + \bar{w} \right) \quad (\text{A. 2})$$

$$\epsilon_\theta = \frac{1}{r_2} (\bar{v} \cot \phi + \bar{w}) \quad (\text{A. 3})$$

$$K_\phi = \frac{1}{r_1} \frac{d}{d\phi} \left[ \frac{1}{r_1} \left( \frac{d\bar{w}}{d\phi} - \bar{v} \right) \right] \quad (\text{A. 4})$$

$$K_\theta = \frac{\cot \phi}{r_2} \left[ \frac{1}{r_1} \left( \frac{d\bar{w}}{d\phi} - \bar{v} \right) \right] \quad (\text{A. 5})$$

$$\rho = \frac{1}{r_1} \left( \frac{d\bar{w}}{d\phi} - \bar{v} \right) \quad (\text{A. 6})$$

where  $r_1$  and  $r_2$  are the radii of curvature of the shell in the meridional and hoop directions, respectively. Hookes law for an orthotropic shell with the principal directions in the hoop and meridional directions takes the form:<sup>9</sup>

$$\begin{Bmatrix} N_{\phi} \\ N_{\theta} \\ M_{\phi} \\ M_{\theta} \end{Bmatrix} = \begin{bmatrix} C_{11} & C_{12} & 0 & 0 \\ C_{12} & C_{22} & 0 & 0 \\ 0 & 0 & C_{33} & C_{34} \\ 0 & 0 & C_{34} & C_{44} \end{bmatrix} \begin{Bmatrix} \epsilon_{\phi} \\ \epsilon_{\theta} \\ K_{\phi} \\ K_{\theta} \end{Bmatrix} \quad (\text{A. 7})$$

The shell configurations to be considered for the bulkheads and the tank walls are listed below with their corresponding geometric parameters defined:

1. Conical Shell (Figure A. 2)

a) General Case

$$\begin{aligned} \phi &= \phi_0 \\ r_1 &= \infty \\ r_2 &= (R_2 / \sin \phi_0) - S \cot \phi_0 \end{aligned} \quad (\text{A. 8})$$

b) Cylinder (radius = R)

$$\begin{aligned} \phi &= \frac{\pi}{2} \\ r_1 &= \infty \\ r_2 &= R \end{aligned} \quad (\text{A. 9})$$

2. Ellipsoid (Figure A. 3)

a) General Case (a = semimajor axis, b = semiminor axis)

$$\begin{aligned} r_1 &= \frac{a^2 b^2}{(a^2 \sin^2 \phi + b^2 \cos^2 \phi)^{3/2}} \\ r_2 &= \frac{a^2}{(a^2 \sin^2 \phi + b^2 \cos^2 \phi)^{1/2}} \end{aligned} \quad (\text{A. 10})$$

b) Hemisphere (radius = R)

$$r_1 = R \tag{A.11}$$

$$r_2 = R$$

For the present analysis, the longitudinal displacement  $u$  and the radial displacement  $v$  will be more convenient. They are related to the displacements  $\bar{v}$  and  $\bar{w}$  by the transformation

$$\bar{v} = -u \sin \phi + v \cos \phi \tag{A.12}$$

$$\bar{w} = u \cos \phi + v \sin \phi$$

Substitution of this transformation into the strains, curvature and rotation yields

$$\epsilon_\phi = \frac{1}{r_1} \left( \frac{du}{d\phi} \sin \phi + \frac{dv}{d\phi} \cos \phi \right) \tag{A.13}$$

$$\epsilon_\theta = \frac{v}{r} \tag{A.14}$$

$$K_\phi = \frac{1}{r_1} \frac{d}{d\phi} \left[ \frac{1}{r_1} \left( \frac{du}{d\phi} \cos \phi + \frac{dv}{d\phi} \sin \phi \right) \right] \tag{A.15}$$

$$K_\theta = \frac{\cos \phi}{r} \left[ \frac{1}{r_1} \left( \frac{du}{d\phi} \cos \phi + \frac{dv}{d\phi} \sin \phi \right) \right] \tag{A.16}$$

$$\rho = \frac{1}{r_1} \frac{d}{d\phi} \left( \frac{du}{d\phi} \cos \phi + \frac{dv}{d\phi} \sin \phi \right) \tag{A.17}$$

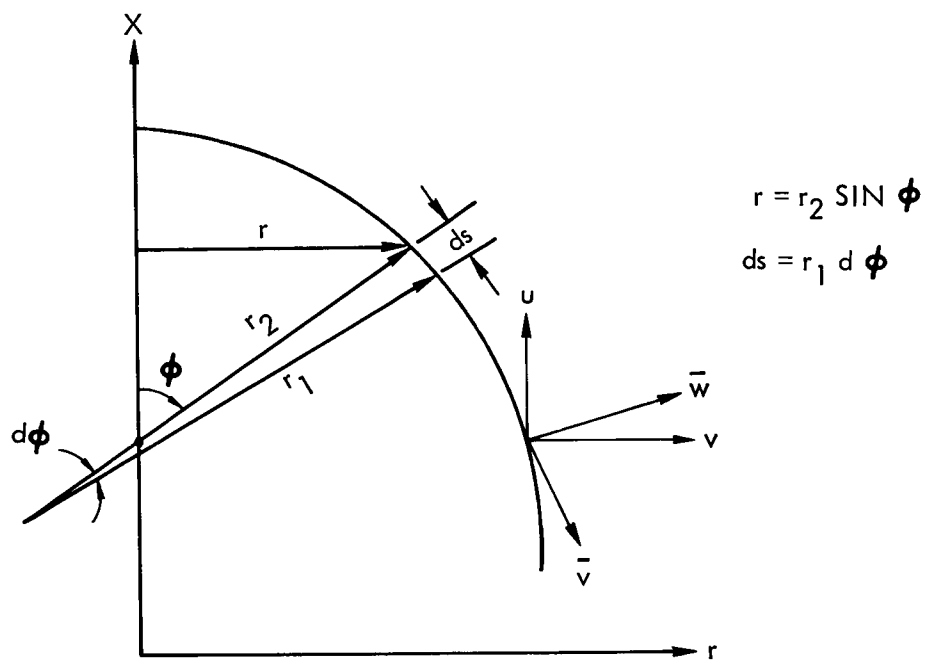


Figure A. 1. Meridian of Shell of Revolution

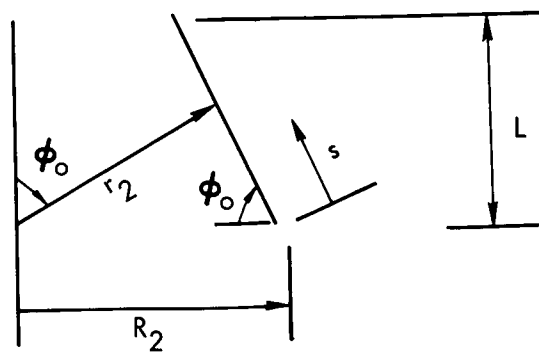


Figure A. 2. Conical Shell

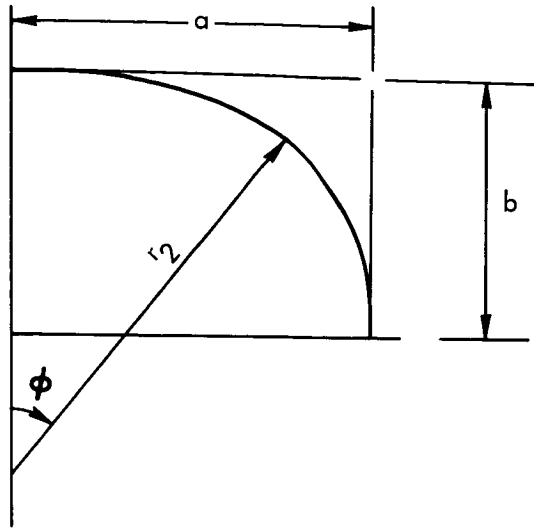


Figure A.3. Ellipsoidal Shell

## APPENDIX B

### INITIAL STRESSES IN SHELL ELEMENTS

In the formulation of the shell stiffness matrix, the effect of the initial meridional stresses is included. Expressions for these stresses are developed below for each of the shell elements to be considered. These derivations are based on membrane theory which is a good first order approximation except in very localized areas where bending predominates.

#### Conical Element

The derivation of the initial stresses in a conical element is divided into three steps. The notation is listed below and shown in Figure B. 1.

$R_2$	lower radius of the conic
$\phi_0$	meridional angle
$L$	length of element
$\bar{w}_i$	effective density of interior fluid
$h_i$	location of interior fluid surface
$\bar{w}_e$	effective density of exterior fluid
$h_e$	location of exterior fluid surface
$p_i$	uniform internal pressure
$p_e$	uniform external pressure
$\pm W$	reactive force at top of conic $\left\{ \begin{array}{l} + \text{ produces tensile stress} \\ - \text{ produces compressive} \\ \text{ stress} \end{array} \right\}$

1. Stress due to uniform pressures and reactive force

$$N_{\phi_1} = \frac{1}{2\pi r \sin \phi_0} \left[ W + (p_i - p_e) \pi (r^2 - R_1^2) \right] \quad 0 \leq x \leq L \quad (\text{B. 1})$$

2. Stress due to interior fluid

Case 1:  $h_i \leq L$

$$\begin{aligned}
 N_{\phi_2} &= \frac{-1}{r \sin \phi_0} \int_x^{h_i} p r \, dr \\
 &= \frac{-1}{r \sin \phi_0} \int_x^{h_i} \bar{w}_i (h_i - x) (R_2 - x \cot \phi_0) (-dx \cot \phi_0) \\
 &= + \frac{\bar{w}_i \cot \phi_0}{r \sin \phi_0} \left[ h_i (h_i - x) R_2 - \frac{1}{2} (h_i^2 - x^2) (R_2 + h_i \cot \phi_0) \right. \\
 &\quad \left. + \frac{1}{3} (h_i^3 - x^3) \cot \phi_0 \right] \quad x \leq h_i \leq L \quad (\text{B. 2})
 \end{aligned}$$

Case 2:  $h_i > L$

$$\begin{aligned}
 N_{\phi_2} &= \frac{-1}{r \sin \phi_0} \int_x^L p r \, dr \\
 &= + \frac{\bar{w}_i \cot \phi_0}{r \sin \phi_0} \left[ h_i (L - x) R_2 - \frac{1}{2} (L^2 - x^2) (R_2 + h_i \cot \phi_0) \right. \\
 &\quad \left. + \frac{1}{3} (L^3 - x^3) \cot \phi_0 \right] \quad 0 \leq x \leq L \quad (\text{B. 3})
 \end{aligned}$$

3. Stress due to exterior fluid

Case 1:  $h_e \leq L$

$$\begin{aligned}
 N_{\phi_3} &= \frac{-1}{r \sin \phi_0} \int_x^{h_e} p r \, dr \\
 &= - \frac{\bar{w}_e \cot \phi_0}{r \sin \phi_0} \left[ h_e (h_e - x) R_2 - \frac{1}{2} (h_e^2 - x^2) (R_2 + h_e \cot \phi_0) \right. \\
 &\quad \left. + \frac{1}{3} (h_e^3 - x^3) \cot \phi_0 \right] \quad 0 \leq x \leq h_e \leq L \quad (\text{B. 4})
 \end{aligned}$$



Case 2:  $h_e > L$

$$\begin{aligned}
 N_{\phi_3} &= \frac{-1}{r \sin \phi_0} \int_x^L pr \, dr \\
 &= \frac{-\bar{w}_e \cot \phi_0}{r \sin \phi_0} \left[ h_e (L - x) R_2 - \frac{1}{2} (L^2 - x^2) (R_2 + h_e \cot \phi_0) \right. \\
 &\quad \left. + \frac{1}{3} (L^3 - x^3) \cot \phi_0 \right] \quad 0 \leq x \leq L \quad (B.5)
 \end{aligned}$$

The total meridional initial stress on the conic will then be the sum of the above stresses

$$N_{\phi} = N_{\phi_1} + N_{\phi_2} + N_{\phi_3} \quad (B.6)$$

### Ellipsoidal Element

The expressions for the initial stress for an ellipsoidal element are developed separately for the upright and inverted bulkheads. The notation for both cases is listed below and shown in Figures B. 2 and B. 3.

- $\bar{a}$  radius of base
- $\bar{b}$  height of element
- $\phi_0$  slope of meridian  
(Note: The semimajor and semiminor axes,  $a$  and  $b$ , can be computed from  $\bar{a}$ ,  $\bar{b}$ , and  $\phi_0$ .)
- $\bar{w}_i$  effective density of interior fluid
- $h_i$  location of surface of interior fluid
- $\bar{w}_e$  effective density of exterior fluid
- $h_e$  location of surface of exterior fluid
- $p_i$  uniform internal pressure
- $p_e$  uniform external pressure

Upright Bulkhead (Figure B. 2)

1. Stress for exterior fluid

Case 1:  $h_e \leq \bar{b}$

$$N_{\phi_1} = -\frac{p_e r_2}{2} + \frac{1}{2\pi r \sin \phi} \int_r^{\bar{r}} 2\pi r p \, dr$$

where

$$\bar{r} = a \sqrt{1 - \frac{(h_e + b - \bar{b})^2}{b^2}} = a \sqrt{1 - \frac{H_e^2}{b^2}}$$

$$p = -\bar{w}_e (h_e - x) \quad (\text{B. 7})$$

$$x + (b - \bar{b}) = b \sqrt{1 - \frac{r^2}{a^2}}$$

This finally leads to

$$N_{\phi_1} = -\frac{p_e r_2}{2} - \frac{\bar{w}_e}{r \sin \phi} \left[ \frac{H_e}{2} (r^2 - \bar{r}^2) - \frac{a^2}{3b} H_e^3 + \frac{a^2 b}{3} \left(1 - \frac{r^2}{a^2}\right)^{3/2} \right]$$

for  $\bar{r} \leq r \leq \bar{a}$

$$N_{\phi_1} = -\frac{p_e r_2}{2} \quad \text{for } 0 \leq r \leq \bar{r} \quad (\text{B. 8})$$

Case 2:  $h_e > \bar{b}$

$$N_{\phi_1} = -\frac{p_e r_2}{2} + \frac{1}{2\pi r \sin \phi} \int_0^r 2\pi r p \, dr$$

$$= -\frac{p_e r_2}{2} - \frac{\bar{w}_e}{r \sin \phi} \left[ \frac{H_e r^2}{2} + \frac{a^2 b}{3} \left(1 - \frac{r^2}{a^2}\right)^{3/2} - \frac{a^2 b}{3} \right] \quad \text{for } 0 \leq r \leq \bar{a} \quad (\text{B. 9})$$

2. Stress for interior fluid

$$N_{\phi_2} = \frac{P_i r_2}{2} + \frac{1}{2\pi r \sin \phi} \int_{\bar{r}}^r 2\pi r p \, dr \quad (\text{B. 10})$$

where

$$\bar{r} = a \sqrt{1 - \frac{(h_i + b - b)^2}{b^2}} = a \sqrt{1 - \frac{H_i^2}{b^2}}$$

$$p = \bar{w}_i (h_i - x)$$

or, after integration,

$$N_{\phi_2} = \frac{P_i r_2}{2} + \frac{\bar{w}_i}{r \sin \phi} \left[ \frac{H_i}{2} (r^2 - \bar{r}^2) - \frac{a^2}{3b} H_i^3 + \frac{a^2 b}{3} \left(1 - \frac{r^2}{a^2}\right)^{3/2} \right] \quad \text{for } \bar{r} < r \leq \bar{a}$$

$$N_{\phi_2} = \frac{P_i r_2}{2} \quad \text{for } 0 \leq r \leq \bar{r} \quad (\text{B. 11})$$

Inverted Bulkhead (Figure B. 3)

1. Stress for interior fluid

$$N_{\phi_1} = \frac{P_i r_2}{2} + \frac{1}{2\pi r \sin \phi} \int_0^r 2\pi r p \, dr \quad (\text{B. 12})$$

for

$$r \leq \bar{r} = a \sqrt{1 - \frac{(h_i + b - \bar{b})^2}{b^2}}$$

$$= a \sqrt{1 - \frac{H_i^2}{b^2}} \quad h_i \geq 0$$

or

$$= \bar{a} \quad h_i < 0$$

where

$$p = w_i (x - h_i) \quad x \geq h_i$$

This leads to the following expressions for the stress:

$$N_{\phi_1} = \frac{p_i r_2}{2} - \frac{\bar{w}_i}{r \sin \phi} \left[ \frac{H_i}{2} r^2 + \frac{a^2 b}{3} \left( 1 - \frac{r^2}{a^2} \right)^{3/2} - \frac{a^2 b}{3} \right] \quad 0 \leq r \leq \bar{r}$$

$$N_{\phi_1} = \frac{p_i r_2}{2} - \frac{\bar{w}_i}{r \sin \phi} \left[ \frac{H_i}{2} \bar{r}^2 + \frac{a^2 b}{3} \left( 1 - \frac{\bar{r}^2}{a^2} \right)^{3/2} - \frac{a^2 b}{3} \right] \quad \bar{r} \leq r \leq \bar{a}$$
(B. 13)

## 2. Stress for lower fluid

$$N_{\phi_2} = -\frac{p_e r_2}{2} + \frac{1}{2\pi r \sin \phi} \int_0^r 2\pi r p \, dr$$

for

$$r \leq \bar{r} = a \sqrt{1 - \frac{(h_e + b - \bar{b})^2}{b^2}} = a \sqrt{1 - \frac{H_e^2}{b^2}}$$
(B. 14)

where

$$p = -\bar{w}_e (x - h_e) \quad x \geq h_e$$

or, after integration

$$N_{\phi_2} = -\frac{p_e r_2}{2} + \frac{\bar{w}_e}{r \sin \phi} \left[ \frac{H_e}{2} r^2 + \frac{a^2 b}{3} \left( 1 - \frac{r^2}{a^2} \right)^{3/2} - \frac{a^2 b}{3} \right] \quad \text{for } 0 \leq r \leq \bar{r}$$

$$N_{\phi_2} = -\frac{p_e r_2}{2} + \frac{\bar{w}_e}{r \sin \phi} \left[ \frac{H_e}{2} \bar{r}^2 + \frac{a^2 b}{3} \left( 1 - \frac{\bar{r}^2}{a^2} \right)^{3/2} - \frac{a^2 b}{3} \right] \quad \bar{r} \leq r \leq \bar{a}$$
(B. 15)

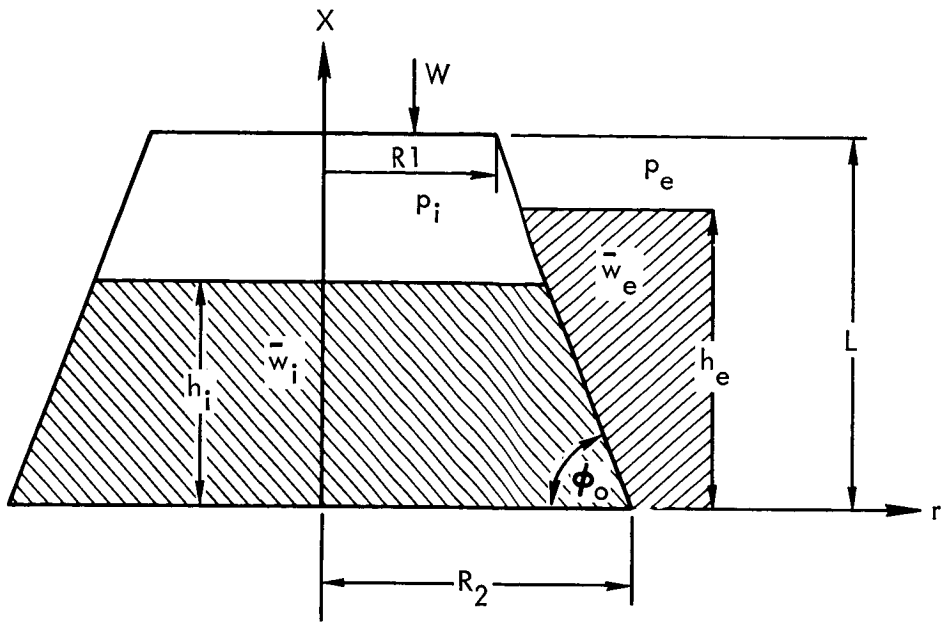


Figure B.1. Conic

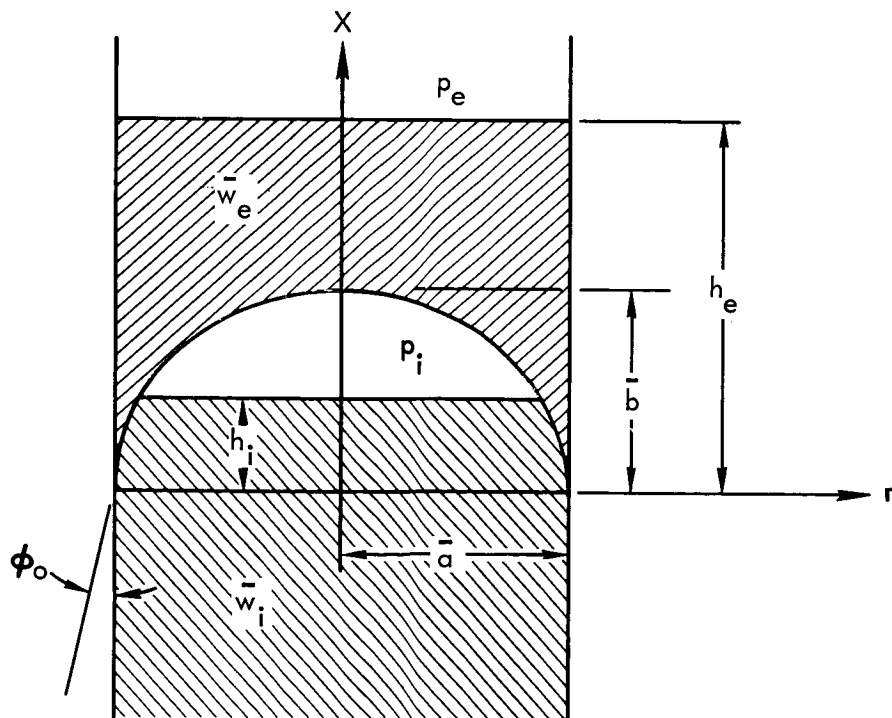


Figure B.2. Upright Ellipsoidal Bulkhead

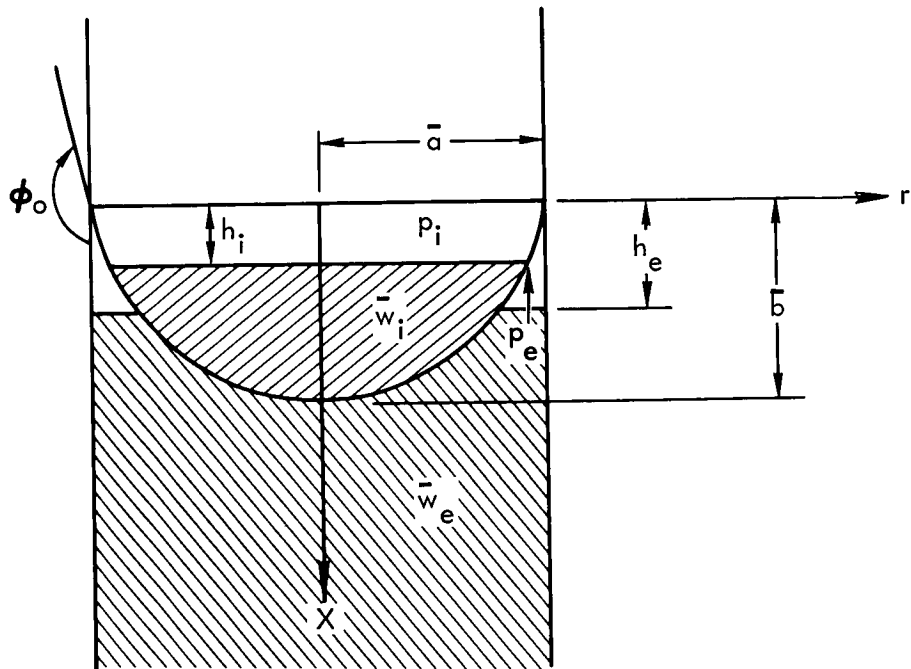


Figure B.3. Inverted Ellipsoidal Bulkhead

## APPENDIX C

### FLUID MASS MATRIX EXPRESSIONS

Detailed expressions are given below for evaluating Equation (4.4) to obtain the fluid component mass matrix. Three cases are involved depending upon whether the upper and lower tank bulkheads are convex upward or convex downward (see Section 2.0). A general description of the program operations utilized to construct the mass matrix for the fluid tanks is described in Appendix E. A brief flow chart followed by the relevant equations in a form suitable for a weighting matrix integration scheme is included to provide the user with a more basic understanding of the digital program.

#### C.1 CASE I. UPPER BULKHEAD CONVEX UPWARD, LOWER BULKHEAD CONVEX DOWNWARD

Equation (4.6) for the general tank shell can be expressed as the sum of contributions to  $\bar{M}_b$  from fluid in three sections of the tank, as illustrated in Figure C.1 for Case I. One of these sections is that located above the base of the upper bulkhead (shell 1). A second lies below the top of lower bulkhead (shell 2). The third lies between the two bulkheads. In general, the motion of the fluid in any section may be affected by the generalized coordinate distortions associated with all three tank shell components. Thus, Equation (4.6) is expressed as

$$\frac{1}{\pi \gamma_b} [\bar{M}_b] = \sum_{m=m_o}^{m=3} \int_0^{\bar{H}_{(m)}} \left( \frac{4}{r_{(m)}} \left\{ \frac{r_{(m)}^2}{2} \hat{u}_{(m)}(x) \right\} \left\{ \frac{r_{(m)}^2}{2} \hat{u}_{(m)}(x) \right\}^T + \frac{1}{2} \left\{ r_{(m)} \hat{v}_{(m)}(x, r) \right\} \left\{ r_{(m)} \hat{v}_{(m)}(x, r) \right\}^T \right) dx \quad (C.1)$$

where  $m_o = 1, 2$  or  $3$ , depending upon whether the fluid surface lies within the range of tank section (1), (2) or (3), as illustrated in Figure C.1.  $\bar{H}_{(m)}$  is the depth of fluid within tank section (m),  $r_{(m)}$  is the radius of shell (m) and, similarly,  $\hat{u}(x)$  and  $\hat{v}_{(m)}(x, r)$  represent the fluid motions

within tank section m. The specific form of the column matrix  $\{\hat{u}_{(m)}(x)\}$  in terms of the component shell generalized coordinates is

$$\left\{ \frac{r_{(1)}^2}{2} \hat{u}_{(1)}(x) \right\} = \left\{ \begin{array}{l} - \int_0^x r_{(1)} \cot \phi_{(1)} \left\{ u_{(1)}(\xi) \right\} dx \\ - \int_0^x r_{(1)} \left\{ v_{(1)}(\xi) \right\} dx \\ \hline - \int_0^{\bar{H}_{(2)}} r_{(2)} \cot \phi_{(2)} \left\{ u_{(2)}(\xi) \right\} dx \\ - \int_0^{\bar{H}_{(2)}} r_{(2)} \left\{ v_{(2)}(\xi) \right\} dx \\ \hline - \int_0^{\bar{H}_{(3)}} r_{(3)} \cot \phi_{(3)} \left\{ u_{(3)}(\xi) \right\} dx \\ - \int_0^{\bar{H}_{(3)}} r_{(3)} \left\{ v_{(3)}(\xi) \right\} dx \end{array} \right. \quad (C.2)$$

$$\left\{ \frac{r_{(2)}^2}{2} \hat{u}_{(2)}(x) \right\} = \left\{ \begin{array}{l} 0 \\ - \int_0^x r_{(2)} \cot \phi_{(2)} \left\{ u_{(2)}(\xi) \right\} dx \\ - \int_0^x r_{(2)} \left\{ v_{(2)}(\xi) \right\} dx \\ \hline - \int_0^{\bar{H}_{(3)}} r_{(3)} \cot \phi_{(3)} \left\{ u_{(3)}(\xi) \right\} dx \\ - \int_0^{\bar{H}_{(3)}} r_{(3)} \left\{ v_{(3)}(\xi) \right\} dx \end{array} \right. \quad (C.3)$$



and

$$\left\{ \frac{r_{(3)}^2}{2} \hat{u}_{(3)}(x) \right\} = \left\{ \begin{array}{c} 0 \\ \text{---} \\ 0 \\ \text{---} \\ - \int_0^x r_{(3)} \cot \phi_{(3)} \left\{ u_{(3)}(\xi) \right\} dx \\ \text{---} \\ - \int_0^x r_{(3)} \left\{ v_{(3)}(\xi) \right\} dx \end{array} \right\} \quad (C.4)$$

where

$$\left\{ u_{(m)}(\xi) \right\} = \left\{ \begin{array}{c} u_1(\xi) \\ \vdots \\ u_{\bar{U}}(\xi) \end{array} \right\}$$

and

$$\left\{ v_{(m)}(\xi) \right\} = \left\{ \begin{array}{c} v_1(\xi) \\ \vdots \\ v_{\bar{V}}(\xi) \end{array} \right\}$$

are the generalized coordinate displacement vectors for tank shell component  $m$ , and  $\phi_{(m)}$  is the meridional angle for tank shell component  $m$ , and  $\bar{U}$  and  $\bar{V}$  are the number of longitudinal and radial generalized coordinates, respectively, in shell component  $m$ .

The column matrix  $\left\{ r_{(m)} \hat{v}_{(m)}(x, r) \right\}$  in terms of the component shell generalized coordinates is

$$\left\{ r_{(1)} \hat{v}_{(1)}(x, r) \right\} = \left\{ \begin{array}{c} r_{(1)} \cot \phi_{(1)} \left\{ u_{(1)}(\xi) \right\} \\ r_{(1)} \left\{ v_{(1)}(\xi) \right\} \\ \text{---} \\ 0 \\ \text{---} \\ 0 \end{array} \right\} - \frac{2 \cot \phi_{(1)}}{r_{(1)}} \left\{ \frac{r_{(1)}^2}{2} \hat{u}_{(1)}(x) \right\} \quad (C.5)$$

$$\left\{ r_{(2)} \hat{v}_{(2)}(x, r) \right\} = \left\{ \begin{array}{c} 0 \\ \text{---} \\ r_{(2)} \cot \phi_{(2)} \left\{ u_{(2)}(\xi) \right\} \\ r_{(2)} \left\{ v_{(2)}(\xi) \right\} \\ \text{---} \\ 0 \end{array} \right\} - \frac{2 \cot \phi_{(2)}}{r_{(2)}} \left\{ \frac{r_{(2)}^2}{2} \hat{u}_{(2)}(x) \right\} \quad (C.6)$$

$$\left\{ r_{(3)} \hat{v}_{(3)}(x, r) \right\} = \left\{ \begin{array}{c} 0 \\ \text{---} \\ 0 \\ \text{---} \\ r_{(3)} \cot \phi_{(3)} \left\{ u_{(3)}(\xi) \right\} \\ r_{(3)} \left\{ v_{(3)}(\xi) \right\} \\ \text{---} \\ 0 \end{array} \right\} - \frac{2 \cot \phi_{(3)}}{r_{(3)}} \left\{ \frac{r_{(3)}^2}{2} \hat{u}_{(3)}(x) \right\} \quad (C.7)$$

C.2 CASE II. UPPER BULKHEAD CONVEX DOWNWARD,  
LOWER BULKHEAD CONVEX DOWNWARD

The Case II configuration is illustrated in Figure C.2 which also defines the tank sections  $m$  for this case. Equation (C.1) for the fluid in tank section (1) is modified as follows. The fluid motion  $\{\hat{u}(x)\}$  in tank section (1) is given by

$$\left\{ \hat{u}_{(1)}(x) \right\} = \frac{2}{(r_{(2)}^2 - r_{(1)}^2)} \left\{ \begin{array}{l} \int_0^x r_{(1)} \cot \phi_{(1)} \left\{ u_{(1)}(\xi) \right\} dx \\ \int_0^x r_{(1)} \left\{ v_{(1)}(\xi) \right\} dx \\ \hline - \int_0^x r_{(2)} \cot \phi_{(2)} \left\{ u_{(2)}(\xi) \right\} dx - \int_0^{\bar{H}_2} r_{(2)} \cot \phi_{(2)} \left\{ u_{(2)}(\xi) \right\} dx \\ - \int_0^x r_{(2)} \left\{ v_{(2)}(\xi) \right\} dx - \int_0^{\bar{H}_2} r_{(2)} \left\{ v_{(2)}(\xi) \right\} dx \\ \hline - \int_0^{\bar{H}_3} r_{(3)} \cot \phi_{(3)} \left\{ u_{(3)}(\xi) \right\} dx \\ - \int_0^{\bar{H}_3} r_{(3)} \left\{ v_{(3)}(\xi) \right\} dx \end{array} \right\} \quad (C. 8)$$

The fluid motion  $\left\{ \hat{v}(x, \hat{r}) \right\}$  in tank section (1) is defined by

$$\left\{ \hat{v}_{(1)}(x, \hat{r}) \right\} = \frac{(\hat{r} - r_{(2)})}{(r_{(1)} - r_{(2)})} \left( \begin{array}{l} \cot \phi_{(1)} \left\{ u_{(1)}(\xi) \right\} \\ \left\{ v_{(1)}(\xi) \right\} \\ \hline 0 \\ \hline 0 \end{array} \right) - \cot \phi_{(1)} \left\{ \hat{u}_{(1)}(x) \right\}$$

$$- \frac{(\hat{r} - r_{(1)})}{(r_{(1)} - r_{(2)})} \left( \begin{array}{l} 0 \\ \hline \cot \phi_{(2)} \left\{ u_{(2)}(\xi) \right\} \\ \left\{ v_{(2)}(\xi) \right\} \\ \hline 0 \end{array} \right) - \cot \phi_{(2)} \left\{ \hat{u}_{(2)}(x) \right\} \quad (C. 9)$$

Upon substitution of Equations (C. 1) and (C. 2) into Equation (4. 1) and integration with respect to  $\hat{r}$  between the limits of  $r_{(1)}$  and  $r_{(2)}$ , one obtains the following expression for the  $m = 1$  portion of Equation (C. 1).

$$\begin{aligned}
 & \frac{1}{\pi \gamma_b} \left[ \overline{M}_b \right]_{(1)} \\
 &= \int_0^{\overline{H}_{(1)}} \frac{4}{\left( r_{(2)}^2 - r_{(1)}^2 \right)} \left\{ \frac{\left( r_{(2)}^2 - r_{(1)}^2 \right)}{2} \hat{u}_{(1)}(x) \right\} \left\{ \frac{\left( r_{(2)}^2 - r_{(1)}^2 \right)}{2} \hat{u}_{(1)}(x) \right\}^T dx \\
 &+ \int_0^{\overline{H}_{(1)}} \frac{\left( r_{(2)}^4 + 8r_{(2)}r_{(1)}^3 - 6r_{(2)}^2r_{(1)}^2 - 3r_{(1)}^4 \right)}{6\left( r_{(1)} - r_{(2)} \right)^2} \left\{ \hat{v}_{(1,1)}(x, r) \right\} \left\{ \hat{v}_{(1,1)}(x, r) \right\}^T dx \\
 &+ \int_0^{\overline{H}_{(1)}} \frac{\left( r_{(2)}^4 + 2r_{(2)}r_{(1)}^3 - 2r_{(1)}r_{(2)}^3 - r_{(1)}^4 \right)}{6\left( r_{(1)} - r_{(2)} \right)^2} \left( \left\{ \hat{v}_{(1,1)}(x, r) \right\} \left\{ \hat{v}_{(1,2)}(x, r) \right\}^T \right. \\
 &\quad \left. + \left\{ \hat{v}_{(1,2)}(x, r) \right\} \left\{ \hat{v}_{(1,1)}(x, r) \right\}^T \right) dx \\
 &+ \int_0^{\overline{H}_{(1)}} \frac{\left( 3r_{(2)}^4 - 8r_{(1)}r_{(2)}^3 + 6r_{(1)}^2r_{(2)}^2 - r_{(1)}^4 \right)}{6\left( r_{(1)} - r_{(2)} \right)^2} \left\{ \hat{v}_{(1,2)}(x, r) \right\} \left\{ \hat{v}_{(1,2)}(x, r) \right\}^T dx
 \end{aligned}
 \tag{C. 10}$$

where

$$\left\{ \frac{r(2)^2 - r(1)^2}{2} \hat{u}_{(1)}(x) \right\} = \left\{ \begin{array}{l} + \int_0^x r(1) \cot \phi(1) \left\{ u_{(1)}(\xi) \right\} dx \\ + \int_0^x r(1) \left\{ v_{(1)}(\xi) \right\} dx \\ \hline - \int_0^{x+\bar{H}(2)} r(2) \cot \phi(2) \left\{ u_{(2)}(\xi) \right\} dx \\ - \int_0^{x+\bar{H}(2)} r(2) \left\{ v_{(2)}(\xi) \right\} dx \\ \hline - \int_0^{\bar{H}(3)} r(3) \cot \phi(3) \left\{ u_{(3)}(\xi) \right\} dx \\ - \int_0^{\bar{H}(3)} r(3) \left\{ v_{(3)}(\xi) \right\} dx \end{array} \right\} \quad (C. 11)$$

$$\left\{ \hat{v}_{(1,1)}(x, r) \right\} = \left\{ \begin{array}{l} \cot \phi(1) \left\{ u_{(1)}(\xi) \right\} \\ \left\{ v_{(1)}(\xi) \right\} \\ \hline 0 \\ \hline 0 \end{array} \right\} - \frac{2 \cot \phi(1)}{r(2)^2 - r(1)^2} \left\{ \frac{r(2)^2 - r(1)^2}{2} \hat{u}_{(1)}(x) \right\} \quad (C. 12)$$

$$\left\{ \hat{v}_{(1,2)}(x, r) \right\} = \left\{ \begin{array}{l} 0 \\ \hline \cot \phi(2) \left\{ u_{(2)}(\xi) \right\} \\ \left\{ v_{(2)}(\xi) \right\} \\ \hline 0 \end{array} \right\} - \frac{2 \cot \phi(2)}{r(2)^2 - r(1)^2} \left\{ \frac{r(2)^2 - r(1)^2}{2} \hat{u}_{(1)}(x) \right\} \quad (C. 13)$$

The expressions for the  $m = 2$  and  $m = 3$  portions of Equation (C. 1) remain unchanged. In summary for evaluating the equivalent of Equation (C. 1) for Case II tank configuration, use Equations (C. 10), (C. 11), (C. 12) and (C. 13) for  $m = 1$ , and Equations (C. 1), (C. 3), (C. 4), (C. 6) and (C. 7) for  $m = 2$  and  $m = 3$ .

**C. 3 CASE III. UPPER BULKHEAD CONVEX UPWARD, LOWER BULKHEAD CONVEX UPWARD**

The Case III configuration is illustrated in Figure C. 3 which also defines the tank sections  $m$  for this case. Equation (C. 1) for the fluid in tank section (3) is modified as follows. The fluid motion  $\{\hat{u}(x)\}$  in tank section (3) is given by

$$\left\{ \hat{u}_{(3)}(x) \right\} = \frac{(r_{(2)}^2 - r_{(3)}^2)}{2} \left\{ \begin{array}{l} 0 \\ - \int_0^x r_{(2)} \cot \phi_{(2)} \left\{ u_{(2)}(\xi) \right\} \\ - \int_0^x r_{(2)} \left\{ v_{(2)}(\xi) \right\} \\ - \int_0^x r_{(3)} \cot \phi_{(3)} \left\{ u_{(3)}(\xi) \right\} \\ - \int_0^x r_{(3)} \left\{ v_{(3)}(\xi) \right\} \end{array} \right\} \quad (C. 14)$$

The fluid motion  $\{\hat{v}(x, \hat{r})\}$  in tank section (3) is given by

$$\begin{aligned}
 \left\{ \hat{v}_{(3)}(x, \hat{r}) \right\} &= \frac{(\hat{r} - r_{(2)})}{(r_{(3)} - r_{(2)})} \left( \begin{array}{c} 0 \\ \text{---} \\ 0 \\ \text{---} \\ \cot \phi_{(3)} \left\{ u_{(3)}(\xi) \right\} \\ \text{---} \\ \left\{ v_{(3)}(\xi) \right\} \end{array} \right) - \cot \phi_{(3)} \left\{ \hat{u}_{(3)}(x) \right\} \\
 &- \frac{(\hat{r} - r_{(3)})}{(r_{(3)} - r_{(2)})} \left( \begin{array}{c} 0 \\ \text{---} \\ \cot \phi_{(2)} \left\{ u_{(2)}(\xi) \right\} \\ \text{---} \\ \left\{ v_{(2)}(\xi) \right\} \\ \text{---} \\ 0 \end{array} \right) - \cot \phi_{(2)} \left\{ \hat{u}_{(3)}(x) \right\}
 \end{aligned} \tag{C. 15}$$

Upon substitution of Equations (C. 14) and (C. 15) into Equation (4. 1) and integration with respect to  $\hat{r}$  between the limits of  $r_{(3)}$  and  $r_{(2)}$ , one obtains the following expression for the  $m = 3$  portion of Equation (C. 1).

$$\begin{aligned}
& \frac{1}{\pi \gamma_b} \left[ \bar{M}_b \right]_{(3)} \\
&= \int_0^{\bar{H}_{(3)}} \frac{4}{(r_{(2)}^2 - r_{(3)}^2)} \left\{ \frac{(r_{(2)}^2 - r_{(3)}^2)}{2} \hat{u}_{(3)}(x) \right\} \left\{ \frac{(r_{(2)}^2 - r_{(3)}^2)}{2} \hat{u}_{(3)}(x) \right\}^T dx \\
&+ \int_0^{\bar{H}_{(3)}} \frac{(r_{(2)}^4 + 8r_{(2)}r_{(3)}^3 - 6r_{(2)}^2r_{(3)}^2 - 3r_{(3)}^4)}{6(r_{(3)} - r_{(2)})^2} \left\{ \hat{v}_{(3,3)}(x, r) \right\} \left\{ \hat{v}_{(3,3)}(x, r) \right\}^T dx \\
&+ \int_0^{\bar{H}_{(3)}} \frac{(r_{(2)}^4 + 2r_{(2)}r_{(3)}^3 - 2r_{(2)}^3r_{(3)} - r_{(3)}^4)}{6(r_{(3)} - r_{(2)})^2} \left( \left\{ \hat{v}_{(3,3)}(x, r) \right\} \left\{ \hat{v}_{(3,2)}(x, r) \right\}^T \right. \\
&\quad \left. + \left\{ \hat{v}_{(3,2)}(x, r) \right\} \left\{ \hat{v}_{(3,3)}(x, r) \right\}^T \right) dx \\
&+ \int_0^{\bar{H}_{(3)}} \frac{(3r_{(2)}^4 - 8r_{(2)}r_{(3)}^3 + 6r_{(2)}^2r_{(3)}^2 - r_{(3)}^4)}{6(r_{(3)} - r_{(2)})^2} \left\{ \hat{v}_{(3,2)}(x, r) \right\} \left\{ \hat{v}_{(3,2)}(x, r) \right\}^T dx
\end{aligned}$$

where

(C. 16)

$$\left\{ \frac{(r_{(2)}^2 - r_{(3)}^2)}{2} \hat{u}_{(3)}(x) \right\} = \left\{ \begin{array}{l} 0 \\ \hline - \int_0^x r_{(2)} \cot \phi_{(2)} \left\{ u_{(2)}(\xi) \right\} dx \\ - \int_0^x r_{(2)} \left\{ v_{(2)}(\xi) \right\} dx \\ \hline + \int_0^x r_{(3)} \cot \phi_{(3)} \left\{ u_{(3)}(\xi) \right\} dx \\ + \int_0^x r_{(3)} \left\{ v_{(3)}(\xi) \right\} dx \end{array} \right\} \quad (C. 17)$$



$$\left\{ \hat{v}_{(3,3)}(x, r) \right\} = \left\{ \begin{array}{c} 0 \\ \text{---} \\ 0 \\ \text{---} \\ \cot \phi_{(3)} \left\{ u_{(3)}(\xi) \right\} \\ \left\{ v_{(3)}(\xi) \right\} \end{array} \right\} - \frac{2 \cot \phi_{(3)}}{r_{(2)}^2 - r_{(3)}^2} \left\{ \frac{r_{(2)}^2 - r_{(3)}^2}{2} \hat{u}_{(3)}(x) \right\} \quad (\text{C. 18})$$

$$\left\{ \hat{v}_{(3,2)}(x, r) \right\} = \left\{ \begin{array}{c} 0 \\ \text{---} \\ \cot \phi_{(2)} \left\{ u_{(2)}(\xi) \right\} \\ \left\{ v_{(2)}(\xi) \right\} \\ \text{---} \\ 0 \end{array} \right\} - \frac{2 \cot \phi_{(2)}}{r_{(2)}^2 - r_{(3)}^2} \left\{ \frac{r_{(2)}^2 - r_{(3)}^2}{2} \hat{u}_{(3)}(x) \right\} \quad (\text{C. 19})$$

Equation (C.1) remains valid for  $m = 1$  and  $m = 2$ , however, Equations (C.2) and (C.3), respectively, become

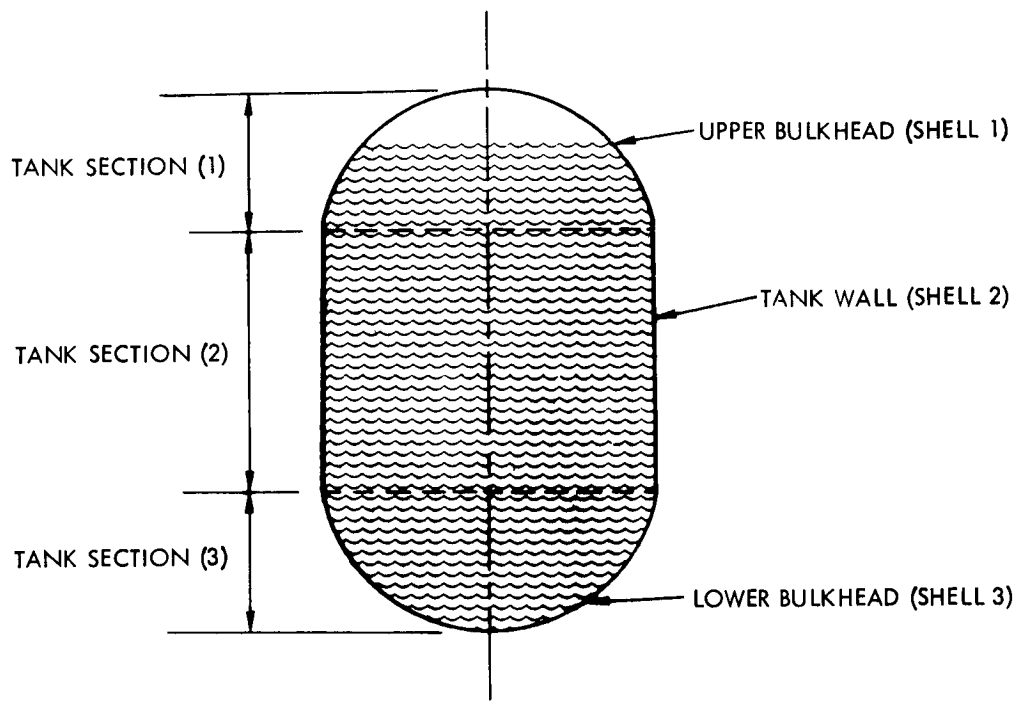
$$\left\{ \frac{r_{(1)}^2}{2} \hat{u}_{(1)}(x) \right\} = \left\{ \begin{array}{l} - \int_0^x r_{(1)} \cot \phi_{(1)} \left\{ u_{(1)}(\xi) \right\} dx \\ - \int_0^x r_{(1)} \left\{ v_{(1)}(\xi) \right\} dx \\ \hline - \int_{\bar{H}_{(3)}}^{\bar{H}_{(2)}} r_{(2)} \cot \phi_{(2)} \left\{ u_{(2)}(\xi) \right\} dx \\ - \int_{\bar{H}_{(3)}}^{\bar{H}_{(2)}} r_{(2)} \left\{ v_{(2)}(\xi) \right\} dx \\ \hline + \int_0^{\bar{H}_{(3)}} r_{(3)} \cot \phi_{(3)} \left\{ u_{(3)}(\xi) \right\} dx \\ + \int_0^{\bar{H}_{(3)}} r_{(3)} \left\{ v_{(3)}(\xi) \right\} dx \end{array} \right. \quad (\text{C.20})$$

$$\left\{ \frac{r_{(2)}^2}{2} \hat{u}_{(2)}(x) \right\} = \left\{ \begin{array}{l} 0 \\ - \int_{\bar{H}_{(3)}}^x r_{(2)} \cot \phi_{(2)} \left\{ u_{(2)}(\xi) \right\} dx \\ - \int_{\bar{H}_{(3)}}^x r_{(2)} \left\{ v_{(2)}(\xi) \right\} dx \\ + \int_0^{\bar{H}_{(3)}} r_{(3)} \cot \phi_{(3)} \left\{ u_{(3)}(\xi) \right\} dx \\ + \int_0^{\bar{H}_{(3)}} r_{(3)} \left\{ v_{(3)}(\xi) \right\} dx \end{array} \right\} \quad (C.21)$$

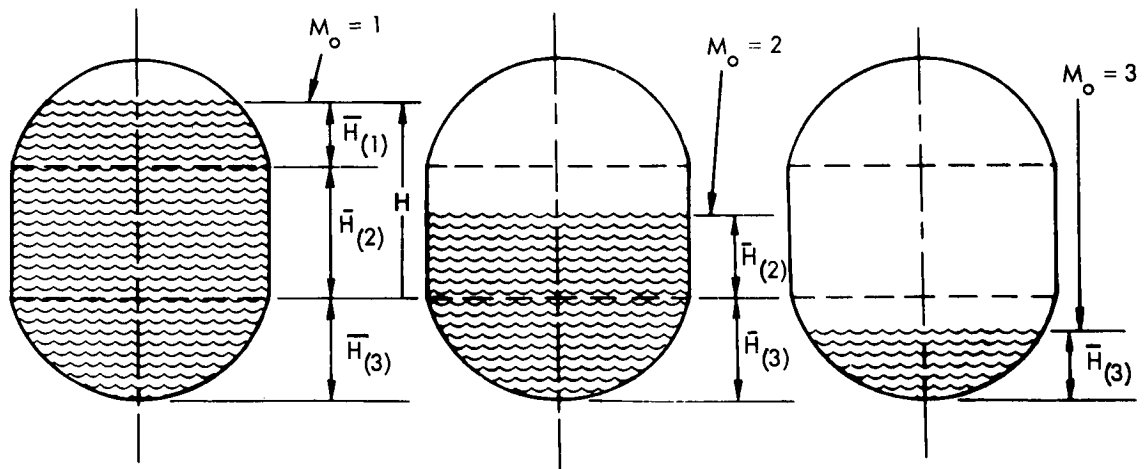
In summary for evaluating the equivalent of Equation (C.1) for Case III tank configuration, use Equations (C.1), (C.20) and (C.5) for  $m = 1$ , use Equations (C.1) with limits of integration

$$\int_{\bar{H}_{(3)}}^{\bar{H}_{(2)}}$$

Equations (C.21) and (C.6) for  $m = 2$ , and use Equations (C.16), (C.14) and (C.15) for  $m = 3$ .



A. DEFINITION OF TANK SECTIONS



B. TANK SECTION FLUID LEVELS

Figure C.1. Case I Tank Configuration

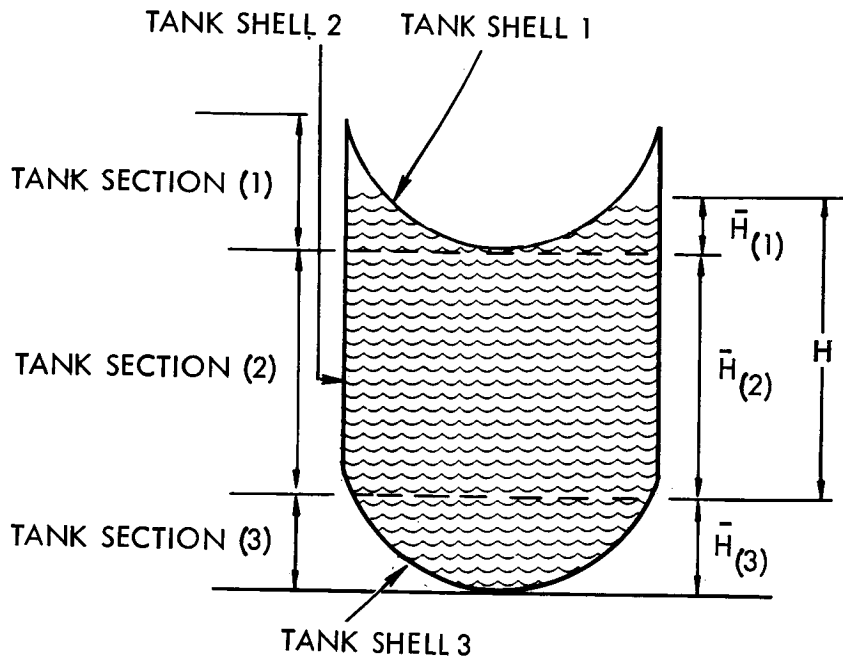


Figure C. 2. Case II Tank Configuration

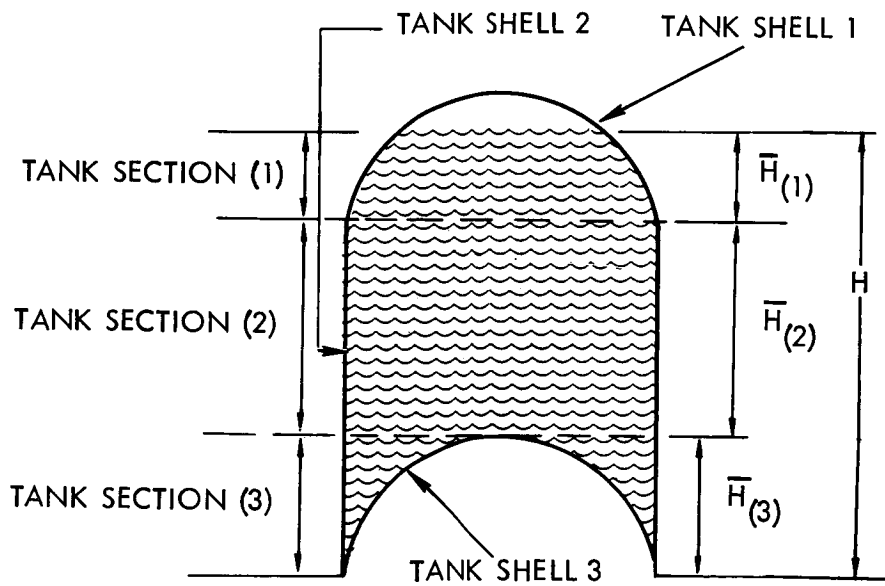


Figure C. 3. Case III Tank Configuration

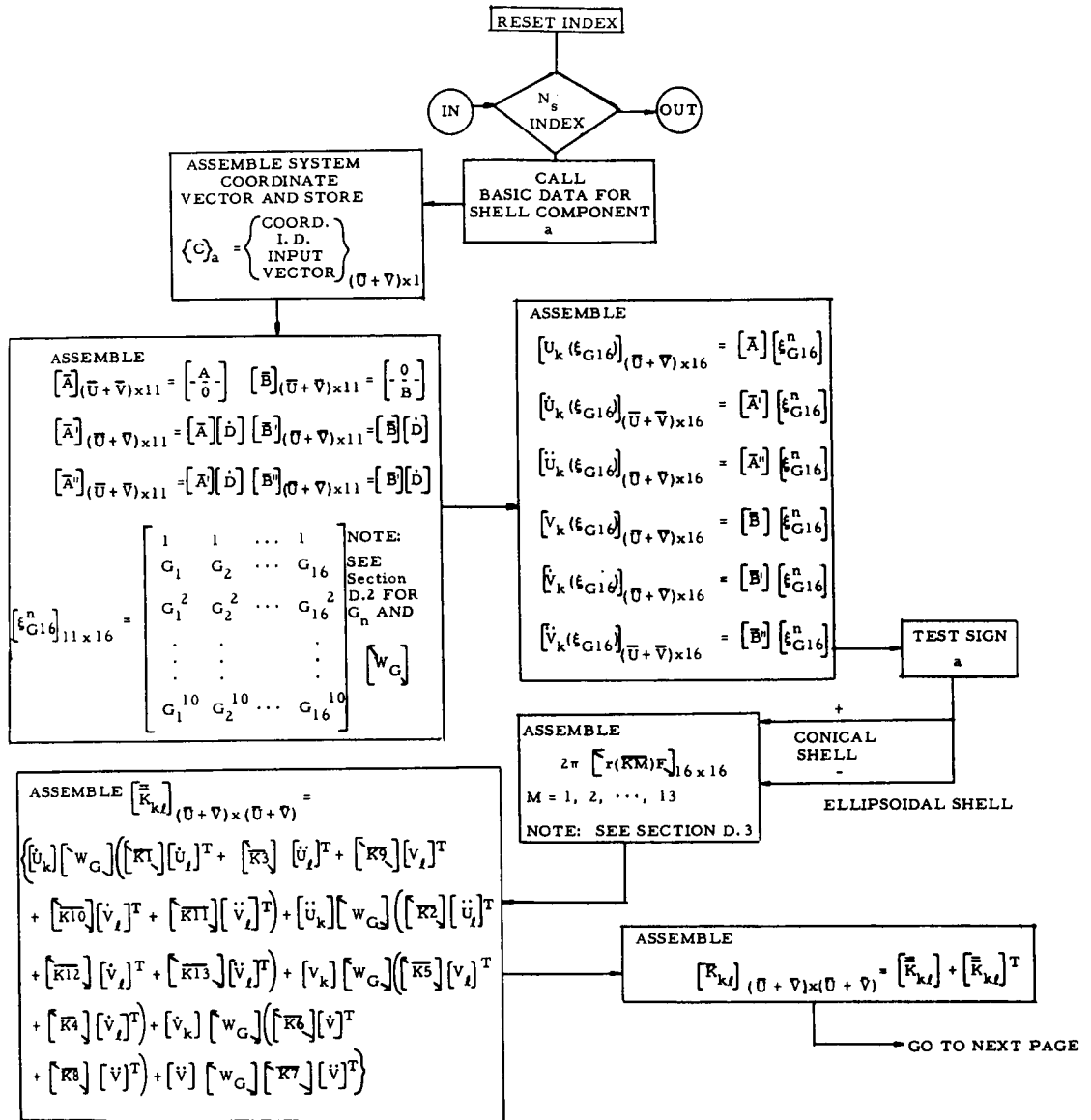
## APPENDIX D

### CALCULATION OF THE SHELL STIFFNESS AND MASS MATRICES

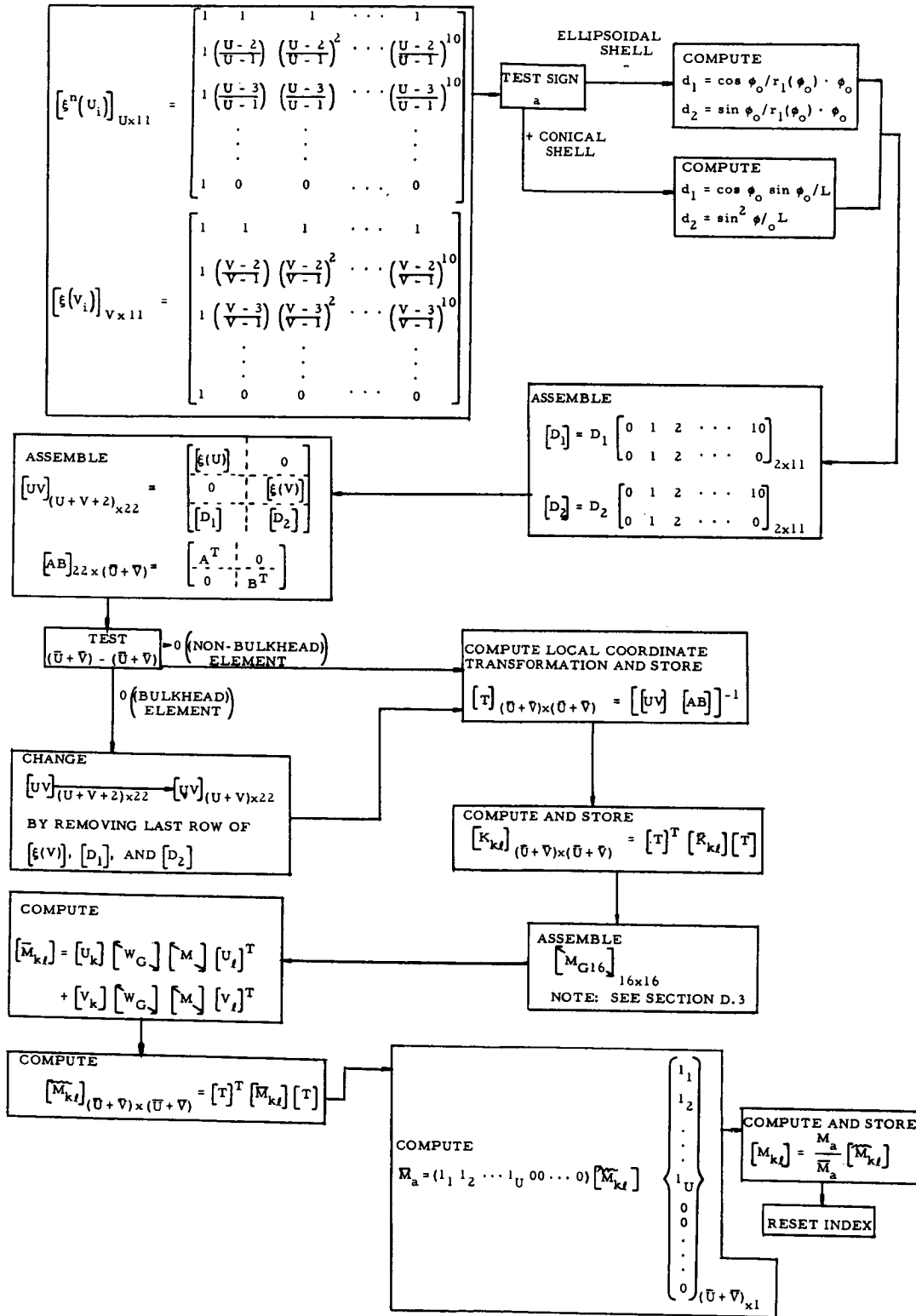
In this section the equations for the shell stiffness and mass matrices presented in Section 3.0 are rewritten in a form more suitable for digital programming. As previously mentioned, integration of these equations is accomplished using a sixteen (16) point Gaussian weighting matrix integration scheme.<sup>5</sup>

These operations may be performed in a straightforward fashion using matrix operations. The equations in this section are, therefore, written in matrix notation and are identical to the equations which are coded into the digital program. For a more complete understanding of the steps required in the construction of the shell stiffness and mass matrices, a functional flow chart depicting the program operations is presented in Section D.1. The weighting matrix coefficients are given in Section D.2 and other detailed expressions are provided in Sections D.3, D.4 and D.5 for elements  $\overline{KM}$ ,  $M$  and for the initial stresses  $N_\phi$ .

# D.1 FUNCTIONAL FLOW CHART FOR CALCULATION OF SHELL STIFFNESS AND MASS MATRICES



### D.1 FUNCTIONAL FLOW CHART FOR CALCULATION OF SHELL STIFFNESS AND MASS MATRICES (Continued)





## D.2 GAUSSIAN WEIGHTING MATRIX TABLES

DATA FOR $\left[ \xi_{G16}^n \right]$			DATA $\left[ W_G \right]$		
G1	0.00529	95325	W1	0.01357	62297
G2	0.02771	24885	W2	0.03112	67620
G3	0.06718	43988	W3	0.04757	92558
G4	0.12229	77958	W4	0.06231	44857
G5	0.19106	18778	W5	0.07479	79944
G6	0.27099	16112	W6	0.08457	82597
G7	0.35919	82246	W7	0.09130	17075
G8	0.45249	37451	W8	0.09472	53052
G9	0.54750	62549	W9	0.09472	53052
G10	0.64080	17754	W10	0.09130	17075
G11	0.72900	83888	W11	0.08457	82597
G12	0.80893	81222	W12	0.07479	79944
G13	0.87770	22042	W13	0.06231	44857
G14	0.93281	56012	W14	0.04757	92558
G15	0.97228	75115	W15	0.03112	67620
G16	0.99470	04675	W16	0.01357	62297

### D.3 ASSEMBLY OF $\left[ \overline{rKMF} \right]$ FOR $M = 1, 2, \dots, 13$ :

The equations for  $\overline{KM}$  and  $F$  are presented below and are evaluated at the points  $\xi = G_1, G_2, \dots, G_{16}$ .

$$\overline{K1} = \frac{1}{2} K1 = \frac{1}{2} \left[ C_{11} \sin^2 \phi + C_{33} \frac{1}{r_1^2} \left( \sin \phi + \frac{\dot{r}_1}{r_1} \cos \phi \right)^2 \right. \\ \left. - C_{34} \frac{2 \cos^2 \phi}{r \cdot r_1} \left( \sin \phi + \frac{\dot{r}_1}{r} \cos \phi \right) + C_{44} \frac{\cos^4 \phi}{r^2} + N_{\phi}^{\circ} \cos^2 \phi \right]$$

$$\overline{K2} = \frac{1}{2} K2 = \frac{1}{2} \left( C_{33} \cos^2 \phi \right)$$

$$\overline{K3} = K3 = -C_{33} \frac{\cos \phi}{r_1} \left( \sin \phi + \frac{\dot{r}_1}{r_1} \cos \phi \right) + C_{34} \frac{\cos^3 \phi}{r}$$

$$\overline{K4} = K4 = C_{12} \frac{\cos \phi}{r}$$

$$\overline{K5} = \frac{1}{2} K5 = \frac{1}{2} \left( C_{22} \frac{1}{r^2} \right)$$

$$\overline{K6} = \frac{1}{2} K6 = \frac{1}{2} \left[ C_{11} \cos^2 \phi + C_{33} \frac{1}{r_1^2} \left( \cos \phi - \frac{\dot{r}_1}{r_1} \sin \phi \right)^2 \right. \\ \left. + C_{34} \frac{2 \sin \phi \cos \phi}{r \cdot r_1} \left( \cos \phi - \frac{\dot{r}_1}{r_1} \sin \phi \right) \right. \\ \left. + C_{44} \frac{\sin^2 \phi \cos^2 \phi}{r^2} + N_{\phi}^{\circ} \sin^2 \phi \right]$$

$$\overline{K7} = \frac{1}{2} K7 = \frac{1}{2} \left( C_{33} \sin^2 \phi \right)$$

$$\overline{K8} = K8 = C_{33} \frac{\sin \phi}{r_1} \left( \cos \phi - \frac{\dot{r}_1}{r_1} \sin \phi \right) + C_{34} \frac{\sin^2 \phi \cos \phi}{r}$$

$$\overline{K9} = K9 = -C_{12} \frac{\sin \phi}{r}$$

$$\begin{aligned} \overline{K10} = K10 = & \left[ -C_{11} \sin \phi \cos \phi - C_{33} \frac{1}{r_1^2} \left( \cos \phi - \frac{\dot{r}_1}{r_1} \sin \phi \right) \left( \sin \phi + \frac{\dot{r}_1}{r_1} \cos \phi \right) \right. \\ & - C_{34} \frac{\sin \phi \cos \phi}{r \cdot r_1} \left( \sin \phi + \frac{\dot{r}_1}{r_1} \cos \phi \right) \\ & + C_{34} \frac{\cos^2 \phi}{r \cdot r_1} \left( \cos \phi - \frac{\dot{r}_1}{r_1} \sin \phi \right) \\ & \left. + C_{44} \frac{\sin \phi \cos^3 \phi}{r^2} + N_\phi^o \sin \phi \cos \phi \right] \end{aligned}$$

$$\overline{K11} = K11 = \left[ -C_{33} \frac{1}{r_1} \left( \sin \phi + \frac{\dot{r}_1}{r_1} \cos \phi \right) \sin \phi + C_{34} \frac{\sin \phi \cos^2 \phi}{r} \right]$$

$$\overline{K12} = K12 = \left[ C_{33} \left( \cos \phi - \frac{\dot{r}_1}{r} \sin \phi \right) \frac{\cos \phi}{r_1} + C_{34} \frac{\sin \phi \cos^2 \phi}{r} \right]$$

$$\overline{K13} = K13 = C_{33} \sin \phi \cos \phi$$

$$\frac{\dot{r}_1}{r} = \frac{-3(k^2 - 1) \sin \phi \cos \phi}{[(k^2 - 1) \sin^2 \phi + 1]}$$

$$M = 2\pi\gamma_a rtF$$

and

$$F = \frac{|L|}{\sin \theta_o} \text{ for conic}$$

$$= r_1 \phi_o \text{ for convex upward ellipsoidal bulkhead}$$

$$= r_1(\phi_o - \pi) \text{ for convex downward ellipsoidal bulkhead}$$

D.4 INITIAL STRESS FOR CONIC

CONIC

INPUT  
 $\phi_o, R_2, L, W$   
 $w_i, h_i, p_i, p_e$

DEFINE

$$N_{\phi_1} = \frac{1}{2\pi r \sin \phi_o} \left[ gW + (p_i - p_e) \pi (r^2 - R_1'^2) \right]$$

$$N_{\phi_2} = \frac{g w_i L^3 \cot \phi_o}{r \sin \phi_o} \left[ \frac{R_2 h_i}{L^2} \left( \frac{h_i}{L} - \xi \right) - \frac{1}{2} \left( \frac{R_2}{L} + \frac{h_i}{L} \cot \phi_o \right) \left( \frac{h_i^2}{L^2} - \xi^2 \right) + \frac{1}{3} \left( \frac{h_i^3}{L^3} - \xi^3 \right) \cot \phi_o \right]$$

$$N_{\phi_3} = \frac{g w_i L^3 \cot \phi_o}{r \sin \phi_o} \left[ \frac{R_2 h_i}{L^2} (1 - \xi) - \frac{1}{2} \left( \frac{R_2}{L} + \frac{h_i}{L} \cot \phi_o \right) (1 - \xi^2) + \frac{1}{3} (1 - \xi^3) \cot \phi_o \right]$$

where

$$r = L \left( \frac{R_2}{L} - \xi \cot \phi_o \right)$$

$\frac{h_i}{L} \leq 1$

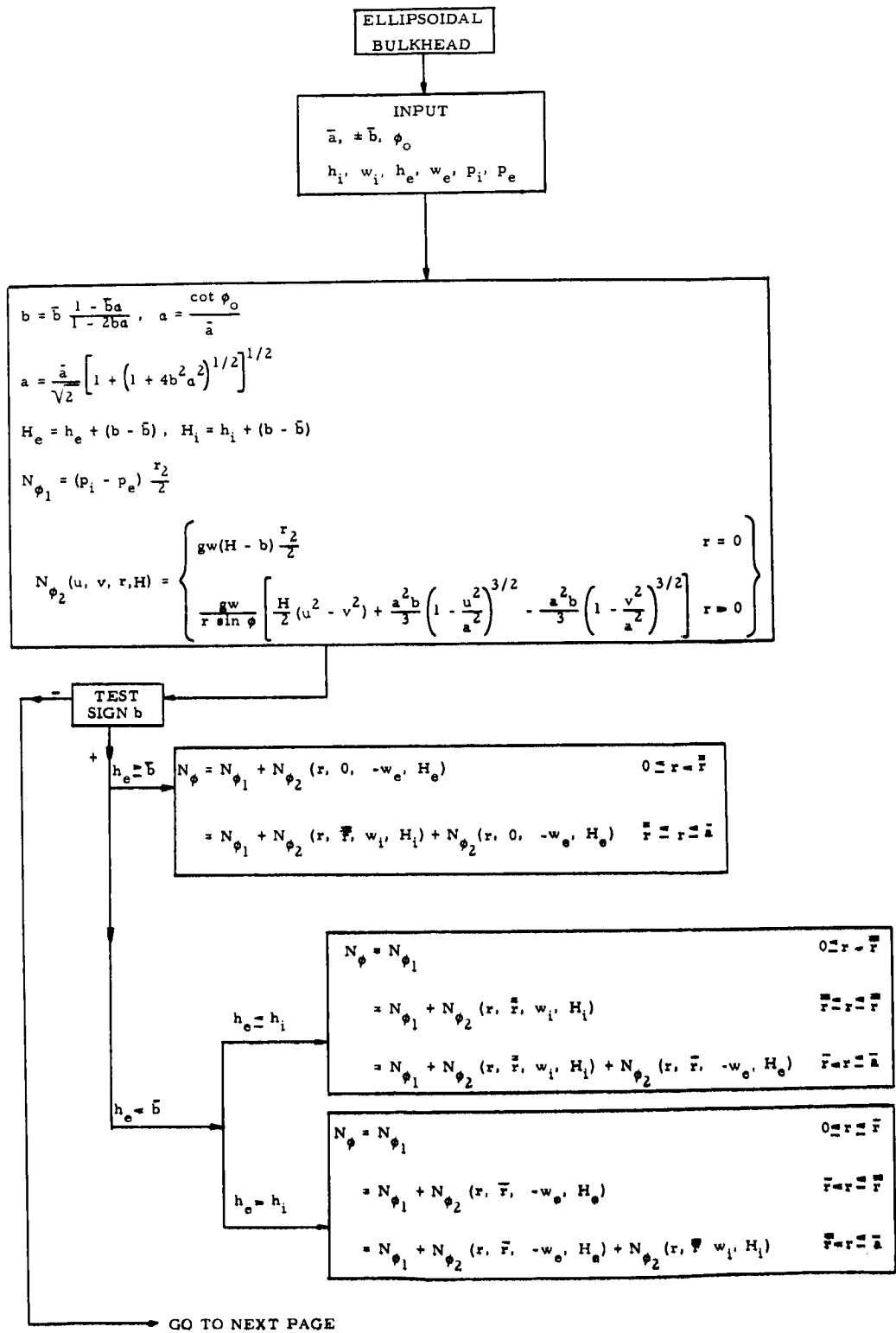
$$N_{\phi} = N_{\phi_1} + N_{\phi_2} \quad 0 < \xi < \frac{h_i}{L}$$

$$= N_{\phi_1} \quad \frac{h_i}{L} \leq \xi < 1$$

$\frac{h_i}{L} > 1$

$$N_{\phi} = N_{\phi_1} + N_{\phi_3} \quad 0 < \xi < 1$$

# D.5 INITIAL STRESS FOR ELLIPSOIDAL BULKHEAD



$$h_i = h_a$$

$$\begin{aligned}
 N_\phi &= N_{\phi_1} + N_{\phi_2}(r, 0, -w_i, H_i) + N_{\phi_2}(r, 0, w_e, H_e) & 0 \leq r \leq \bar{r} \\
 &= N_{\phi_1} + N_{\phi_2}(\bar{r}, 0, -w_i, H_i) + N_{\phi_2}(r, 0, w_e, H_e) & \bar{r} \leq r \leq \bar{\bar{r}} \\
 &= N_{\phi_1} + N_{\phi_2}(\bar{r}, 0, -w_i, H_i) + N_{\phi_2}(\bar{\bar{r}}, 0, w_e, H_e) & \bar{\bar{r}} \leq r \leq \bar{a}
 \end{aligned}$$

$$h_i \leq h_e \leq \bar{b}$$

$$\begin{aligned}
 N_\phi &= N_{\phi_1} + N_{\phi_2}(r, 0, -w_i, H_i) + N_{\phi_2}(r, 0, w_e, H_e) & 0 \leq r \leq \bar{r} \\
 &= N_{\phi_1} + N_{\phi_2}(r, 0, -w_i, H_i) + N_{\phi_2}(\bar{\bar{r}}, 0, w_e, H_e) & \bar{r} \leq r \leq \bar{\bar{r}} \\
 &= N_{\phi_1} + N_{\phi_2}(\bar{r}, 0, -w_i, H_i) + N_{\phi_2}(\bar{\bar{r}}, 0, w_e, H_e) & \bar{\bar{r}} \leq r \leq \bar{a}
 \end{aligned}$$

Note: when

$$b > 0, \quad \bar{r} = a \sqrt{1 - \frac{(h_e + b - |\bar{b}|)^2}{b^2}}$$

$$\bar{\bar{r}} = a \sqrt{1 - \frac{(h_i + b - |\bar{b}|)^2}{b^2}}$$

$$b < 0, \quad \bar{r} = a \sqrt{1 - \frac{(h_i + b - |\bar{b}|)^2}{b^2}}$$

$$\bar{\bar{r}} = a \sqrt{1 - \frac{(h_e + b - |\bar{b}|)^2}{b^2}}$$

## APPENDIX E

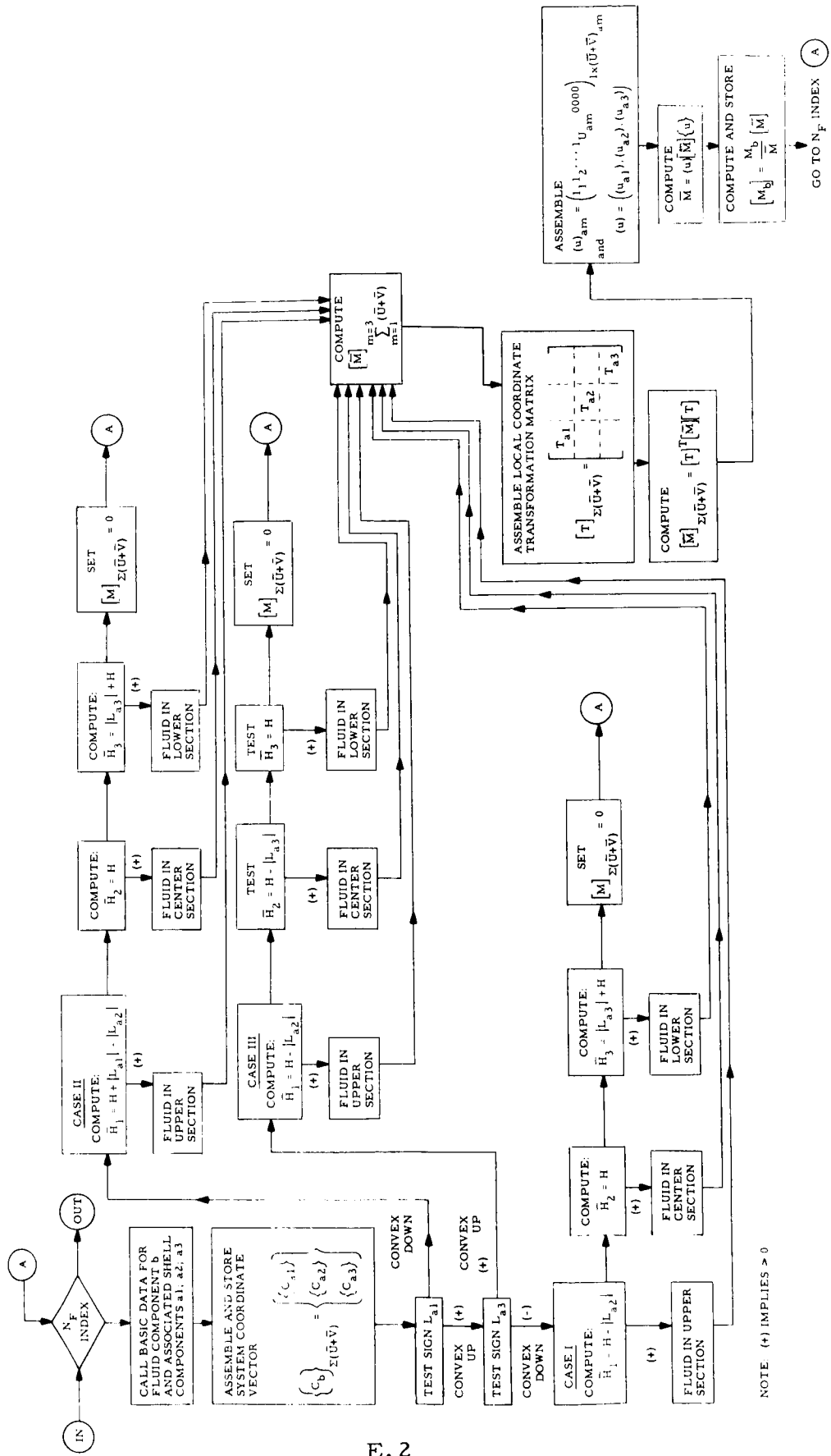
### CALCULATION OF FLUID MASS MATRIX

The construction of the fluid mass matrix presented in Section 4.0 for three tank configurations differs from the construction of the shell inertial and stiffness characteristics insofar as the fluid equations involve double integrations. As mentioned in Section 4.0, these integrations are performed using a Lagrangian integration scheme. Although this technique is similar to the Gaussian method of integration used in the computation of the shell matrices described in Appendix D, only the Lagrangian technique is adaptable to double integration. The digital program utilizes a 21-point Lagrangian weighting matrix which is constructed by combining two 11-point matrices tabulated in the above reference. The increased number of points provides additional numerical accuracy. In the following pages, the fluid equations are rewritten to accommodate the integrations using the weighting matrix technique.\* A functional flow chart outlining the complete mass matrix calculation is provided.

---

\*The notation of this appendix corresponds to the notation utilized in the digital program.

# E.1 FUNCTIONAL FLOW CHART FOR CALCULATION OF FLUID MASS MATRIX





## E. 2 GENERAL MATRIX EQUATION FOR MASS MATRIX $[\overline{M}]$

$$\begin{aligned}
 [\overline{M}]_{\sum_{m=1}^{m=3} (\overline{U}+\overline{V})_{a(m)}} &= [\overline{M}_1] + [\overline{M}_2] \\
 [\overline{M}_1]_{\sum_{m=1}^{m=3} (\overline{U}+\overline{V})_{am}} &= \begin{bmatrix} [\overline{U}_k^1] [K1] [W] [\overline{U}_k^1]^T \\ + [\overline{U}_k^2] [K2] [W] [\overline{U}_k^2]^T \\ + [\overline{U}_k^3] [K3] [W] [\overline{U}_k^3]^T \end{bmatrix} \\
 [\overline{M}_2]_{\sum_{m=1}^{m=3} (\overline{U}+\overline{V})_{am}} &= \begin{bmatrix} [\overline{V}_k^1] [C1] [W] [\overline{V}_k^1]^T + [\overline{V}_k^1] [C2] [W] [\overline{\overline{V}}_k^1]^T \\ [\overline{\overline{V}}_k^1] [C2] [W] [\overline{V}_k^1]^T + [\overline{\overline{V}}_k^1] [C3] [W] [\overline{\overline{V}}_k^1]^T \\ [\overline{V}_k^2] [C4] [W] [\overline{V}_k^2]^T \\ [\overline{V}_k^3] [C5] [W] [\overline{V}_k^3]^T + [\overline{V}_k^3] [C6] [W] [\overline{\overline{V}}_k^3]^T \\ [\overline{\overline{V}}_k^3] [C6] [W] [\overline{V}_k^3]^T + [\overline{\overline{V}}_k^3] [C7] [W] [\overline{\overline{V}}_k^3]^T \end{bmatrix}
 \end{aligned}$$

$$\begin{aligned}
 \begin{bmatrix} \bar{U}_k^1 \\ \sum (U+V)_{x21} \end{bmatrix} &= \begin{bmatrix} \begin{bmatrix} U_{k1} \\ V_{k1} \end{bmatrix} \begin{bmatrix} KU_1 \\ KV_1 \end{bmatrix} \begin{bmatrix} \bar{W} \end{bmatrix} \\ \hline \begin{bmatrix} U_{k2} \\ V_{k2} \end{bmatrix} \begin{bmatrix} KU_2 \\ KV_2 \end{bmatrix} \begin{bmatrix} \bar{W} \end{bmatrix} + \begin{bmatrix} \bar{U}_{k2} \\ \bar{V}_{k2} \end{bmatrix} \begin{bmatrix} \overline{KU}_2 \\ \overline{KV}_2 \end{bmatrix} \begin{bmatrix} \bar{W} \end{bmatrix} \\ \hline \begin{bmatrix} U_{k3} \\ V_{k3} \end{bmatrix} \begin{bmatrix} KU_3 \\ KV_3 \end{bmatrix} \begin{bmatrix} \bar{W} \end{bmatrix} \end{bmatrix}
 \end{aligned}$$

$$\begin{aligned}
 \begin{bmatrix} \bar{U}_k^2 \\ \sum (\bar{U}+\bar{V})_{x21} \end{bmatrix} &= \begin{bmatrix} \begin{bmatrix} U_{k2} \\ V_{k2} \end{bmatrix} \begin{bmatrix} KU_2 \\ KV_2 \end{bmatrix} \begin{bmatrix} \bar{W} \end{bmatrix} + \begin{bmatrix} \bar{U}_{k2} \\ \bar{V}_{k2} \end{bmatrix} \begin{bmatrix} \overline{KU}_2 \\ \overline{KV}_2 \end{bmatrix} \begin{bmatrix} \bar{W} \end{bmatrix} \\ \hline \begin{bmatrix} U_{k3} \\ V_{k3} \end{bmatrix} \begin{bmatrix} KU_3 \\ KV_3 \end{bmatrix} \begin{bmatrix} \bar{W} \end{bmatrix} \end{bmatrix}
 \end{aligned}$$

$$\begin{aligned}
 \begin{bmatrix} \bar{U}_k^3 \\ \sum (\bar{U}+\bar{V})_{x21} \end{bmatrix} &= \begin{bmatrix} \begin{bmatrix} \bar{U}_{k2} \\ \bar{V}_{k2} \end{bmatrix} \begin{bmatrix} \overline{KU}_2 \\ \overline{KV}_2 \end{bmatrix} \begin{bmatrix} \bar{W} \end{bmatrix} \\ \hline \begin{bmatrix} U_{k3} \\ V_{k3} \end{bmatrix} \begin{bmatrix} KU_3 \\ KV_3 \end{bmatrix} \begin{bmatrix} \bar{W} \end{bmatrix} \end{bmatrix}
 \end{aligned}$$

$$\begin{bmatrix} \bar{V}_k^1 \\ \sum(\bar{U}+\bar{V})_{x21} \end{bmatrix} = \begin{bmatrix} [U_{k1}] & [KU_4] \\ [V_{k1}] & [KV_4] \\ \hline 0 \\ \hline 0 \end{bmatrix} + \begin{bmatrix} \bar{U}_k^1 \\ [K4] \end{bmatrix}$$

$$\begin{bmatrix} \bar{V}_k^1 \\ \sum(\bar{U}+\bar{V})_{x21} \end{bmatrix} = \begin{bmatrix} 0 \\ \hline [\bar{U}_{k2}] & [\bar{KU}_5] \\ [V_{k2}] & [\bar{KV}_5] \\ \hline 0 \end{bmatrix} + \begin{bmatrix} \bar{U}_k^1 \\ [\bar{K5}] \end{bmatrix}$$

$$\begin{bmatrix} \bar{V}_k^2 \\ \sum(\bar{U}+\bar{V})_{x21} \end{bmatrix} = \begin{bmatrix} 0 \\ \hline [U_{k2}] & [KU_5] \\ [V_{k2}] & [KV_5] \\ \hline 0 \end{bmatrix} + \begin{bmatrix} \bar{U}_k^2 \\ [K5] \end{bmatrix}$$

$$\begin{bmatrix} \bar{V}_k^3 \\ \sum (\bar{U} + \bar{V})_{x21} \end{bmatrix} = \begin{bmatrix} 0 \\ \text{---} \\ 0 \\ \text{---} \\ \begin{bmatrix} U_{k3} & KU_6 \\ V_{k3} & KV_6 \end{bmatrix} \end{bmatrix} + \begin{bmatrix} \bar{U}_k^3 \\ \bar{K6} \end{bmatrix}$$

$$\begin{bmatrix} \bar{\bar{V}}_k^3 \\ \sum (\bar{U} + \bar{V})_{x21} \end{bmatrix} = \begin{bmatrix} 0 \\ \text{---} \\ \begin{bmatrix} \bar{\bar{U}}_{k2} & \bar{\bar{KU}}_5 \\ \bar{\bar{V}}_{k2} & \bar{\bar{KV}}_5 \end{bmatrix} \\ \text{---} \\ 0 \end{bmatrix} + \begin{bmatrix} \bar{\bar{U}}_k^3 \\ \bar{\bar{K5}} \end{bmatrix}$$

$$\begin{bmatrix} U_{k1} \\ \bar{U}_{a1} \end{bmatrix}_{x21} = \begin{bmatrix} A_{a1} \\ \xi_{a1}^n \end{bmatrix}$$

$$\begin{bmatrix} V_{k1} \\ \bar{V}_{a1} \end{bmatrix}_{x21} = \begin{bmatrix} B_{a1} \\ \xi_{a1}^n \end{bmatrix}$$

$$\begin{bmatrix} U_{k2} \\ \bar{U}_{a2} \end{bmatrix}_{x21} = \begin{bmatrix} A_{a2} \\ \xi_{a2}^n \end{bmatrix} \quad \begin{bmatrix} \bar{U}_{k2} \\ \bar{U}_{a2} \end{bmatrix}_{x21} = \begin{bmatrix} A_{a2} \\ \bar{\xi}_{a2}^n \end{bmatrix}$$

$$\begin{bmatrix} V_{k2} \\ \bar{V}_{a2} \end{bmatrix}_{x21} = \begin{bmatrix} B_{a2} \\ \xi_{a2}^n \end{bmatrix} \quad ; \quad \begin{bmatrix} \bar{V}_{k2} \\ \bar{V}_{a2} \end{bmatrix}_{x21} = \begin{bmatrix} B_{a2} \\ \bar{\xi}_{a2}^n \end{bmatrix}$$

$$\begin{bmatrix} U_{k3} \\ \bar{U}_{a3} \end{bmatrix}_{x21} = \begin{bmatrix} A_{a3} \\ \xi_{a3}^n \end{bmatrix}$$

$$\begin{bmatrix} V_{k3} \\ \bar{V}_{a3} \end{bmatrix}_{x21} = \begin{bmatrix} B_{a3} \\ \xi_{a3}^n \end{bmatrix}$$

$$\begin{bmatrix} \bar{\bar{U}}_{k2} \\ \bar{\bar{U}}_{a2} \end{bmatrix}_{x21} = \begin{bmatrix} A_{a2} \\ \bar{\bar{\xi}}_{a2}^n \end{bmatrix}$$

$$\begin{bmatrix} \bar{\bar{V}}_{k2} \\ \bar{\bar{V}}_{a2} \end{bmatrix}_{x21} = \begin{bmatrix} B_{a2} \\ \bar{\bar{\xi}}_{a2}^n \end{bmatrix}$$

Note:  $\begin{bmatrix} A_{am} \\ B_{am} \end{bmatrix}$  and  $\begin{bmatrix} \xi_{am}^n \\ \bar{\xi}_{am}^n \end{bmatrix}$  are provided as initial input

$$\begin{bmatrix} \xi_{a1}^n \\ \xi_{a2}^n \end{bmatrix}_{11 \times 21} = \begin{bmatrix} 1 & & & & 1 & & & & 1 & & & & \dots & & & & 1 \\ \xi_{m0} & (0.95 \xi_{m0} + 0.05 \xi_{m1}) & (0.90 \xi_{m0} + 0.10 \xi_{m1}) & \dots & \xi_{m1} \\ \xi_{m0}^2 & (0.95 \xi_{m0} + 0.05 \xi_{m1})^2 & (0.90 \xi_{m0} + 0.10 \xi_{m1})^2 & \dots & \xi_{m1}^2 \\ \vdots & \vdots & \vdots & & \vdots \\ \xi_{m0}^{10} & (0.95 \xi_{m0} + 0.05 \xi_{m1})^{10} & (0.90 \xi_{m0} + 0.10 \xi_{m1}) & \dots & \xi_{m1}^{10} \end{bmatrix}$$

for  
m = 1, 2, 3

$$\begin{bmatrix} \bar{\xi}_{a2}^n \end{bmatrix}_{11 \times 21} = \begin{bmatrix} 1 & & & & 1 & & & & 1 & & & & 1 & & & & 1 \\ \bar{\xi}_{2,1}(\xi_{10}) & \bar{\xi}_{2,2}(0.95 \xi_{10} + 0.05 \xi_{11}) & \bar{\xi}_{2,3}(0.90 \xi_{10} + 0.10 \xi_{11}) & \dots & \bar{\xi}_{2,21}(\xi_{11}) \\ \bar{\xi}_{2,1}^2 & \bar{\xi}_{2,2}^2 & \bar{\xi}_{2,3}^2 & \dots & \bar{\xi}_{2,21}^2 \\ \vdots & \vdots & \vdots & & \vdots \\ \bar{\xi}_{2,1}^{10} & \bar{\xi}_{2,2}^{10} & \bar{\xi}_{2,3}^{10} & \dots & \bar{\xi}_{2,21}^{10} \end{bmatrix}$$

Note:

See Functional Relationship  $\bar{\xi}_{a2}(\xi_{a1})$  defined below.

$$\begin{bmatrix} \bar{\bar{\xi}}_{a2}^n \end{bmatrix}_{11 \times 21} = \begin{bmatrix} 1 & & & & 1 & & & & 1 & & & & 1 & & & & 1 \\ \bar{\bar{\xi}}_{2,1}(\xi_{30}) & \bar{\bar{\xi}}_{2,2}(0.95 \xi_{30} + 0.05 \xi_{31}) & \bar{\bar{\xi}}_{2,3}(0.90 \xi_{30} + 0.10 \xi_{31}) & \dots & \bar{\bar{\xi}}_{2,21}(\xi_{31}) \\ \bar{\bar{\xi}}_{2,1}^2 & \bar{\bar{\xi}}_{2,2}^2 & \bar{\bar{\xi}}_{2,3}^2 & \dots & \bar{\bar{\xi}}_{2,21}^2 \\ \vdots & \vdots & \vdots & & \vdots \\ \bar{\bar{\xi}}_{2,1}^{10} & \bar{\bar{\xi}}_{2,2}^{10} & \bar{\bar{\xi}}_{2,3}^{10} & \dots & \bar{\bar{\xi}}_{2,21}^{10} \end{bmatrix}$$

Note:

See functional relationship  $\bar{\bar{\xi}}_{a2}(\xi_{a3})$  defined below.

$$F_1(r_{a1}, r_{a2}) = \frac{r_{a2}^4 + 8r_{a2}r_{a1}^3 - 6r_{a2}^2r_{a1}^2 - 3r_{a1}^4}{6(r_{a1} - r_{a2})^2}$$

$$F_2(r_{a1}, r_{a2}) = \frac{r_{a2}^4 + 2r_{a2}r_{a1}^3 - 2r_{a1}r_{a2}^3 - r_{a1}^4}{6(r_{a1} - r_{a2})^2}$$

Functional Relationship  $\bar{\xi}_{a2}(\xi_{a1})$

$$\bar{\xi}_{a2} = \frac{x}{|L|} = \frac{b}{|L|} \left[ 1 - \sqrt{1 - \frac{r^2}{a^2}} \right]$$

where

$$r^2 = f(\xi_{a1})$$

$$= \frac{a^4 \sin^2 \phi}{(a^2 \sin^2 \phi + b^2 \cos^2 \phi)}$$

and

$$\xi_{a1} = \frac{\pi - \phi}{\pi - \phi_0}$$

Functional Relationship  $\bar{\bar{\xi}}_{a2}(\xi_{a3})$

$$\bar{\bar{\xi}}_{a2} = \frac{1}{|L|} \left\{ \bar{b} - b \left[ 1 - \sqrt{1 - \frac{r^2}{a^2}} \right] \right\}$$

where

$$r^2 = f(\xi_{a3})$$

$$= \frac{a^4 \sin^2 \phi}{(a^2 \sin^2 \phi + b^2 \cos^2 \phi)}$$

and

$$\xi_{a3} = \frac{\phi}{\phi_0}$$

E.3 CASE I (a1 - Convex Up Ellipsoid; a2 - Conic;  
a3 - {IA: Convex Down Ellipsoid  
IB: Conic})

E.3.1 Integral Equation Relationships

$$\begin{aligned}
[\bar{M}] &= -4\pi\bar{\gamma}_1 (\phi_0)_{a1} \int_{\xi_{10}}^{\xi_{11}} \left( \frac{r_1 \sin \phi}{r^2} \right)_{a1} \left\{ \frac{r^2}{2} \hat{u}(x) \right\}_1 \left\{ \frac{r^2}{2} \hat{u}(x) \right\}_1^T d\xi_{a1} \\
&\quad + 4\pi\bar{\gamma}_2 (|L|)_{a2} \int_{\xi_{20}}^{\xi_{21}} \left( \frac{1}{r^2} \right)_{a2} \left\{ \frac{r^2}{2} \hat{u}(x) \right\}_2 \left\{ \frac{r^2}{2} \hat{u}(x) \right\}_2^T d\xi_{a2} \\
\text{IA:} &\left\{ -4\pi\bar{\gamma}_3 (\phi_0 - \pi)_{a3} \int_{\xi_{30}}^{\xi_{31}} \left( \frac{r_1 \sin \phi}{r^2} \right)_{a3} \left\{ \frac{r^2}{2} \hat{u}(x) \right\}_3 \left\{ \frac{r^2}{2} \hat{u}(x) \right\}_3^T d\xi_{a3} \right. \\
\text{IB:} &\left\{ +4\pi\bar{\gamma}_3 (|L|)_{a3} \int_{\xi_{30}}^{\xi_{31}} \left( \frac{1}{r^2} \right)_{a3} \left\{ \frac{r^2}{2} \hat{u}(x) \right\}_3 \left\{ \frac{r^2}{2} \hat{u}(x) \right\}_3^T d\xi_{a3} \right. \\
&\quad - \frac{\pi\bar{\gamma}_1 (\phi_0)_{a1}}{2} \int_{\xi_{10}}^{\xi_{11}} (r_1 \sin \phi)_{a1} \left\{ r\hat{v}(x, r) \right\}_1 \left\{ r\hat{v}(x, r) \right\}_1^T d\xi_{a1} \\
&\quad + \frac{\pi\bar{\gamma}_2 (|L|)_{a2}}{2} \int_{\xi_{20}}^{\xi_{21}} \left\{ r\hat{v}(x, r) \right\}_2 \left\{ r\hat{v}(x, r) \right\}_2^T d\xi_{a2} \\
\text{IA:} &\left\{ - \frac{\pi\bar{\gamma}_3 (\phi_0 - \pi)_{a3}}{2} \int_{\xi_{30}}^{\xi_{31}} (r_1 \sin \phi)_{a3} \left\{ r\hat{v}(x, r) \right\}_3 \left\{ r\hat{v}(x, r) \right\}_3^T d\xi_{a3} \right. \\
\text{IB:} &\left\{ + \frac{\pi\bar{\gamma}_3 (|L|)_{a3}}{2} \int_{\xi_{30}}^{\xi_{31}} \left\{ r\hat{v}(x, r) \right\}_3 \left\{ r\hat{v}(x, r) \right\}_3^T d\xi_{a3} \right.
\end{aligned}$$

where

$$\left\{ \frac{r^2}{2} \hat{u}(x) \right\}_1 = \left\{ \begin{array}{l} + \int_{\xi_{10}}^{\xi} (r \cdot r_1 \phi_0 \cos \phi \{u(\xi)\})_{a1} d\xi_{a1} \\ + \int_{\xi_{10}}^{\xi} (r \cdot r_1 \phi_0 \sin \phi \{v(\xi)\})_{a1} d\xi_{a1} \\ \hline - \int_{\xi_{20}}^{\xi_{21}} (r |L| \cot \phi_0 \{u(\xi)\})_{a2} d\xi_{a2} \\ - \int_{\xi_{20}}^{\xi_{21}} (r |L| \{v(\xi)\})_{a2} d\xi_{a2} \\ \hline \text{IA: } \left\{ \begin{array}{l} \int_{\xi_{30}}^{\xi_{31}} (r \cdot r_1 (\phi_0 - \pi) \cos \phi \{u(\xi)\})_{a3} d\xi_{a3} \\ \int_{\xi_{30}}^{\xi_{31}} (r \cdot r_1 (\phi_0 - \pi) \sin \phi \{v(\xi)\})_{a3} d\xi_{a3} \end{array} \right. \\ \text{IB: } \left\{ \begin{array}{l} - \int_{\xi_{30}}^{\xi_{31}} (r |L| \cot \phi_0 \{u(\xi)\})_{a3} d\xi_{a3} \\ - \int_{\xi_{30}}^{\xi_{31}} (r |L| \{v(\xi)\})_{a3} d\xi_{a3} \end{array} \right. \end{array} \right.$$



$$\left\{ \frac{r^2}{2} \hat{u}(x) \right\}_2 = \left\{ \begin{array}{l} 0 \\ \hline - \int_{\xi_{20}}^{\xi} (r|L| \cot \phi_o \{u(\xi)\})_{a2} d\xi_{a2} \\ - \int_{\xi_{20}}^{\xi} (r|L| \{v(\xi)\})_{a2} d\xi_{a2} \\ \hline \text{IA: } \left\{ \begin{array}{l} \int_{\xi_{30}}^{\xi_{31}} (r \cdot r_1 (\phi_o - \pi) \cos \phi \{u(\xi)\})_{a3} d\xi_{a3} \\ \int_{\xi_{30}}^{\xi_{31}} (r \cdot r_1 (\phi_o - \pi) \sin \phi \{v(\xi)\})_{a3} d\xi_{a3} \end{array} \right. \end{array} \right.$$

$$\text{IB: } \left\{ \begin{array}{l} - \int_{\xi_{30}}^{\xi_{31}} (r|L| \cot \phi_o \{u(\xi)\})_{a3} d\xi_{a3} \\ - \int_{\xi_{30}}^{\xi_{31}} (r|L| \{v(\xi)\})_{a3} d\xi_{a3} \end{array} \right.$$

$$\left\{ \frac{r^2}{2} \hat{u}(x) \right\}_3 = \left\{ \begin{array}{c} 0 \\ \hline 0 \\ \hline \int_{\xi_{30}}^{\xi} \left( r \cdot r_1 (\phi_0 - \pi) \cos \phi \{u(\xi)\} \right)_{a3} d\xi_{a3} \\ \text{IA:} \\ \int_{\xi_{30}}^{\xi} \left( r \cdot r_1 (\phi_0 - \pi) \sin \phi \{v(\xi)\} \right)_{a3} d\xi_{a3} \end{array} \right\}$$

$$\text{IB:} \left\{ \begin{array}{c} - \int_{\xi_{30}}^{\xi} \left( r |L| \cot \phi_0 \{u(\xi)\} \right)_{a3} d\xi_{a3} \\ - \int_{\xi_{30}}^{\xi} \left( r |L| \{v(\xi)\} \right)_{a3} d\xi_{a3} \end{array} \right\}$$

$$\left\{ r \hat{v}(x, r) \right\}_1 = \left\{ \begin{array}{c} \left( r \cdot \cot \phi \{u(\xi)\} \right)_{a1} \\ \left( r \{v(\xi)\} \right)_{a1} \\ \hline 0 \\ \hline 0 \end{array} \right\} - \left( \frac{2 \cot \phi}{r} \right)_{a1} \cdot \left\{ \frac{r^2}{2} \hat{u}(x) \right\}_{a1}$$

$$\left\{ \hat{r}v(x, r) \right\}_2 = \left\{ \begin{array}{c} 0 \\ \hline (r \cdot \cot \phi_0 \{u(\xi)\})_{a2} \\ (r \cdot \{v(\xi)\})_{a2} \\ \hline 0 \end{array} \right\} - \left( \frac{2 \cot \phi_0}{r} \right)_{a2} \cdot \left\{ \frac{r^2}{2} \hat{u}(x) \right\}_{a2}$$

$$\left\{ \hat{r}v(x, r) \right\}_3 = \left\{ \begin{array}{c} 0 \\ \hline 0 \\ \hline (r \cdot \cot \phi \{u(\xi)\})_{a3} \\ (r \{v(\xi)\})_{a3} \end{array} \right\} - \left( \frac{2 \cot \phi}{r} \right)_{a3} \cdot \left\{ \frac{r^2}{2} \hat{u}(x) \right\}_{a3}$$

### E. 3. 2 Integration Limit Data

#### Fluid Surface in Section 1

$$\xi_{11} = \left( \frac{\bar{\phi}}{\phi_0} \right)_{a1}$$

$$\xi_{20} = \xi_{30} = 0$$

$$\xi_{10} = \xi_{21} = \xi_{31} = 1$$

$$\bar{\gamma}_1 = \bar{\gamma}_2 = \bar{\gamma}_3 = \gamma$$

Note:

$$\bar{\phi} = \sin^{-1} \left\{ \frac{\bar{r}}{\left[ a^2 k^2 - \bar{r}^2 (k^2 - 1) \right]^{1/2}} \right\}$$

$$k = a/b$$

$$\bar{r} = a \sqrt{1 - \frac{(\bar{H}_1 + b - \bar{b})^2}{b^2}}$$

if  $(\bar{H}_1 + b - \bar{b}) > 0$  ,  $0 < \bar{\phi} < 90^\circ$  , if  $< 0$  ,  $90^\circ < \bar{\phi} < 180^\circ$

### Fluid Surface in Section 2

$$\xi_{21} = \left( \frac{\bar{H}_2}{|L|} \right)_{a2}$$

$$\xi_{10} = \xi_{11} = \xi_{31} = 1$$

$$\xi_{20} = \xi_{30} = 0$$

$$\bar{\gamma}_1 = 0$$

$$\bar{\gamma}_2 = \bar{\gamma}_3 = \gamma$$

### Fluid Surface in Section 3

$$\text{IA: } \left\{ \xi_{31} = \left( \frac{\pi - \bar{\phi}}{\pi - \phi_0} \right)_{a3} \right.$$

$$\text{IB: } \left\{ \xi_{31} = \left( \frac{\bar{H}_3}{|L|} \right)_{a3} \right.$$

$$\xi_{10} = \xi_{11} = 1$$

$$\xi_{20} = \xi_{21} = \xi_{30} = 0$$

$$\bar{\gamma}_1 = \bar{\gamma}_2 = 0$$

$$\bar{\gamma}_3 = \gamma$$

Note:

$$\bar{\phi} = \sin^{-1} \left\{ \frac{\bar{r}}{-[a^2 k^2 - \bar{r}^2 (k^2 - 1)]^{1/2}} \right\}$$

$$k = a/b$$

$$\bar{r} = a \sqrt{1 - \frac{(b - \bar{H}_3)^2}{b^2}}$$

### E. 3.3 Specific Matrix Data

Note: Quantities  $\left\{ \left( \quad \right)_{am} \right\}_{am, i}$  are evaluated at

points  $\xi_{am, i}$  ( $i = 1, 2, 3, \dots, 21$ ) where

$$\xi_{am, 1} = \xi_{m0}; \quad \xi_{am, 2} = (0.95 \xi_{m0} + 0.05 \xi_{m1});$$

$$\xi_{am, 3} = (0.90 \xi_{m0} + 0.10 \xi_{m1}); \quad \xi_{am, 4} = (0.85 \xi_{m0} + 0.15 \xi_{m1});$$

$$\dots, \quad \xi_{am, 20} = (0.05 \xi_{m0} + 0.95 \xi_{m1}); \quad \xi_{am, 21} = \xi_{m1}$$

$$K1_i = -4\pi\bar{\gamma}_1(\phi_o)_{a1} \left\{ \left( \frac{r_1 \sin \phi}{r^2} \right)_{a1} \right\}_{a1, i} \cdot (\xi_{11} - \xi_{10})$$

$$K2_i = +4\pi\bar{\gamma}_2(|L|)_{a2} \left\{ \left( \frac{1}{r^2} \right)_{a2} \right\}_{a2, i} \cdot (\xi_{21} - \xi_{20})$$

$$IA: \left\{ K3_i = -4\pi\bar{\gamma}_3(\phi_o - \pi)_{a3} \left\{ \left( \frac{r_1 \sin \phi}{r^2} \right)_{a3} \right\}_{a3, i} \right\} \cdot (\xi_{31} - \xi_{30})$$

$$IB: \left\{ K3_i = +4\pi\bar{\gamma}_3(|L|)_{a3} \left\{ \left( \frac{1}{r^2} \right)_{a3} \right\}_{a3, i} \right\} \cdot (\xi_{31} - \xi_{30})$$

$$K4_i = - \left\{ \left( \frac{2 \cot \phi}{r} \right)_{a1} \right\}_{a1, i}$$

$$K5_i = -2(\cot \phi_o)_{a2} \left\{ \left( \frac{1}{r} \right)_{a2} \right\}_{a2, i} ; \bar{K}_{5i} = \bar{\bar{K}}_{5i} = 0$$

$$\text{IA: } \left\{ K6_i = - \left\{ \left( \frac{2 \cot \phi}{r} \right)_{a3} \right\} \right\}_{a3, i}$$

$$\text{IB: } \left\{ K6_i = -2(\cot \alpha)_{a3} \left\{ \left( \frac{1}{r} \right)_{a3} \right\} \right\}_{a3, i}$$

$$C1_i = -\frac{\pi \bar{Y}_1}{2} (\phi_o)_{21} \left\{ (r_1 \sin \phi)_{a1} \right\}_{a1, i} \cdot (\xi_{11} - \xi_{10})$$

$$C2_i = C3_i = 0$$

$$C4_i = +\frac{\pi \bar{Y}_2}{2} (|L|)_{a2} \{1\}_{a2, i} \cdot (\xi_{21} - \xi_{20})$$

$$\text{IA: } \left\{ C5_i = -\frac{\pi \bar{Y}_3}{2} (\phi_o - \pi)_{a3} \left\{ (r_1 \sin \phi)_{a3} \right\} \right\}_{a3, i} \cdot (\xi_{31} - \xi_{30})$$

$$\text{IB: } \left\{ C5_i = +\frac{\pi \bar{Y}_3}{2} (|L|)_{a3} \{1\}_{a3, i} \right\} \cdot (\xi_{31} - \xi_{30})$$

$$C6_i = C7_i = 0$$

$$(KU_1)_i = +(\phi_o)_{a1} \left\{ (r \cdot r_1 \cos \phi)_{a1} \right\}_{a1, i} \cdot (\xi_{11} - \xi_{10})$$

$$(KV_1)_i = +(\phi_o)_{a1} \left\{ (r \cdot r_1 \sin \phi)_{a1} \right\}_{a1, i} \cdot (\xi_{11} - \xi_{10})$$

$$\left( \text{KU}_2 \right)_i = -(|L| \cot \phi_o)_{a2} \left\{ (r)_{a2} \right\}_{a2,i} \cdot (\xi_{21} - \xi_{20}) ;$$

$$\overline{\text{KU}}_2 = \overline{\overline{\text{KU}}}_2 = \overline{\text{KV}}_2 = \overline{\overline{\text{KV}}}_2 = 0$$

$$\left( \text{KV}_2 \right)_i = -(|L|)_{a2} \left\{ (r)_{a2} \right\}_{a2,i} \cdot (\xi_{21} - \xi_{20})$$

$$\text{IA: } \begin{cases} \left( \text{KU}_3 \right)_i = +(\phi_o - \pi)_{a3} \left\{ (r \cdot r_1 \cos \phi)_{a3} \right\}_{a3,i} \cdot (\xi_{31} - \xi_{30}) \\ \left( \text{KV}_3 \right)_i = +(\phi_o - \pi)_{a3} \left\{ (r \cdot r_1 \sin \phi)_{a3} \right\}_{a3,i} \cdot (\xi_{31} - \xi_{30}) \end{cases}$$

$$\text{IB: } \begin{cases} \left( \text{KU}_3 \right)_i = -(|L| \cot \phi_o)_{a3} \left\{ (r)_{a3} \right\}_{a3,i} \cdot (\xi_{31} - \xi_{30}) \\ \left( \text{KV}_3 \right)_i = -(|L|)_{a3} \left\{ (r)_{a3} \right\}_{a3,i} \cdot (\xi_{31} - \xi_{30}) \end{cases}$$

$$\left( \text{KU}_4 \right)_i = + \left\{ (r \cot \phi)_{a1} \right\}_{a1,i}$$

$$\left( \text{KV}_4 \right)_i = + \left\{ (r)_{a1} \right\}_{a1,i}$$

$$\left( \text{KU}_5 \right)_i = +(\cot \phi_o)_{a2} \left\{ (r)_{a2} \right\}_{a2,i}$$

$$\left( \text{KV}_5 \right)_i = + \left\{ (r)_{a2} \right\}_{a2,i} ; \quad \overline{\text{KU}}_5 = \overline{\overline{\text{KU}}}_5 = \overline{\text{KV}}_5 = \overline{\overline{\text{KV}}}_5 = 0$$

$$\text{IA: } \begin{cases} (KU_6)_i = + \left\{ (r \cot \phi)_{a3} \right\}_{a3, i} \\ (KV_6)_i = + \left\{ (r)_{a3} \right\}_{a3, i} \end{cases}$$

$$\text{IB: } \begin{cases} (KU_6)_i = + (\cot \phi_o)_{a3} \left\{ (r)_{a3} \right\}_{a3, i} \\ (KV_6)_i = + \left\{ (r)_{a3} \right\}_{a3, i} \end{cases}$$



E. 4 CASE II (a1 - Convex Down Ellipsoid; a2 - Conic;  
a3 - {IIA: Convex Down Ellipsoid  
IIB: Conic})

E. 4. 1 Integral Equation Relationships

$$\begin{aligned}
[\bar{M}] = & -4\bar{v}_1 (\phi_o - \pi)_{a1} \int_{\xi_{10}}^{\xi_{11}} \frac{(r_1 \sin \phi)_{a1}}{(r_{a2}^2 - r_{a1}^2)} \left\{ \frac{(r_{a2}^2 - r_{a1}^2)}{2} \hat{u}(x) \right\}_1 \left\{ \frac{(r_{a2}^2 - r_{a1}^2)}{2} \hat{u}(x) \right\}_1^T d\xi_{a1} \\
& + 4\bar{v}_2 (|L|)_{a2} \int_{\xi_{20}}^{\xi_{21}} \left( \frac{1}{r^2} \right)_{a2} \left\{ \frac{r^2}{2} \hat{u}(x) \right\}_2 \left\{ \frac{r^2}{2} \hat{u}(x) \right\}_2^T d\xi_{a2}^* \\
\text{IIA: } & \left\{ -4\bar{v}_3 (\phi_o - \pi)_{a3} \int_{\xi_{30}}^{\xi_{31}} \left( \frac{r_1 \sin \phi}{r^2} \right)_{a3} \left\{ \frac{r^2}{2} \hat{u}(x) \right\}_3 \left\{ \frac{r^2}{2} \hat{u}(x) \right\}_3^T d\xi_{a3}^* \right. \\
\text{IIB: } & \left\{ +4\bar{v}_3 (|L|)_{a3} \int_{\xi_{30}}^{\xi_{31}} \left( \frac{1}{r^2} \right)_{a3} \left\{ \frac{r^2}{2} \hat{u}(x) \right\}_3 \left\{ \frac{r^2}{2} \hat{u}(x) \right\}_3^T d\xi_{a3}^* \right. \\
& - \bar{v}_1 (\phi_o - \pi)_{a1} \int_{\xi_{10}}^{\xi_{11}} F_1 (r_{a1}, r_{a2}) \cdot (r_1 \sin \phi)_{a1} \left\{ \hat{v}(x, r) \right\}_{1,1} \left\{ \hat{v}(x, r) \right\}_{1,1}^T d\xi_{a1} \\
& - \bar{v}_1 (\phi_o - \pi)_{a1} \int_{\xi_{10}}^{\xi_{11}} F_2 (r_{a1}, r_{a2}) \cdot (r_1 \sin \phi)_{a1} \left[ \left\{ \hat{v}(x, r) \right\}_{1,1} \left\{ \hat{v}(x, r) \right\}_{1,2}^T + \left\{ \hat{v}(x, r) \right\}_{1,2} \left\{ \hat{v}(x, r) \right\}_{1,1}^T \right] d\xi_{a1} \\
& + \bar{v}_1 (\phi_o - \pi)_{a1} \int_{\xi_{10}}^{\xi_{11}} F_1 (r_{a2}, r_{a1}) \cdot (r_1 \sin \phi)_{a1} \left\{ \hat{v}(x, r) \right\}_{1,2} \left\{ \hat{v}(x, r) \right\}_{1,2}^T d\xi_{a1} \\
& + \frac{\bar{v}_2 (|L|)_{a2}}{2} \int_{\xi_{20}}^{\xi_{21}} \left\{ r \hat{v}(x, r) \right\}_2 \left\{ r \hat{v}(x, r) \right\}_2^T d\xi_{a2}^* \\
\text{IIA: } & \left\{ - \frac{\bar{v}_3 (\phi_o - \pi)_{a3}}{2} \int_{\xi_{30}}^{\xi_{31}} (r_1 \sin \phi)_{a3} \left\{ r \hat{v}(x, r) \right\}_3 \left\{ r \hat{v}(x, r) \right\}_3^T d\xi_{a3}^* \right. \\
\text{IIB: } & \left\{ + \frac{\bar{v}_3 (|L|)_{a3}}{2} \int_{\xi_{30}}^{\xi_{31}} \left\{ r \hat{v}(x, r) \right\}_3 \left\{ r \hat{v}(x, r) \right\}_3^T d\xi_{a3}^* \right.
\end{aligned}$$

\* Identical with Case I.

where

$$\left\{ \frac{(r_{a2}^2 - r_{a1}^2)}{2} \hat{u}(x) \right\}_1 = \left\{ \begin{array}{l}
 - \int_{\xi_{10}}^{\xi} (r \cdot r_1 (\phi_0 - \pi) \cos \phi \{u(\xi)\})_{a1} d\xi_{a1} \\
 - \int_{\xi_{10}}^{\xi} (r \cdot r_1 (\phi_0 - \pi) \sin \phi \{v(\xi)\})_{a1} d\xi_{a1} \\
 \hline
 - \int_{\xi_{20}}^{\xi_{21}} (r|L| \cot \phi_0 \{u(\xi)\})_{a2} d\xi_{a2} \\
 + \int_{\xi_{10}}^{\xi} (r \cot \phi_0 \{u(\xi)\})_{a2} \cdot (r_2 (\phi_0 - \pi) \sin \phi)_{a1} d\xi_{a1} \\
 - \int_{\xi_{20}}^{\xi_{21}} (r|L| \{v(\xi)\})_{a2} d\xi_{a2} \\
 + \int_{\xi_{10}}^{\xi} (r \{v(\xi)\})_{a2} \cdot (r_2 (\phi_0 - \pi) \sin \phi)_{a1} d\xi_{a1} \\
 \hline
 \text{IIA: } \left\{ \begin{array}{l}
 \int_{\xi_{30}}^{\xi_{31}} (r \cdot r_1 (\phi_0 - \pi) \cos \phi \{u(\xi)\})_{a3} d\xi_{a3} \\
 \int_{\xi_{30}}^{\xi_{31}} (r \cdot r_1 (\phi_0 - \pi) \sin \phi \{v(\xi)\})_{a3} d\xi_{a3}
 \end{array} \right. \\
 \text{IIB: } \left\{ \begin{array}{l}
 - \int_{\xi_{30}}^{\xi_{31}} (r|L| \cot \phi_0 \{u(\xi)\})_{a3} d\xi_{a3} \\
 - \int_{\xi_{30}}^{\xi_{31}} (r|L| \{v(\xi)\})_{a3} d\xi_{a3}
 \end{array} \right.
 \end{array} \right.$$

Note:  $\left\{ \frac{r^2}{2} \hat{u}(x) \right\}_2$  and  $\left\{ \frac{r^2}{2} \hat{u}(x) \right\}_3$  are the same as for Case I.

$$\left\{ \hat{v}(x, r) \right\}_{1,1} = \left\{ \begin{array}{c} (\cot \phi \{u(\xi)\})_{a1} \\ \{v(\xi)\}_{a1} \\ \hline 0 \\ \hline 0 \end{array} \right\} - \frac{2(\cot \phi)_{a1}}{(r_{a2}^2 - r_{a1}^2)} \cdot \left\{ \frac{r_{a2}^2 - r_{a1}^2}{2} \hat{u}(x) \right\}_1$$

$$\left\{ \hat{v}(x, r) \right\}_{1,2} = \left\{ \begin{array}{c} 0 \\ \hline (\cot \phi_o \{u(\xi)\})_{a2} \\ \{v(\xi)\}_{a2} \\ \hline 0 \end{array} \right\} - \frac{2(\cot \phi_o)_{a2}}{(r_{a2}^2 - r_{a1}^2)} \cdot \left\{ \frac{r_{a2}^2 - r_{a1}^2}{2} \hat{u}(x) \right\}_1$$

Note:  $\left\{ \hat{v}(x, r) \right\}_2$  and  $\left\{ \hat{v}(x, r) \right\}_3$  same as for Case I.

## E.4.2 Integration Limit Data

### Fluid Surface in Section 1

$$\xi_{10} = \xi_{20} = \xi_{30} = 0 ; \quad \xi_{31} = 1$$

$$\xi_{11} = \left( \frac{\pi - \bar{\phi}}{\pi - \phi_0} \right)_{a1}$$

$$\xi_{21} = 1 - (|\bar{b}|)_{a1} / (|L|)_{a2}$$

$$\bar{y}_1 = \bar{y}_2 = \bar{y}_3 = \gamma$$

Note:

$$\bar{\phi} = \sin^{-1} \left\{ \frac{\bar{r}}{-[a^2 k^2 - \bar{r}^2 (k^2 - 1)]^{1/2}} \right\}$$

$$k = a/b$$

$$\bar{r} = a \sqrt{1 - \frac{(b - \bar{H}_1)^2}{b^2}}$$

### Fluid Surface in Section 2

$$\xi_{10} = \xi_{11} = 0.5$$

$$\xi_{20} = \xi_{30} = 0$$

$$\xi_{31} = 1$$

$$\xi_{21} = (\bar{H}_2 / |L|)_{a2}$$

$$\bar{y}_1 = 0 ; \quad \bar{y}_2 = \bar{y}_3 = \gamma$$

### Fluid Surface in Section 3

$$\xi_{10} = \xi_{11} = 0.5 , \quad \xi_{20} = \xi_{21} = \xi_{30} = 0$$

$$\text{IIA: } \left\{ \xi_{31} = \left( \frac{\bar{\phi}}{\phi_0} \right)_{a3} \right.$$

$$\text{IIB: } \left\{ \xi_{31} = \left( \frac{\bar{H}_3}{|L|} \right)_{a3} \right.$$

### E.4.3 Specific Matrix Data

$$(K1)_i = -4\pi\bar{Y}_1 (\phi_o - \pi)_{a1} \left\{ \frac{(r_1 \sin \phi)_{a1}}{(r_{a2}^2 - r_{a1}^2)} \right\}_{a1,i} \cdot (\xi_{11} - \xi_{10})$$

$$(K2)_i = +4\pi\bar{Y}_2 (|L|)_{a2} \left\{ \left( \frac{1}{r^2} \right)_{a2} \right\}_{a2,i} \cdot (\xi_{21} - \xi_{20})^*$$

$$\text{IIA: } \left\{ (K3)_i = -4\pi\bar{Y}_3 (\phi_o - \pi)_{a3} \left\{ \frac{(r_1 \sin \phi)}{r^2} \right\}_{a3} \right\}_{a3,i} \cdot (\xi_{31} - \xi_{30})^*$$

$$\text{IIB: } \left\{ (K3)_i = +4\pi\bar{Y}_3 (|L|)_{a3} \left\{ \left( \frac{1}{r^2} \right)_{a3} \right\}_{a3,i} \right\}_{a3,i} \cdot (\xi_{31} - \xi_{30})^*$$

$$(C1)_i = -\pi\bar{Y}_1 (\phi_o - \pi)_{a1} \left\{ F_1(r_{a1}, r_{a2}) \cdot (r_1 \sin \phi)_{a1} \right\}_{a1,i} \cdot (\xi_{11} - \xi_{10})$$

$$(C2)_i = -\pi\bar{Y}_1 (\phi_o - \pi)_{a1} \left\{ F_2(r_{a1}, r_{a2}) \cdot (r_1 \sin \phi)_{a1} \right\}_{a1,i} \cdot (\xi_{11} - \xi_{10})$$

$$(C3)_i = +\pi\bar{Y}_1 (\phi_o - \pi)_{a1} \left\{ F_1(r_{a2}, r_{a1}) \cdot (r_1 \sin \phi)_{a1} \right\}_{a1,i} \cdot (\xi_{11} - \xi_{10})$$

$$(C4)_i = +\frac{\pi\bar{Y}_2}{2} (|L|)_{a2} \left\{ 1 \right\}_{a2,i} \cdot (\xi_{21} - \xi_{20})^*$$

$$\text{IIA: } \left\{ (C5)_i = -\frac{\pi\bar{Y}_3}{2} (\phi_o - \pi)_{a3} \left\{ (r_1 \sin \phi)_{a3} \right\}_{a3,i} \right\}_{a3,i} \cdot (\xi_{31} - \xi_{30})^*$$

$$\text{IIB: } \left\{ (C5)_i = +\frac{\pi\bar{Y}_3}{2} (|L|)_{a3} \left\{ 1 \right\}_{a3,i} \right\}_{a3,i} \cdot (\xi_{31} - \xi_{30})^*$$

$$(C6)_i = (C7)_i = 0^*$$

---

\* Same as for Case I

$$(KU_1)_i = -(\phi_0 - \pi)_{a1} \left\{ (r \cdot r_1 \cos \phi)_{a1} \right\}_{a1,i} (\xi_{11} - \xi_{10})$$

$$(KV_1)_i = -(\phi_0 - \pi)_{a1} \left\{ (r \cdot r_1 \sin \phi)_{a1} \right\}_{a1,i} (\xi_{11} - \xi_{10})$$

$$(KU_2)_i = -(|L| \cot \phi_0)_{a2} \left\{ (r)_{a2} \right\}_{a2,i} (\xi_{21} - \xi_{20})^*$$

$$(KV_2)_i = -(|L|)_{a2} \left\{ (r)_{a2} \right\}_{a2,i} (\xi_{21} - \xi_{20})^*$$

$$\text{IIA:} \begin{cases} (KU_3)_i = (\phi_0 - \pi)_{a3} \left\{ (r \cdot r_1 \cos \phi)_{a3} \right\}_{a3,i} (\xi_{31} - \xi_{30})^* \\ (KV_3)_i = (\phi_0 - \pi)_{a3} \left\{ (r \cdot r_1 \sin \phi)_{a3} \right\}_{a3,i} (\xi_{31} - \xi_{30})^* \end{cases}$$

$$\text{IIB:} \begin{cases} (KU_3)_i = -(|L| \cot \phi_0)_{a3} \left\{ (r)_{a3} \right\}_{a3,i} (\xi_{31} - \xi_{30})^* \\ (KV_3)_i = -(|L|)_{a3} \left\{ (r)_{a3} \right\}_{a3,i} (\xi_{31} - \xi_{30})^* \end{cases}$$

$$(\overline{KU}_2)_i = (\phi_0 - \pi)_{a1} (\cot \phi_0)_{a2} \left\{ (r_1 \sin \phi)_{a1} (r)_{a2} \right\}_{a1,i} (\xi_{11} - \xi_{10})$$

$$(\overline{KV}_2)_i = (\phi_1 - \pi)_{a1} \left\{ (r_1 \sin \phi)_{a1} (r)_{a2} \right\}_{a1,i} (\xi_{11} - \xi_{10})$$

$$(\overline{\overline{KU}}_2)_i = 0^*$$

$$(\overline{\overline{KV}}_2)_i = 0^*$$

$$(KU_4)_i = \left\{ (\cot \phi)_{a1} \right\}_{a1,i}$$

$$(KV_4)_i = (1)$$

\* Same as for Case I

$$\left(\overline{KU}_5\right)_i = (\cot \phi_o)_{a2}$$

$$\left(\overline{KV}_5\right)_i = (1)$$

$$\left(KU_5\right)_i = +(\cot \phi_o)_{a2} \left\{ (r)_{a2} \right\}_{a2,i}^*$$

$$\left(KV_5\right)_i = + \left\{ (r)_{a2} \right\}_{a2,i}^*$$

$$\text{IIA: } \begin{cases} \left(KU_6\right)_i = + \left\{ (r \cot \phi)_{a3} \right\}_{a3,i}^* \\ \left(KV_6\right)_i = + \left\{ (r)_{a3} \right\}_{a3,i}^* \end{cases}$$

$$\text{IIB: } \begin{cases} \left(KU_6\right)_i = +(\cot \phi_o)_{a3} \left\{ (r)_{a3} \right\}_{a3,i}^* \\ \left(KV_6\right)_i = + \left\{ (r)_{a3} \right\}_{a3,i}^* \end{cases}$$

$$\left(\overline{\overline{KU}}_5\right)_i = 0^*$$

$$\left(\overline{\overline{KV}}_5\right)_i = 0^*$$

$$\left(K4\right)_i = -2 \left\{ \frac{(\cot \phi)_{a1}}{(r^2)_{a2} - (r^2)_{a1}} \right\}_{a1,i}$$

$$\left(\overline{K5}\right)_i = -2 \left\{ \frac{(\cot \phi)_{a2}}{(r^2)_{a2} - (r^2)_{a1}} \right\}_{a1,i}$$

---

\* Same as for Case I

$$(K5)_i = -2 (\cot \phi_o)_{a2} \left\{ \left( \frac{1}{r} \right)_{a2} \right\}_{a2, i}^*$$

$$(\overline{K5})_i = 0^*$$

$$\text{IIA: } \left\{ (K6)_i = - \left\{ \left( \frac{2 \cot \phi}{r} \right)_{a3} \right\}_{a3, i}^* \right.$$

$$\text{IIB: } \left\{ (K6)_i = -2 (\cot \phi_o)_{a3} \left\{ \left( \frac{1}{r} \right)_{a3} \right\}_{a3, i}^* \right.$$

---

\* Same as for Case I



E.5 CASE III (a1 - Convex Up Ellipsoid; a2 - Conic;  
a3 - Convex Up Ellipsoid)

E.5.1 Integral Equation Relationships

$$\begin{aligned}
 [\bar{M}] = & -4\pi\bar{\gamma}_1(\phi_0)_{a1} \int_{\xi_{10}}^{\xi_{11}} \left( \frac{r_1 \sin \phi}{r^2} \right)_{a1} \left\{ \frac{r^2}{2} \hat{u}(x) \right\}_1 \left\{ \frac{r^2}{2} \hat{u}(x) \right\}_1^T d\xi_{a1} \\
 & + 4\pi\bar{\gamma}_2(|L|)_{a2} \int_{\xi_{20}}^{\xi_{21}} \left( \frac{1}{r^2} \right)_{a2} \left\{ \frac{r^2}{2} \hat{u}(x) \right\}_2 \left\{ \frac{r^2}{2} \hat{u}(x) \right\}_2^T d\xi_{a2} \\
 & - 4\pi\bar{\gamma}_3(\phi_0)_{a3} \int_{\xi_{30}}^{\xi_{31}} \frac{(r_1 \sin \phi)_{a3}}{(r_{a2}^2 - r_{a3}^2)} \left\{ \frac{(r_{a2}^2 - r_{a3}^2)}{2} \hat{u}(x) \right\}_3 \left\{ \frac{(r_{a2}^2 - r_{a3}^2)}{2} \hat{u}(x) \right\}_3^T d\xi_{a3} \\
 & - \frac{\pi\bar{\gamma}_1(\phi_0)_{a1}}{2} \int_{\xi_{10}}^{\xi_{11}} (r_1 \sin \phi)_{a1} \left\{ r\hat{v}(x, r) \right\}_1 \left\{ r\hat{v}(x, r) \right\}_1^T d\xi_{a1} \\
 & + \frac{\pi\bar{\gamma}_2(|L|)_{a2}}{2} \int_{\xi_{20}}^{\xi_{21}} \left\{ r\hat{v}(x, r) \right\}_2 \left\{ r\hat{v}(x, r) \right\}_2^T d\xi_{a2} \\
 & - \pi\bar{\gamma}_3(\phi_0)_{a3} \int_{\xi_{30}}^{\xi_{31}} F_1(r_{a3}; r_{a2}) \cdot (r_1 \sin \phi)_{a3} \left\{ \hat{v}(x, r) \right\}_{3,3} \left\{ \hat{v}(x, r) \right\}_{3,3}^T d\xi_{a3} \\
 & - \pi\bar{\gamma}_3(\phi_0)_{a3} \int_{\xi_{30}}^{\xi_{31}} F_2(r_{a3}; r_{a2}) \cdot (r_1 \sin \phi)_{a3} \left[ \left\{ \hat{v}(x, r) \right\}_{3,3} \left\{ \hat{v}(x, r) \right\}_{3,2}^T \right. \\
 & \qquad \qquad \qquad \left. + \left\{ \hat{v}(x, r) \right\}_{3,2} \left\{ \hat{v}(x, r) \right\}_{3,3}^T \right] d\xi_{a3} \\
 & + \pi\bar{\gamma}_3(\phi_0)_{a3} \int_{\xi_{30}}^{\xi_{31}} F_1(r_{a2}; r_{a3}) \cdot (r_1 \sin \phi)_{a3} \left\{ \hat{v}(x, r) \right\}_{3,2} \left\{ \hat{v}(x, r) \right\}_{3,2}^T d\xi_{a3}
 \end{aligned}$$

where

$$\left\{ \frac{r^2}{2} \hat{u}(\mathbf{x}) \right\}_1 = \left\{ \begin{array}{l}
 + \int_{\xi_{10}}^{\xi} \left( r \cdot r_1 \phi_0 \cos \phi \{u(\xi)\} \right)_{a1} d\xi_{a1} \\
 + \int_{\xi_{10}}^{\xi} \left( r \cdot r_1 \phi_0 \sin \phi \{v(\xi)\} \right)_{a1} d\xi_{a1} \\
 \hline
 - \int_{\xi_{20}}^{\xi_{21}} \left( r |L| \cot \phi_0 \{u(\xi)\} \right)_{a2} d\xi_{a2} \\
 + \int_{\xi_{30}}^{\xi_{31}} \left( r \cot \phi_0 \{u(\xi)\} \right)_{a2} \cdot \left( r_1 \phi_0 \sin \phi \right)_{a3} d\xi_{a3} \\
 - \int_{\xi_{20}}^{\xi_{21}} \left( r |L| \{v(\xi)\} \right)_{a2} d\xi_{a2} \\
 + \int_{\xi_{30}}^{\xi_{31}} \left( r \{v(\xi)\} \right)_{a2} \cdot \left( r_1 \phi_0 \sin \phi \right)_{a3} d\xi_{a3} \\
 \hline
 - \int_{\xi_{30}}^{\xi_{31}} \left( r \cdot r_1 \phi_0 \cos \phi \{u(\xi)\} \right)_{a3} d\xi_{a3} \\
 - \int_{\xi_{30}}^{\xi_{31}} \left( r \cdot r_1 \phi_0 \sin \phi \{v(\xi)\} \right)_{a3} d\xi_{a3}
 \end{array} \right.$$

$$\left\{ \frac{r^2}{2} \hat{u}(x) \right\}_2 = \left\{ \begin{array}{l} 0 \\ - \int_{\xi_{20}}^{\xi} (r |L| \cot \phi_o \{u(\xi)\})_{a2} d\xi_{a2} \\ \quad + \int_{\xi_{30}}^{\xi_{31}} (r \cot \phi_o \{u(\xi)\})_{a2} (r_1 \phi_o \sin \phi)_{a3} d\xi_{a3} \\ - \int_{\xi_{20}}^{\xi} (r |L| \{v(\xi)\})_{a2} d\xi_{a2} \\ \quad + \int_{\xi_{30}}^{\xi_{31}} r \{v(\xi)\}_{a2} (r_1 \phi_o \sin \phi)_{a3} d\xi_{a3} \\ - \int_{\xi_{30}}^{\xi_{31}} (r \cdot r_1 \phi_o \cos \phi \{u(\xi)\})_{a3} d\xi_{a3} \\ - \int_{\xi_{30}}^{\xi_{31}} (r \cdot r_1 \phi_o \sin \phi \{v(\xi)\})_{a3} d\xi_{a3} \end{array} \right\}$$

$$\left\{ \frac{(r_{a2}^2 - r_{a3}^2)}{2} \hat{u}(x) \right\}_3 = \left\{ \begin{array}{l} 0 \\ + \int_{\xi_{30}}^{\xi} (r \cot \phi \{u(\xi)\})_{a2} (r_1 \phi_0 \sin \phi)_{a3} d \xi_{a3} \\ + \int_{\xi_{30}}^{\xi} (r \{v(\xi)\})_{a2} (r_1 \phi_0 \sin \phi)_{a3} d \xi_{a3} \\ + \int_{\xi_{30}}^{\xi} (r \cdot r_1 \phi_0 \cos \phi \{u(\xi)\})_{a3} d \xi_{a3} \\ - \int_{\xi_{30}}^{\xi} (r \cdot r_1 \phi_0 \sin \phi \{v(\xi)\})_{a3} d \xi_{a3} \end{array} \right\}$$

$\left\{ \hat{r}v(x, r) \right\}_1$  and  $\left\{ \hat{r}v(x, r) \right\}_2$  are same as Case I.

$$\left\{ \hat{v}(x, r) \right\}_{3,3} = \left\{ \begin{array}{l} 0 \\ 0 \\ (\cot \phi \{u(\xi)\})_{a3} \\ \{v(\xi)\}_{a3} \end{array} \right\} - \frac{2(\cot \phi)_{a3}}{(r_{a2}^2 - r_{a3}^2)} \left\{ \frac{(r_{a2}^2 - r_{a3}^2)}{2} \hat{u}(x) \right\}_3$$

$$\left\{ \hat{v}(x, r) \right\}_{3,2} = \left\{ \begin{array}{c} 0 \\ \text{---} \\ (\cot \phi_0 \{u(\xi)\})_{a2} \\ \{v(\xi)\}_{a2} \\ \text{---} \\ 0 \end{array} \right\} - \frac{2(\cot \phi_0)_{a2}}{(r_{a2}^2 - r_{a3}^2)} \left\{ \frac{(r_{a2}^2 - r_{a3}^2)}{2} \hat{u}(x) \right\}_3$$

### E. 5. 2 Integration Limit Data

#### Fluid Surface in Section 1

$$\xi_{11} = \left( \bar{\phi} / \phi_o \right)_{a1}$$

$$\xi_{20} = (|b|)_{a3} / (|L|)_{a2}$$

$$\xi_{31} = 0$$

$$\xi_{10} = \xi_{21} = \xi_{30} = 1$$

$$\bar{y}_1 = \bar{y}_2 = \bar{y}_3 = \gamma$$

#### Fluid Surface in Section 2

$$\xi_{10} = \xi_{11} = \xi_{30} = 1$$

$$\xi_{21} = (H/|L|)_{a2}$$

$$\xi_{20} = (|b|)_{a3} / (|L|)_{a2}$$

$$\xi_{31} = 0$$

$$\bar{y}_1 = 0$$

$$\bar{y}_2 = \bar{y}_3 = \gamma$$

#### Fluid Surface in Section 3

$$\xi_{10} = \xi_{11} = 1$$

$$\xi_{20} = \xi_{21} = \left( \bar{H}_3 / |L| \right)_{a2}$$

$$\xi_{30} = 1$$

$$\xi_{31} = \left( \bar{\phi} / \phi_o \right)_{a3}$$

$$\bar{\gamma}_1 = \bar{\gamma}_2 = 0$$

$$\bar{\gamma}_3 = \gamma$$

### E.5.3 Specific Matrix Data

$$(K1)_i = -4\pi\bar{\gamma}_1(\phi_o)_{a1} \left\{ \left( \frac{r_1 \sin \phi}{r^2} \right)_{a1} \right\}_{a1,i} \cdot (\xi_{11} - \xi_{10})^*$$

$$(K2)_i = +4\pi\bar{\gamma}_2(|L|)_{a2} \left\{ \left( \frac{1}{r^2} \right)_{a2} \right\}_{a2,i} \cdot (\xi_{21} - \xi_{20})^*$$

$$(K3)_i = -4\pi\bar{\gamma}_3(\phi_o)_{a3} \left\{ \left( \frac{r_1 \sin \phi}{r_{a2}^2 - r_{a3}^2} \right)_{a3} \right\}_{a3,i} \cdot (\xi_{31} - \xi_{30})$$

$$(C1)_i = -\frac{\pi\bar{\gamma}_1}{2}(\phi_o)_{a1} \left\{ (r_1 \sin \phi)_{a1} \right\}_{a1,i} \cdot (\xi_{11} - \xi_{10})^*$$

$$(C2)_i = (C3)_i = 0^*$$

$$(C4)_i = +\frac{\pi\bar{\gamma}_2}{2}(|L|)_{a2} \{1\}_{a2,i} \cdot (\xi_{21} - \xi_{20})^*$$

$$(C5)_i = -\pi\bar{\gamma}_3(\phi_o)_{a3} \left\{ F_1(r_{a3}, r_{a2}) \cdot (r_1 \sin \phi)_{a3} \right\}_{a3,i} \cdot (\xi_{31} - \xi_{30})$$

$$(C6)_i = -\pi\bar{\gamma}_3(\phi_o)_{a3} \left\{ F_2(r_{a3}, r_{a2}) \cdot (r_1 \sin \phi)_{a3} \right\}_{a3,i} \cdot (\xi_{31} - \xi_{30})$$

$$(C7)_i = +\pi\bar{\gamma}_3(\phi_o)_{a3} \left\{ F_1(r_{a2}, r_{a3}) \cdot (r_1 \sin \phi)_{a3} \right\}_{a3,i} \cdot (\xi_{31} - \xi_{30})$$

\* Same as for Case I

$$(KU_1)_i = +(\phi_o)_{a1} \left\{ (r \cdot r_1 \cos \phi)_{a1} \right\}_{a1,i} \cdot (\xi_{11} - \xi_{10})^*$$

$$(KV_1)_i = +(\phi_o)_{a1} \left\{ (r \cdot r_1 \sin \phi)_{a1} \right\}_{a1,i} \cdot (\xi_{11} - \xi_{10})^*$$

$$(KU_2)_i = -(L| \cot \phi_o)_{a2} \left\{ (r)_{a2} \right\}_{a2,i} \cdot (\xi_{21} - \xi_{20})^*$$

$$(KV_2)_i = -(L|)_{a2} \left\{ (r)_{a2} \right\}_{a2,i} \cdot (\xi_{21} - \xi_{20})^*$$

$$(\overline{KU}_2)_i = (\overline{KV}_2) = 0^*$$

$$(\overline{\overline{KU}}_2)_i = +(\cot \phi_o)_{a2} (\phi_o)_{a3} \left\{ (r)_{a2} (r_1 \sin \phi)_{a3} \right\}_{a3,i} \cdot (\xi_{31} - \xi_{30})$$

$$(\overline{\overline{KV}}_2)_i = +(\phi_o)_{a3} \left\{ (r)_{a2} (r_1 \sin \phi)_{a3} \right\}_{a3,i} \cdot (\xi_{31} - \xi_{30})$$

$$(KU_3)_i = -(\phi_o)_{a3} \left\{ (r \cdot r_1 \cos \phi)_{a3} \right\}_{a3,i} \cdot (\xi_{31} - \xi_{30})$$

$$(KV_3)_i = -(\phi_o)_{a3} \left\{ (r \cdot r_1 \sin \phi)_{a3} \right\}_{a3,i} \cdot (\xi_{31} - \xi_{30})$$

$$(KU_4)_i = + \left\{ (r \cot \phi)_{a1} \right\}_{a1,i}^*$$

$$(KV_4)_i = + \left\{ (r)_{a1} \right\}_{a1,i}^*$$

$$(\overline{KU}_5)_i = (\overline{KV}_5) = 0^*$$

---

\* Same as for Case I



$$(KU_5)_i = +(\cot \phi_o)_{a2} \left\{ (r)_{a2} \right\}_{a2,i}^*$$

$$(KV_5)_i = + \left\{ (r)_{a2} \right\}_{a2,i}^*$$

$$(KU_6)_i = + \left\{ (\cot \phi)_{a3} \right\}_{a3,i}$$

$$(KV_6)_i = +1$$

$$(\overline{\overline{KU}}_5)_i = + \left\{ (\cot \phi_o)_{a3} \right\}_{a3,i}$$

$$(\overline{\overline{KV}}_5)_i = +1$$

$$(K_4)_i = - \left\{ \left( \frac{2 \cot \phi}{r} \right)_{a1} \right\}_{a1,i}^*$$

$$(\overline{K}_5)_i = 0^*$$

$$(K_5)_i = -2(\cot \phi_o)_{a2} \left\{ \left( \frac{1}{r} \right)_{a2} \right\}_{a2,i}^*$$

$$(\overline{\overline{K}}_5)_i = -2(\cot \phi_o)_{a2} \left\{ \frac{1}{(r_{a2}^2 - r_{a3}^2)} \right\}_{a3,i}$$

$$(K_6)_i = -2 \left\{ (\cot \phi)_{a3} \cdot \frac{1}{(r_{a2}^2 - r_{a3}^2)} \right\}_{a3,i}$$

---

\* Same as for Case I

E. 6 LAGRANGIAN WEIGHTING MATRIX TABLES

DATA FOR $[W]$			DATA* FOR $[\bar{W}]_{21 \times 21}$		
$W_1$	0.01341	70742	$W_1$	0.01341	70742
$W_2$	0.08876	79707	$W_2$	0.08876	79707
$W_3$	-0.04052	17853	$W_3$	-0.04052	17853
$W_4$	0.22747	31442	$W_4$	0.22747	31442
$W_5$	-0.21757	75613	$W_5$	-0.21757	75613
$W_6$	0.35688	23152	$W_6$	0.35688	23152
$W_7$	-0.21757	75613	$W_7$	-0.21757	75613
$W_8$	0.22747	31442	$W_8$	0.22747	31442
$W_9$	-0.04052	17853	$W_9$	-0.04052	17853
$W_{10}$	0.08876	79707	$W_{10}$	0.08876	79707
$W_{11}$	0.02683	41484	$W_{11}$	0.02683	41484
$W_{12}$	0.08876	79707	$W_{12}$	0.08876	79707
$W_{13}$	-0.04052	17853	$W_{13}$	-0.04052	17853
$W_{14}$	0.22747	31442	$W_{14}$	0.22747	31442
$W_{15}$	-0.21757	75613	$W_{15}$	-0.21757	75613
$W_{16}$	0.35688	23152	$W_{16}$	0.35688	23152
$W_{17}$	-0.21757	75613	$W_{17}$	-0.21757	75613
$W_{18}$	0.22747	31442	$W_{18}$	0.22747	31442
$W_{19}$	-0.04052	17853	$W_{19}$	-0.04052	17853
$W_{20}$	0.08876	79707	$W_{20}$	0.08876	79707
$W_{21}$	0.01341	70742	$W_{21}$	0.01341	70742

\* This column is identical for all 21 columns of the matrix.



## APPENDIX F

### SAMPLE INPUT DATA

Sample input data for a typical one stage launch vehicle (Figure F. 1) is presented to illustrate the basic data requirements. For simplicity all structural components are constructed of aluminum. The vehicle oxidizer and fuel tanks are both assumed to be simple tanks according to the terminology used in Section 2.0. To demonstrate the capability of handling stringers and ribs, two shell sections are given orthotropic properties as indicated in Figure F. 1.

The physical model is first subdivided into a consistent set of shell, fluid and mass-spring components as shown in Figure F. 2. In this example the vehicle is represented by eleven (11) shell components, two (2) fluid components and four (4) spring-mass components to account for the payload, engine and equipment. The displacement coordinate locations are then selected and numbered according to the requirements discussed in Section 8.0. For this sample problem the vehicle is assumed to be unsupported, i. e., no fixed coordinates are specified.

The input data load sheets have been prepared for the launch vehicle illustrated in Figure F. 1 and are included in this appendix to illustrate the input format. The system data appears first followed in order by the data specifications for each of the shell, fluid and spring-mass components.

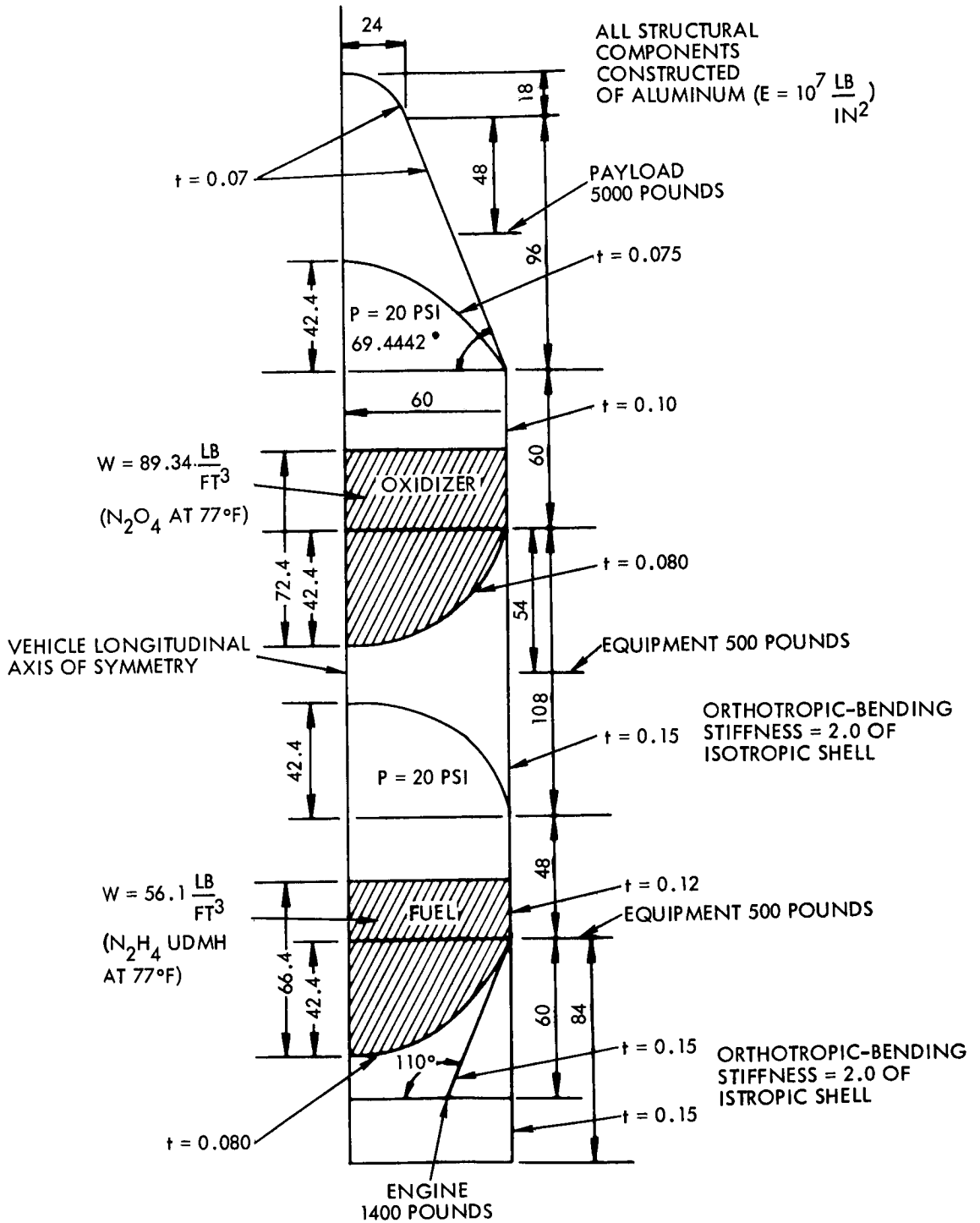


Figure F. 1. Typical One-Stage Launch Vehicle

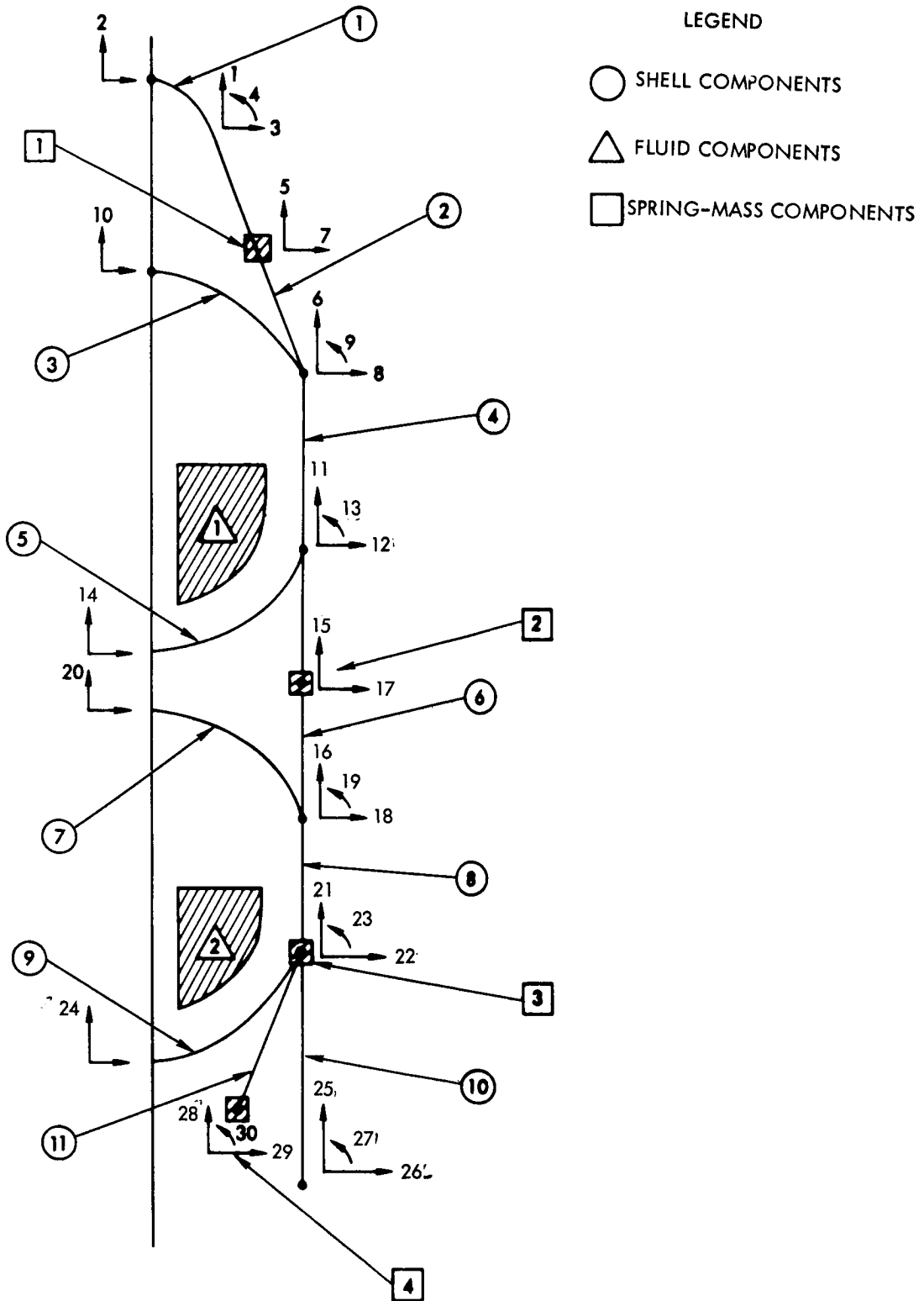


Figure F.2. System Components and Coordinates



SPACE TECHNOLOGY LABORATORIES  
COMPUTATION AND DATA REDUCTION CENTER

PAGE 2 OF 14

DATE \_\_\_\_\_  
NAME \_\_\_\_\_  
PROBLEM NO. \_\_\_\_\_  
NO. OF CARDS \_\_\_\_\_

PRIORITY \_\_\_\_\_  
KEYPUNCHED BY *[Signature]*  
VERIFIED BY \_\_\_\_\_

1 7 78

**X1**

SYMBOL	P R E	LOC.	VALUE	EXP.
I	INA	-1		
I	IU	2		
I	IV	2		
I	IUB	2		
I	IVB	2		
I	IDVT	1		
I		2		
I		3		
I		4		
I	INK	1		
	RHIN	69.444		
	XL	0.		
	R2IN	0.		
	BBAR	18.0		
	ABAR	24.0		
	C11I	.7692307	06	
		.7692307	06	
	C12I	.2307692	06	
		.2307692	06	
	C22I	.7692307	06	
		.7692307	06	
	C33I	.31410256	03	
		.31410256	03	
		.31410256	03	
	C34I	.94230769	02	
		.94230769	02	
		.94230769	02	
		.94230769	02	
	C44I	.31410256	03	
		.31410256	03	
		.31410256	03	
		.31410256	03	
	THI	.07		
		.07		
	DESTA	.2588	-3	
	AM	0.		
	HI	0.		
	DETI	0.		
	PRE	0.		

SYMBOL	P R E	LOC.	VALUE	EXP.
		HE	0.	
		DESTA	0.	
		PRE	0.	
		WEAR	0.	
		END		

**X1**



SPACE TECHNOLOGY LABORATORIES  
COMPUTATION AND DATA REDUCTION CENTER

PAGE 3 OF 14

DATE \_\_\_\_\_

NAME \_\_\_\_\_

PRIORITY \_\_\_\_\_

PROBLEM NO. \_\_\_\_\_

KEYPUNCHED BY *St*

NO. OF CARDS \_\_\_\_\_

VERIFIED BY *St*

1 7

78

SYMBOL	LOC.	VALUE	EXP.
I INA	2		
I IU	3		
I IV	3		
I IUB	3		
I TVB	5		
I IDVT	1		
I	5		
I	6		
I	3		
I	7		
I	8		
I	4		
I	9		
I INK	3		
PHIN	69.444		
XL	96.		
RZIN	60.		
BBAR	0.		
ABAR	0.		
C11I	.7692307		06
	.7692307		06
C12I	.2307692		06
	.2307692		06
C22I	.7692307		06
	.7692307		06
C33I	.31410256		03
	.31410256		03
	.31410256		03
	.31410256		03
C34I	.94230769		02
	.94230769		02
	.94230769		02
	.94230769		02
C44I	.31410256		03
	.31410256		03
	.31410256		03
	.31410256		03
THI	.07		
	.07		
DEGRA	.2555		-3

SYMBOL	LOC.	VALUE	EXP.
AM		.490146	
HI		0.	
DESTE		0.	
PRI		0.	
HE		0.	
DESTE		0.	
PRE		0.	
WEAR		-19.8	
END			

SPACE TECHNOLOGY LABORATORIES  
COMPUTATION AND DATA REDUCTION CENTER

PAGE 4 OF 14

DATE \_\_\_\_\_

NAME \_\_\_\_\_

PROBLEM NO. \_\_\_\_\_

NO. OF CARDS \_\_\_\_\_

PRIORITY \_\_\_\_\_

KEYPUNCHED BY *GH*

VERIFIED BY *GH*

**IX**

SYMBOL	1 2		7	17
	P	R	LOC.	VALUE
I	INA	-3		
I	IU	2		
I	IV	2		
I	IUB	2		
I	IVB	2		
I	IDVT	6		
I		10		
I		8		
I		9		
I	INK	1		
	PHEN	69.444		
	XL	0.		
	R2IN	0.		
	B.BAR	42.4		
	ABAR	60.		
	C11Z	.8241758	06	
		.8241758	06	
	C12Z	.2472527	06	
		.2472527	06	
	C22Z	.8241759	06	
		.8241759	06	
	C33Z	.38633241	03	
		.38633241	03	
		.38633241	03	
	C34Z	.11589972	03	
		.11589972	03	
		.11589972	03	
		.11589972	03	
	C44Z	.38633241	03	
		.38633241	03	
		.38633241	03	
		.38633241	03	
	THZ	.075		
		.075		
	DFSTA	.2588	-3	
	AM	0.		
	HZ	0.		
	DESTZ	0.		
	PRZ	0.		

SYMBOL	1 2		7	17
	P	R	LOC.	VALUE
			HE	0.
			DESTE	0.
			PRF	0.
			WEPRC	0.
			END	

**IX**

SPACE TECHNOLOGY LABORATORIES  
COMPUTATION AND DATA REDUCTION CENTER

PAGE 5 of 14

DATE

NAME

PRIORITY

PROBLEM NO.

KEYPUNCHED BY

NO. OF CARDS

VERIFIED BY

1

7

78

IX

SYMBOL	1 2 7 17			
	19 20	28	36	43
	37 38	43	53	61
	66 66	61	71	
SYMBOL	LOC.	VALUE	EXP.	
I	ZVA	4		
I	ZU	2		
I	ZV	2		
I	ZUB	2		
I	ZVB	4		
I	ZDVT	6		
I		11		
I		8		
I		12		
I		9		
I		13		
Z	INK	2		
	PHIN	90.		
	XL	60.		
	RRIN	60.		
	BBAR	0.		
	ABAR	0.		
	C11E	1.098901	06	
		1.098901	06	
	C12T	.3296703	06	
		.3296703	06	
	C22I	1.098901	06	
		1.098901	06	
	C33T	.915750	03	
		.915750	03	
		.915750	03	
		.915750	03	
	C34T	.2747250	03	
		.2747250	03	
		.2747250	03	
		.2747250	03	
	C44I	.915750	03	
		.915750	03	
		.915750	03	
		.915750	03	
	THI	10		
		.10		
	DESTA	1.2588	-3	
	AM	.585389		
	HT	30.		

IX

SYMBOL	1 2 7 17			
	19 20	28	36	43
	37 38	43	53	61
	66 66	61	71	
SYMBOL	LOC.	VALUE	EXP.	
	DESTI	.51701388	-1	
	PRE	20.		
	HE	0.		
	DESTE	0.		
	PRE	0.		
	WEPRC	-5347.022		
	END			

SPACE TECHNOLOGY LABORATORIES  
COMPUTATION AND DATA REDUCTION CENTER

PAGE 6 OF 14

DATE \_\_\_\_\_

NAME \_\_\_\_\_

PROBLEM NO. \_\_\_\_\_

NO. OF CARDS \_\_\_\_\_

PRIORITY \_\_\_\_\_

KEYPUNCHED BY *[Signature]*

VERIFIED BY *[Signature]*

**X**

SYMBOL	1 2		7		17	
	R	E	LOC.	VALUE	EXP.	
I	INA	-5				
I	IU	2				
I	IV	2				
I	IUB	2				
I	IVB	2				
I	IDVT	11				
I		14				
I		12				
I		13				
I	INX	1				
	PHIN	90.				
	XL	0.				
	R2IN	0.				
	BBAR	-42.4				
	ABAR	60.				
	C11Z	.87912			06	
		.87912			06	
	C12Z	.263736			06	
		.263736			06	
	C22Z	.87912			06	
		.87912			06	
	C33Z	.46886447			03	
		.46886447			03	
		.46886447			03	
		.46886447			03	
	C34Z	.14065934			03	
		.14065934			03	
		.14065934			03	
		.14065934			03	
	C44Z	.46886447			03	
		.46886447			03	
		.46886447			03	
		.46886447			03	
	THZ	.08				
		.08				
	DESTA	.2588			-3	
	AM	.380503				
	HI	-30.				
	DESTE	.51701388			-1	
	PRI	20.				

**X1**

SYMBOL	1 2		7		17	
	R	E	LOC.	VALUE	EXP.	
			HE	0.		
			DESTE	0.		
			PRI	0.		
			WEARC	0.		
			END			

SPACE TECHNOLOGY LABORATORIES  
COMPUTATION AND DATA REDUCTION CENTER

PAGE 7 OF 14

DATE \_\_\_\_\_  
NAME \_\_\_\_\_  
PROBLEM NO. \_\_\_\_\_  
NO. OF CARDS \_\_\_\_\_

PRIORITY \_\_\_\_\_  
KEYPUNCHED BY *pt*  
VERIFIED BY *AK*

1	7	78
---	---	----

**X**

SYMBOL	1 2		7		17	
	P	R	28	38	68	71
I	I	NA	6			
I	I	IU	3			
I	I	IV	3			
I	I	IUB	3			
I	I	IVB	5			
I	I	IDVT	11			
I			15			
I			16			
I			12			
I			12			
I			18			
I			13			
I			19			
I		INK	3			
		PHIN	90.			
		XL	108.			
		RAIN	60.			
		BBAR	0.			
		ABAR	0.			
		C11I	1.64835	06		
			1.64835	06		
		C12I	.494505	06		
			.494505	06		
		C22I	1.64835	06		
			1.64835	06		
		C33I	.618	04		
			.618	04		
			.618	04		
			.618	04		
		C34I	.185	04		
			.185	04		
			.185	04		
			.185	04		
		C44I	.618	04		
			.618	04		
			.618	04		
			.618	04		
		THI	.15			
			.15			
		DESTA	2588	-3		

**X**

SYMBOL	1 2		7		17	
	P	R	28	38	68	71
		AM	1.580557			
		HZ	0.			
		DESTI	0.			
		PRI	0.			
		HE	0.			
		DESTE	0.			
		PPE	0.			
		WEARG.	-39479.357			
		END				

SPACE TECHNOLOGY LABORATORIES  
COMPUTATION AND DATA REDUCTION CENTER

PAGE 8 OF 14

DATE \_\_\_\_\_  
NAME \_\_\_\_\_  
PROBLEM NO. \_\_\_\_\_  
NO. OF CARDS \_\_\_\_\_

PRIORITY \_\_\_\_\_  
KEYPUNCHED BY *[Signature]*  
VERIFIED BY \_\_\_\_\_

1	7	79
<b>IX</b>		

SYMBOL	1 2		7		17	
	P	LOC.	VALUE	EXP.	38	59
I	INA	-7				
I	IU	2				
I	IV	2				
I	IUB	2				
I	IUB	2				
I	IDVT	16				
I	.	20				
I	.	18				
I	.	19				
I	INK	1				
	PHIN	90				
	XL	0.				
	R2IN	0.				
	BBAR	42.4				
	ABAR	60.				
	C11E	.8241758	06			
		.8241758	06			
	C12E	.2472527	06			
		.2472527	06			
	C22E	.8241758	06			
		.8241758	06			
	C33E	.38633241	03			
		.38633241	03			
		.38633241	03			
		.38633241	03			
	C34E	.11589972	03			
		.11589972	03			
		.11589972	03			
		.11589972	03			
	C44E	.38633241	03			
		.38633241	03			
		.38633241	03			
		.38633241	03			
	THZ	.075				
		.075				
	DESTA	.2588	-3			
	AM	.356721				
	HI	0.				
	DESTI	0.				
	PRZ	20.				

SYMBOL	1 2		7		17	
	P	LOC.	VALUE	EXP.	38	59
	HE	0.				
	DESTE	0.				
	PRE	0.				
	WFARC	0.				
	END					

**IX**

SPACE TECHNOLOGY LABORATORIES  
COMPUTATION AND DATA REDUCTION CENTER

PAGE 9 OF 14

DATE \_\_\_\_\_

NAME \_\_\_\_\_

PRIORITY \_\_\_\_\_

PROBLEM NO. \_\_\_\_\_

KEYPUNCHED BY *[Signature]*

NO. OF CARDS \_\_\_\_\_

VERIFIED BY \_\_\_\_\_

1	7



SYMBOL	P R E		LOC.	VALUE	EXP.
	1	2			
I	19	20	8		
I	37	38	2		
I	88	88	2		
I			2		
I			4		
I			16		
I			21		
I			18		
I			22		
I			19		
I			23		
I			2		
			PHIN	90.	
			X4	40.	
			R2IN	60.	
			BRAR	0.	
			ABAR	0.	
			C11I	1.31868	06
				1.31868	06
			C12I	1.395604	06
				.395604	06
			C22I	1.31868	06
				1.31868	06
			C33I	1.5824176	03
				1.5824176	03
				1.5824176	03
			C34I	.47472528	03
				.47472528	03
				.47472528	03
				.42172528	03
			C44I	1.5824176	03
				1.5824176	03
				1.5824176	03
			T44I	.12	
				.12	
			DESTA	.2588	-3
			AM	.561973	
			HF	24.	



SYMBOL	P R E		LOC.	VALUE	EXP.
	1	2			
	19	20	DESTI	.32465277	-1
	37	38	PRZ	20.	
	88	88	HE	0.	
			DESTF	0.	
			PRE	0.	
			WFARL	70720.379	
			E	NO	

SPACE TECHNOLOGY LABORATORIES  
COMPUTATION AND DATA REDUCTION CENTER

DATE \_\_\_\_\_

NAME \_\_\_\_\_

PROBLEM NO. \_\_\_\_\_

NO. OF CARDS \_\_\_\_\_

PRIORITY \_\_\_\_\_

KEYPUNCHED BY *illg*

VERIFIED BY \_\_\_\_\_

1	7	75
		<b>X</b>

SYMBOL	1 2		7		17	
	P	E	LOC.	VALUE	EXP.	
I	INA	-9				
I	IU	2				
I	IV	2				
I	IUB	2				
I	IUB	2				
I	IVB	2				
I	FDVT	21				
I		24				
I		22				
I		23				
I	INK	1				
	PHZN	110.				
	XL	0				
	R2IN	0				
	B BAR	-42.4				
	A BAR	60.				
	C11I	.87912	06			
		.87912	06			
	C12I	.263736	06			
		.263736	06			
	C22I	.87912	06			
		.87912	06			
	C33I	.46886447	03			
		.46886447	03			
		.46886447	03			
		.46886447	03			
	C34I	.14065934	03			
		.14065934	03			
		.14065934	03			
		.14065934	03			
	C44I	.46886447	03			
		.46886447	03			
		.46886447	03			
		.46886447	03			
	THI	.08				
		.08				
	DESTA	.2588	-3			
	AM	0				
	HZ	-24.				
	DESTI	.32465277	-1			
	CRJ	20.				

SYMBOL	1 2		7		17	
	P	E	LOC.	VALUE	EXP.	
	HE	0.				
	DESTE	0.				
	PRE	0.				
	WENRC	0.				
	END					

**X**



SPACE TECHNOLOGY LABORATORIES  
COMPUTATION AND DATA REDUCTION CENTER

PAGE 11 of 14

DATE \_\_\_\_\_  
NAME \_\_\_\_\_  
PROBLEM NO. \_\_\_\_\_  
NO. OF CARDS \_\_\_\_\_

PRIORITY \_\_\_\_\_  
KEYPUNCHED BY *WJ*  
VERIFIED BY *WJ*

1	7	73
		<b>X</b>

SYMBOL	P R E		LOC.	VALUE	EXP.
	1 19 37 55	2 20 38 56			
I			INA	10	
I			IU	2	
I			IV	2	
I			IIR	2	
I			IYB	4	
I			IDUT	21	
I				25	
I				22	
I				26	
T				23	
I				27	
I			INK	2	
			PHIN	90.	
			XL	54.	
			RZIN	60.	
			BRAR	0.	
			ABAR	0.	
			C11Z	1.64835	06
				1.64835	06
			C12Z	1.494505	06
				.494505	06
			C22Z	1.64835	06
				1.64835	06
			C33Z	.618	04
				.618	04
				.618	04
				.618	04
			C34Z	.185	04
				.185	04
				.185	04
				.185	04
			C44Z	.618	04
				.618	04
				.618	04
				.618	04
			T44Z	.15	
				.15	
			DISA	.2588	-3
			(AD)	1.227317	
			PZ	0.	

SYMBOL	P R E		LOC.	VALUE	EXP.
	1 19 37 55	2 20 38 56			
			DETI	0.	
			PRI	0.	
			HE	0.	
			DETE	0.	
			PRE	0.	
			WFARC	-62607.878	
			END		

**X** AM

SPACE TECHNOLOGY LABORATORIES  
COMPUTATION AND DATA REDUCTION CENTER

PAGE 12 OF 14

DATE \_\_\_\_\_

NAME \_\_\_\_\_

PROBLEM NO. \_\_\_\_\_

NO. OF CARDS \_\_\_\_\_

PRIORITY \_\_\_\_\_

KEYPUNCHED BY *WJG*

VERIFIED BY *WJG*

**X**

SYMBOL	1 2 7 17		EXP.
	P R E	LOC.	
I INA		11	
I IU		2	
I IV		2	
I TUB		2	
I IVB		4	
I IDVT		21	
I		28	
I		22	
I		27	
I		23	
I		30	
I INK		2	
PHIN		110.	
XL		-60.	
R2IN		38.1618	
RAMR		0.	
ABAR		0.	
C11Z		1.64835	06
		1.64835	06
C12Z		.494505	06
		.494505	06
C22Z		1.64835	06
		1.64835	06
C33Z		3.0906593	03
		3.0906593	03
		3.0906593	03
		3.0906593	03
C34Z		.9271978	03
		.9271978	03
		.9271978	03
C44Z		3.0906593	03
		3.0906593	03
		3.0906593	03
THZ		.15	
		.15	
DESTA		.2588	-3
AM		.764387	
HT		0.	

SYMBOL	1 2 7 17		EXP.
	P R E	LOC.	
DESTI		0.	
PRI		0.	
HE		0.	
DESTI		0.	
PRE		0.	
WFARC		1695.3252	
END			



SPACE TECHNOLOGY LABORATORIES  
COMPUTATION AND DATA REDUCTION CENTER

PAGE 14 OF 14

DATE \_\_\_\_\_

NAME \_\_\_\_\_

PRIORITY \_\_\_\_\_

PROBLEM NO. \_\_\_\_\_

KEYPUNCHED BY \_\_\_\_\_

NO. OF CARDS \_\_\_\_\_

VERIFIED BY \_\_\_\_\_

70



SYMBOL	P R E	LOC.	VALUE	EXP.
1	I	INC	1	
	I	IN	2	
	M	CK	10,10	
		02,02	1.0	3
	M	CM	10,10	
		01,01	12.939958	
	I	IDVTC	5	
	I	7		
		END		
2	I	INC	2	
	I	IN	2	
	M	CK	10,10	
		02,02	1.0	3
	M	CM	10,10	
		01,01	1.293995	
	I	IDVTC	15	
	I	17		
		END		
3	I	INC	3	
	I	IN	2	
	M	CK	10,10	
		02,02	1.0	3
	M	CM	10,10	
		01,01	1.293995	
	I	IDVTC	2.1	
	I	2.2		
		END		
4	I	INC	4	
	I	IN	3	
	M	CK	10,10	
		02,02	1.0	3



SYMBOL	P R E	LOC.	VALUE	EXP.
		03,03	1.0	4
M	CM	10,10		
	01,01	3.623188		
I	IDVTC	28		
	I	29		
	I	30		
		END		